MDC-TR-66-110

AIR FORCE MISSILE DEVELOPMENT CENTER
TECHNICAL REPORT

FEASIBILITY STUDY OF AIR BEARING ROCKET SLED SLIPPERS

R. C. Meier and A. F. Smith

JULY 1966

HOLLOMAN AIR FORCE BASE
NEW MEXICO

MDC-TR-66-110

FEASIBILITY STUDY OF AIR BEARING ROCKET SLED SLIPPERS

R. C. Meier and A. F. Smith
Kaman Aircraft Corporation

TECHNICAL REPORT MDC-TR-66-110
July 1966

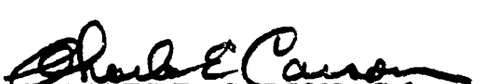

CHARLES E. CARSON, Colonel, USAF
Director, Test Track

Air Force Missile Development Center
Air Force Systems Command
Holloman Air Force Base, New Mexico

FOREWORD

The investigation reported herein was initiated and sponsored by the Air Force Missile Development Center (AFMDC), Air Force Systems Command (AFSC), United States Air Force, under Project No. 6876, Task No. 687602-B-6.

The study was performed by Kaman Aircraft Corporation, Bloomfield, Connecticut, from February 16 to July 1, 1966, under Contract No. AF 29(600)-5516. The final report was submitted on July 5, 1966.

Grateful acknowledgement is expressed to Major John Frazier and 1st Lt. William Gallant, Air Force Project Engineer, for the technical information and assistance provided during the performance of the study.

ABSTRACT

A study was conducted for the Air Force Missile Development Center to investigate the feasibility of applying the principle of air film lubrication to rocket sled slippers to: (1) overcome erosive oxidation and severe melting effects experienced at hypersonic speeds and (2) alleviate rail-induced vibrations. Results of the study indicate that a simple self-acting type of bearing can support a typical monorail rocket sled, without contact between the slipper and the rail, at speeds between Mach 1.5 and Mach 6. With contact eliminated, the slipper can be coated with a refractory material to prevent erosive oxidation and melting of slipper structural material. This type of air bearing slipper appears to be the most suitable for AFMDC requirements. An externally pressurized type of slipper bearing is capable of preventing slipper-rail contact over the entire speed range of typical monorail and dual rail sleds. However, the weight and volume of the associated pressurization system are large, and are considered prohibitive for a practical design. The most critical track requirements for an application of air lubricated slippers are the vertical alignment and dimensional tolerances of the rail. It is recommended that AFMDC proceed with the development of a self-acting type of slipper bearing.

TABLE OF CONTENTS

		PAGE
	ABSTRACT	iii
	NOMENCLATURE	xi
I.	INTRODUCTION	1
	1.1 Purpose of the Study	1
	1.2 Types of Bearings and Lubricants	1
	1.3 Application of Air Bearings to Rocket Sled Slippers	3
	1.4 Applicable Technology	3
II.	REQUIREMENTS	5
	2.1 Performance Requirements	5
	2.2 Constraints	5
	2.3 Evaluation	5
III.	SELF-ACTING SLIPPER BEARINGS	9
	3.1 General Considerations	9
	3.2 Bearing Analysis	12
	3.3 Self-Acting Slipper Bearing Performance	13
	3.4 Factors Affecting Self-Acting Slipper Bearing Design	13
	3.5 Monorail Sled Self-Acting Slipper Bearing	16
	3.6 Dual Rail Sled Self-Acting Slipper Bearing	29

TABLE OF CONTENTS (Continued)

		PAGE
IV.	EXTERNALLY PRESSURIZED SLIPPER BEARINGS.	31
	4.1 General Considerations	31
	4.2 Bearing Analysis	35
	4.3 Factors Affecting Externally Pressurized Slipper Bearing Design	37
	4.4 Dual Rail Sled Externally Pressurized Slipper Bearing.	38
	4.5 Monorail Sled Externally Pressurized Slipper Bearing.	50
V.	EFFECT OF TRACK CONDITIONS	57
	5.1 Effect of Rail Alignment and Dimensional Variations	57
	5.2 Effects of Roughness on Slipper Bearing Performance.	61
	5.3 Effects of Foreign Objects on Slipper Performance.	68
VI.	HIGH SPEED SLIPPER COATINGS.	70
	6.1 Candidate Materials.	70
	6.2 Current Coating Program.	70
VII.	OPERATIONAL REQUIREMENTS AND DEVELOPMENT EFFORT	72
	7.1 Self-Acting Slipper Bearing System . .	72
	7.2 Externally Pressurized Slipper Bearing System	73

TABLE OF CONTENTS (Continued)

	PAGE
VIII. CONCLUSIONS AND RECOMMENDATIONS.	75
8.1 Conclusions on Self-Acting Slipper Bearings	75
8.2 Conclusions on Externally Pressurized Slipper Bearings	75
8.3 Recommendations.	76
IX. PHASE II PROPOSALS	78
9.1 Performance Program Modification . . .	78
9.2 Slipper Designs.	78
9.3 Slipper Fabrication.	79
9.4 Test Program	79
9.5 Test Data Correlation.	79
REFERENCES.	80
APPENDIX I - SELF-ACTING SLIPPER BEARING ANALYSIS AND RESULTS	81
APPENDIX II - USE OF THE SLIPPER PERFORMANCE CURVES. .	91
APPENDIX III - EXTERNAL AERODYNAMIC LOADS	97
APPENDIX IV - TURBULENT BEARING ANALYSIS	101

LIST OF ILLUSTRATIONS

FIGURE		PAGE
1	Air Lubricated Rocket Sled Slippers	2
2	Typical Monorail Sled Load-Velocity Curve	6
3	Typical Dual Rail Sled Load-Velocity Curve. . . .	7
4	Typical Self-Acting Bearing Configurations. . . .	8
5	Typical Self-Acting Air Bearing Pressure Profile	10
6	Typical Self-Acting Slipper Bearing Performance	12
7	Pressure Distribution in Large Slipper-Rail Gaps	15
8	Comparison of Full and Partial Monorail Slippers at Mach 6.	17
9	Monorail Self-Acting Slipper Bearing.	18
10	Variation of Minimum Slipper-Rail Gap During Monorail Sled Acceleration Run.	20
11	Effect of Sled Loading on Slipper Slope	22
12	Lateral Load Capacity of Self-Acting Monorail Sled Slipper Bearing	23
13	Monorail Sled Slipper Position When Reacting an Applied Rolling Moment.	25
14	Monorail Self-Acting Slipper Bearing Moment Capacity	26
15	Net Increase in Slipper Aerodynamic Drag Over Standard Slipper	28
16	Types of Externally Pressurized Air Bearings. . .	30
17	Preferred Design Features for Externally Pressurized Slippers.	34

LIST OF ILLUSTRATIONS (Continued)

FIGURE		PAGE
18	Externally Pressurized Slipper Bearing Design	36
19	Dual Rail Sled Externally Pressurized Slipper Requirements	39
20	Effect of Supply Pressure on Flow Rate of Dual Rail Sled Externally Pressurized Slipper	41
21	Tank Volume and Compressor Power For Dual Rail Sled Externally Pressurized Slipper	42
22	Effect of Slipper-Rail Gap on Dual Rail Sled Externally Pressurized Slipper Penalties	43
23	Weight and Volume Penalties of Dual Rail Sled Externally Pressurized Slipper	45
24	Lateral Load Capacity of Dual Rail Sled Externally Pressurized Slipper	47
25	Excess Force of Dual Rail Sled Externally Pressurized Slipper	49
26	Weight and Volume Penalties of Monorail Sled Externally Pressurized Slipper	51
27	Monorail Sled Externally Pressurized Slipper Requirements	52
28	Lateral Load Capacity of Monorail Sled Externally Pressurized Slipper	54
29	Moment Capacity of Monorail Sled Externally Pressurized Slipper at Rest	56
30	Motion of Slipper Due to Variation in Rail Alignment or Dimensions	58
31	Minimum Slipper-Rail Gap on Initial Section of Ramp	60

LIST OF ILLUSTRATIONS (Continued)

FIGURE		PAGE
32	Variation of Slipper-Rail Gap on Ramp	62
33	Effect of Ramp Length on Slipper-Rail Gap Variation	63
34	Effect of Roughness on Slipper Drag	67
35	Typical Flow Pattern at the Slipper-Rail Gap Inlet	84
36	Typical Velocity Profiles in the Slipper-Rail Gap.	85
37	Self-Acting Slipper Bearing Performance	87
38	Forces on the Slipper Bearing	92
39	Gap Inlet Pressure Vs Mach Number	93
40	Effect of Slipper Slope on Performance.	95
41	Slipper Model for External Flow Analysis. . . .	98
42	External Aerodynamic Slipper Loads.	100
43	Bearing Coordinate System	104
44	Turbulent Bearing Performance Parameters. . . .	108
45	Numerical Integration Method.	110

NOMENCLATURE

F	Force - Lbf, Bearing load per unit surface width - Lbf/Ft
h	Slipper-rail gap - Ft, In.
L	Slipper length - Ft, In.
l	Turbulent mixing length - Ft, In.
n	Polytropic exponent
$\bar{n}$	Number of increments in the numerical integration
p	Pressure - Lbf/Ft^2
R	Reynolds number
u,v,w	Flow velocities, Ft/Sec.
V	Sled velocity, Ft/Sec.
t	Time - Sec.
x,y,z	Coordinates - Ft, In.
$\bar{x}$	Slipper center of pressure - Ft, In.
α	Slipper gap slope, rail slope - Ft/Ft, In/In
μ	Viscosity - Lbm/Ft.Sec., Lbf Sec/Ft^2
ρ	Density - Lbm/Ft^3, $Slugs/Ft^3$
σ	Gradient of the mixing length - Ft/Ft, In/In
τ	Characteristic time - Sec., Turbulent shear stress - Lbf/Ft^2

SECTION I

INTRODUCTION

1.1 Purpose of the Study

This investigation was undertaken to assess the feasibility and practicality of air film lubrication for rocket sled slippers. The slippers, which are wrapped around the rail to constrain the rocket sled to the test track, have two operational problems. First, at high supersonic and hypersonic speeds, the combination of high air temperature and sliding friction causes severe erosive oxidation and melting of slipper material. Second, rail-induced vibrations occur over the entire operating speed range from subsonic to hypersonic. Due to slight variations in rail alignment and dimensions, a clearance must be provided between the rail and slipper. This clearance allows the sled to jump or bounce as it travels down the track.

Lubrication of the slipper would alleviate both of these problems. At high test speeds, elimination of sliding friction between the slipper and rail would reduce the slipper operating environment to that experienced by other portions of the sled. For very high speed tests, where critical portions of the sled would be covered with protective coatings, the same coatings could be used on the slippers without danger of their being sheared off. In addition to eliminating sliding friction, a lubricating film between the slipper and rail would provide a cushioning effect to any rail-induced vibrations.

1.2 Types of Bearings and Lubricants

Generally, bearings are divided into two classes - those which are self-acting, or hydrodynamic, and those which are externally pressurized, or hydrostatic. Self-acting bearings develop an average pressure greater than the lubricant inlet pressure due to viscous forces generated by relative motion of the bearing surfaces. The lubricant inlet pressure is usually ambient so that the bearing load capacity is directly measurable in terms of the average pressure increase. Externally pressurized bearings develop load capacity by injecting the lubricant into the bearing at a pressure higher than ambient. This type of bearing is employed when the relative motion of the two bearing surfaces is not sufficient to produce the required load capacity. The definition given above for a self-acting bearing also applies to hybrid types where the lubricant is supplied at a pressure higher than ambient and relative

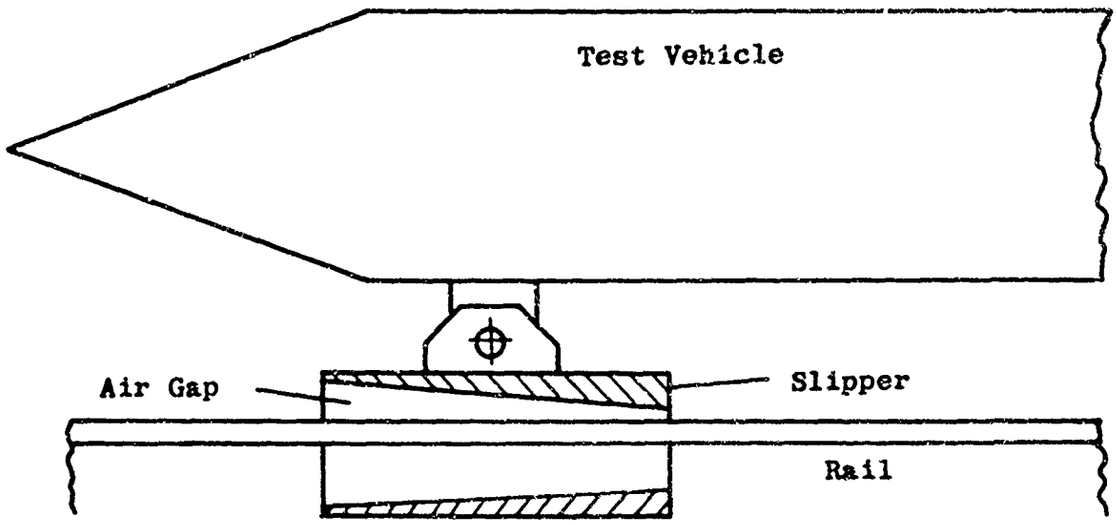

(a) Self-Acting Slipper Bearing

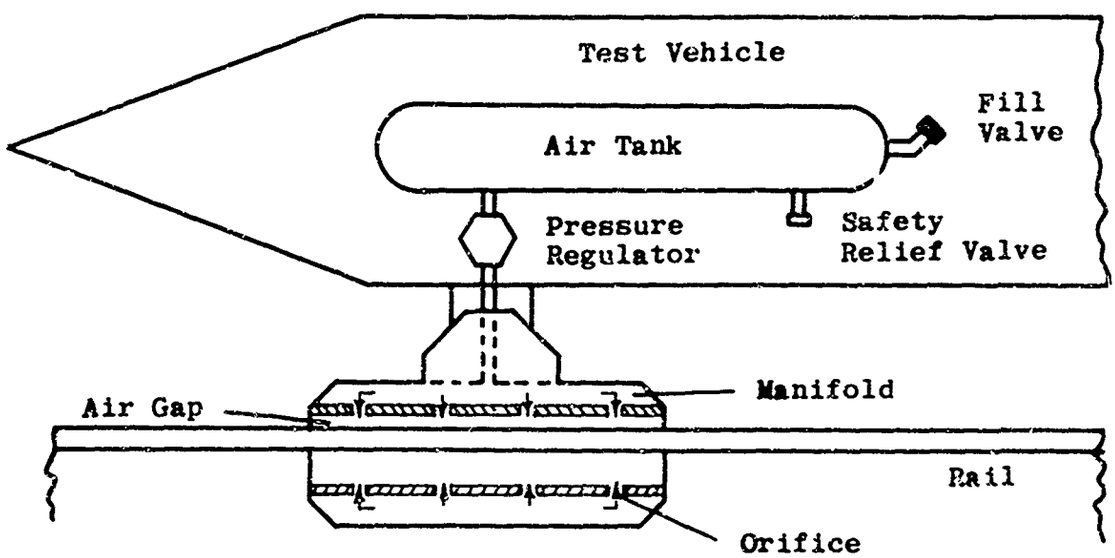

(b) Externally Pressurized Slipper Bearing

Figure 1. Air Lubricated Rocket Sled Slippers

motion of the bearing surfaces increases the load capacity over that due to the injected lubricant alone.

Virtually any lubricant may be considered for a rocket sled slipper. Oils, greases, water and air (or any other gas) can be used. However, any liquid lubricant which is painted on the track may be scraped off by the forward slipper of a sled thus "starving" rear slippers. Even if the lubricant is carried on board, operation at hypersonic speeds subjects the lubricant to extremely high temperatures (about 3300°F at Mach 6), thus ruling out most liquids. Gases are quite suitable at these high temperatures, and of the gases, air is the most logical candidate. For the self-acting type of bearing, the lubricant supply is effectively infinite and exerts no weight penalty on the sled. Unlike liquids, the viscosity of air increases with increasing temperature. This property is especially desirable for high speed operation.

1.3 Application of Air Bearings to Rocket Sled Slippers

For a rocket sled application, the rail and slipper serve as the two bearing surfaces. If the slipper is inclined at a slight angle to the rail, as shown in Figure 1(a), a force will be developed by the air film and surface interaction tending to keep the surfaces separated; in this case, to carry a load on the slipper. This type of bearing, a self-acting plane wedge, is the simplest to fabricate, weighs no more than a standard slipper, and exhibits virtually no stability problems. In addition, its development cost would be very small compared to other types. However, if contact with the rail is to be avoided at all speeds, an externally pressurized bearing, operating at least part of the time, is required. A schematic of such a bearing and its subsystem are shown in Figure 1(b). This type of bearing requires a support system whose weight is dependent on the slipper loading and operating time. In addition, the lubricant supply system is subject to instabilities when coupled to the bearing. Its development costs would probably be an inverse function of the amount of weight penalty allowable.

1.4 Applicable Technology

Air lubricated bearings have only recently received a substantial amount of attention due to their relatively limited performance characteristics, especially load capacity. Until such requirements as computer memory discs, small gyroscopes, etc., indicated a need for air lubricated bearings, they remained a relatively undeveloped technology. The recent pro-

gress in air lubricated bearings has been confined to areas far removed from a rocket sled application. Almost all air bearing analysis, design, and construction has been limited to applications where the velocities involved are more than an order of magnitude lower than for a rocket sled. And, almost all of the available analyses on air bearings are for bearings operating with a laminar gas film in the bearing gap. For a rocket sled, this film is highly turbulent and the results obtained by applying laminar theory analysis can yield very pessimistic designs.

SECTION II

REQUIREMENTS

The major requirements of an air bearing rocket sled slipper are summarized below. These are condensed from the Technical Exhibit of the contract, Reference (1), and are included here to clarify the results discussed in subsequent sections. Only the specific requirements and objectives are included here and the parameters considered in the study are included in the appropriate sections.

2.1 Performance Requirements

The principal performance requirement of an air lubricated slipper bearing is to prevent contact between the slipper and rail under the highly transient loading specifications given in Reference (1). These loading specifications are shown in Figure 2 for a typical monorail sled, and in Figure 3 for a typical dual rail sled. In addition, an air lubricated slipper bearing must be capable of reacting moments and incidental lateral loading without rail contact. Similarly, no instabilities causing slipper-rail contact are acceptable.

2.2 Constraints

The principal constraint on an air bearing slipper is that it must be compatible with the present AFMDC track at Holloman Air Force Base. No changes of the track are permissible.

2.3 Evaluation

The major characteristics of an air bearing slipper to be evaluated include the penalties with respect to weight, drag, and operational complications such a system would incur and the level of development effort required to provide a prototype system. In addition, the ability of such a system to overcome the problem of erosive oxidation at hypersonic speeds must be evaluated.

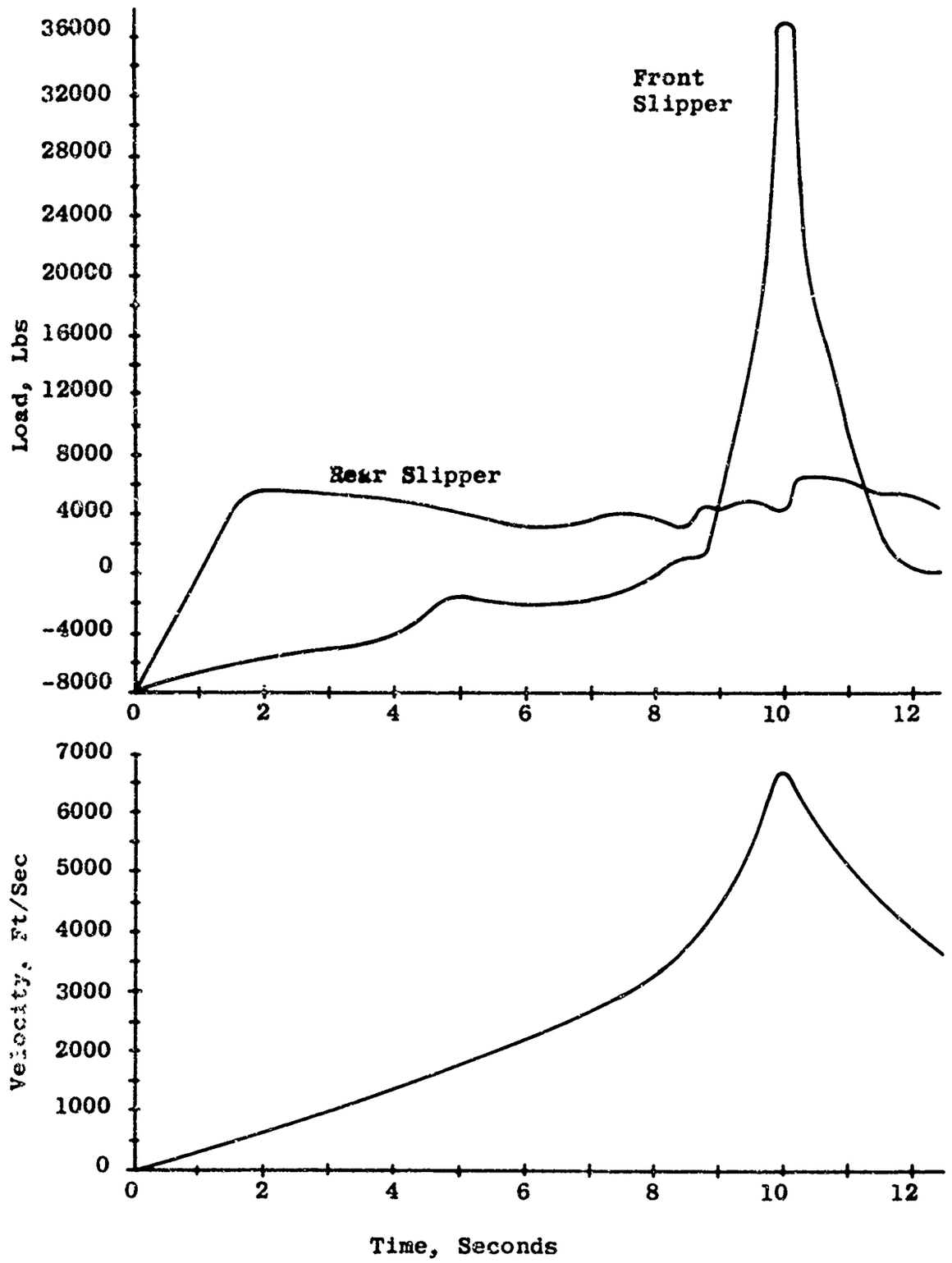

Figure 2. Typical Monorail Sled Load-Velocity Curve

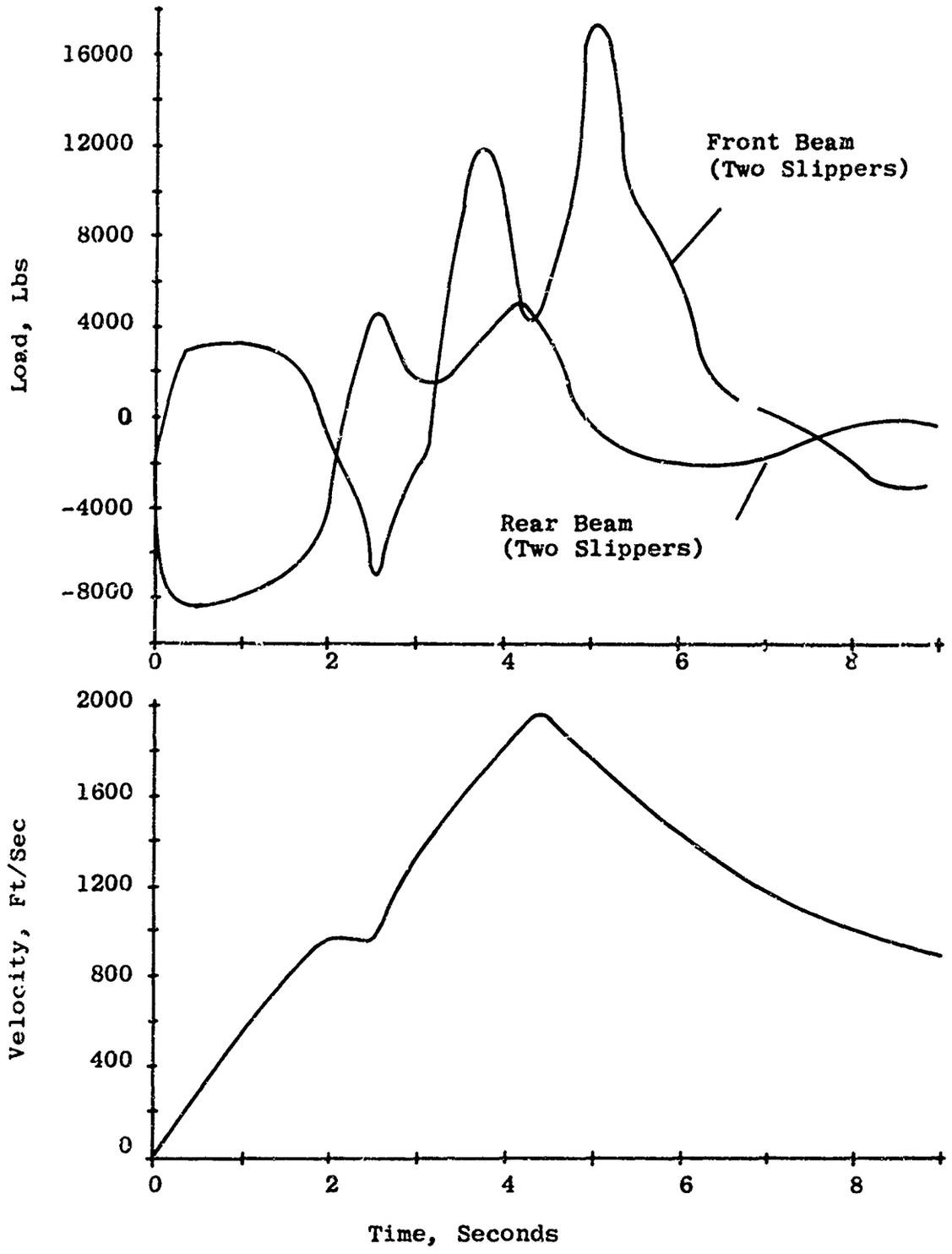

Figure 3. Typical Dual Rail Sled Load-Velocity Curve

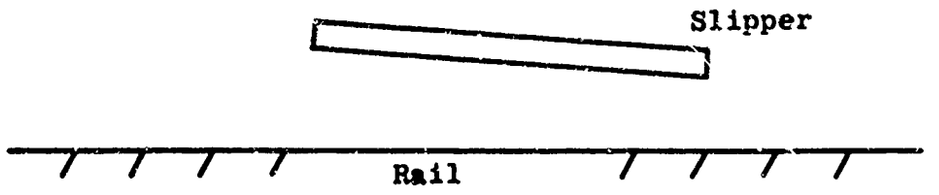

(a) Plane Wedge or Tapered

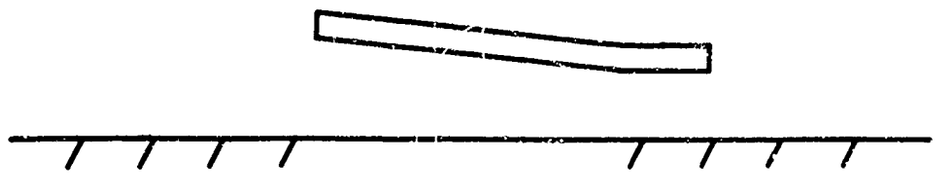

(b) Tapered-Flat

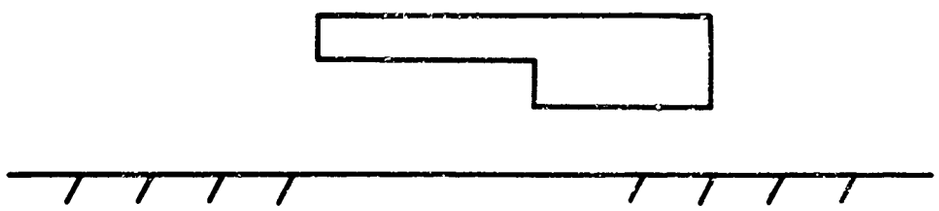

(c) Step

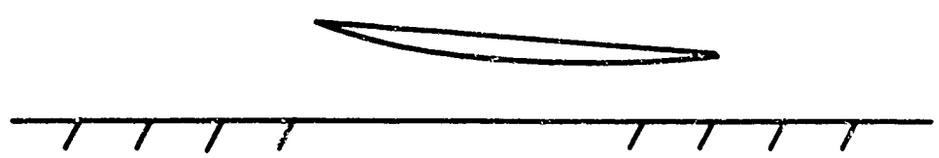

(d) Curved

Figure 4. Typical Self-Acting Bearing Configurations

SECTION III

SELF-ACTING SLIPPER BEARINGS

3.1 General Considerations

The use of a simple, self-acting air bearing for a rocket sled slipper application is most attractive due to its light weight, low development cost, and operational simplicity. Virtually any two surfaces in close proximity with relative motion act as a bearing, but the effectiveness of the bearing is a strong function of the shape, operating environment, and arrangement of the elements. The most important parameter to be considered for a rocket sled application is the minimum slipper-rail gap. This dimension should be as large as possible to minimize the requirements on track alignment, dimensional variations of the rail, and surface roughness.

3.1.1 Bearing Geometry

Various shapes for self-acting bearings are possible, depending on requirements of the particular application. Four typical configurations are shown in Figure 4. The simplest of these is the plane wedge or tapered bearing, which is the easiest to fabricate. The other types have higher load capacities for the same length, width and minimum gap, on a theoretical basis which ignores side flow. The step bearing shown in Figure 4(c) has a higher side flow than the other types and therefore does not achieve its theoretical advantage in practice. Even theoretically, the load capacities of the different shapes do not vary by large amounts. For these reasons, the simple wedge shape bearing was chosen for subsequent analysis.

3.1.2 Effect of Inlet and Exit Pressures

The flow field in the immediate vicinity of the slipper directly affects its operation as a bearing. The gap inlet pressure is the most important parameter since the bearing load capacity is almost directly proportional to this pressure. A typical pressure profile for an air-lubricated slipper bearing is shown in Figure 5. This pressure profile is nondimensionalized in terms of the inlet pressure and bearing length for a Mach 6 operating condition. For the same slipper geometry, this profile would apply for almost any inlet pressure.

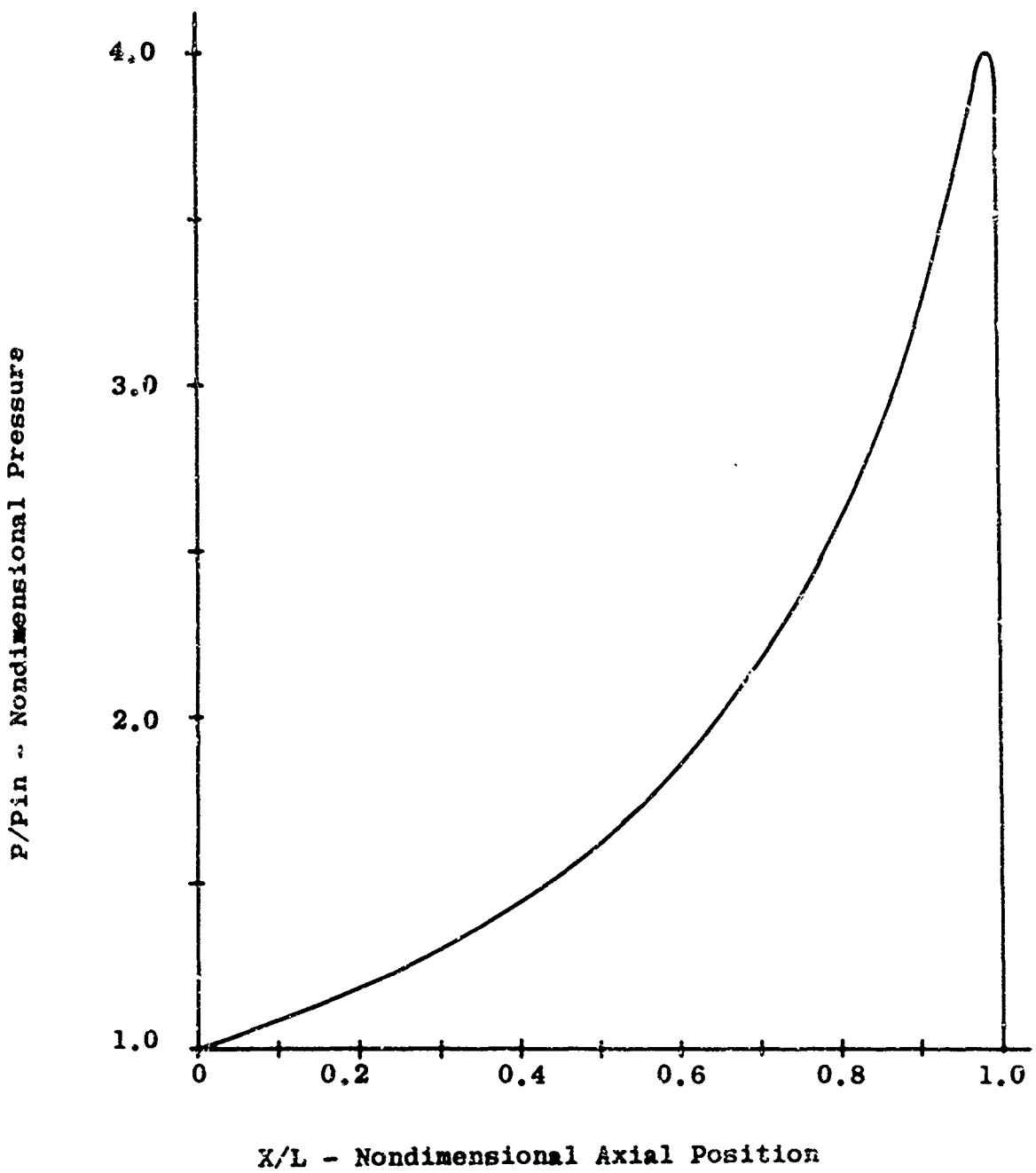

Figure 5. Typical Self-Acting Air Bearing Pressure Profile

Since the integrated pressure profile yields the load capacity, the highest inlet pressure will produce the highest load capacity. The use of a flow deflection device to shield the slipper is therefore precluded for a self-acting slipper bearing due to the low pressure region behind such a device.

The pressure profile in Figure 5 also shows that the pressure drops off from the maximum value to the exit value very rapidly. From a load capacity viewpoint, the exit pressure can vary over a large range without appreciably affecting the bearing load.

3.1.3 Flow Within the Gap and Shock Formation

The flow within the slipper-rail gap is determined by the sled velocity. Relative to a coordinate system fixed to the slipper, the flow velocity is zero on the slipper surface and equal to the sled velocity on the rail. The situation is reversed if the coordinate system is fixed on the rail. When a sled is operating at supersonic velocities, portions of the flow within the slipper-rail gap are supersonic, transonic, and subsonic. The pressure profile in Figure 5 shows that the maximum pressure point is close to the exit of the slipper and the pressure gradient up to this point is quite high. The high pressure gradient will generate regions or layers of the flow close to the slipper surface where the flow is reversed. The relatively large area of subsonic flow and the layer of reversed flow provide a mechanism for pressure signals to propagate upstream and modify the flow. This characteristic minimizes the possibility of a shock ahead of the maximum pressure point.

The flow aft of the maximum pressure location is affected by a steep accelerating pressure gradient and most of the flow within the gap, excluding a small region near the slipper, will become supersonic. The possibility of shocks forming within the gap is much greater in this region. However, the very small area over which this may occur would cause the effect of shock formation to be negligible. The only serious problem would be the possibility of altering the upstream flow. However, conventional air bearings also operate with pressure gradients near the end of the bearing sufficient to cause supersonic flow and no corrections have been found necessary. Trailing edge discontinuities are neglected in standard bearing analyses and, as pointed out in Reference (2), experiments have verified that these discontinuities are usually negligible.

3.2 Bearing Analysis

The basic bearing analysis used to evaluate the feasibility of self-acting slipper bearings was adopted from the work of N. Tipie and V. N. Constantinescu of the Institute of Applied Mechanics, Academy of the Rumanian Peoples' Republic. The results of their studies on turbulent lubricating films have been published in Reference (3), which was used for this study.

The approach taken in this work parallels the analysis of turbulent boundary layers. The Prandtl mixing length theory is applied to the reduced Navier-Stokes equation and a modified version of the standard lubricating equation is formed. Details of the analysis and the associated assumptions used are given in Appendix I.

The solution of the basic differential equation given in Reference (3) requires an assumption on the form of the equation to render it integrable. In order to insure that this assumption did not limit the applicability of the analysis, the basic differential equation was numerically integrated with a computer program developed for this purpose.

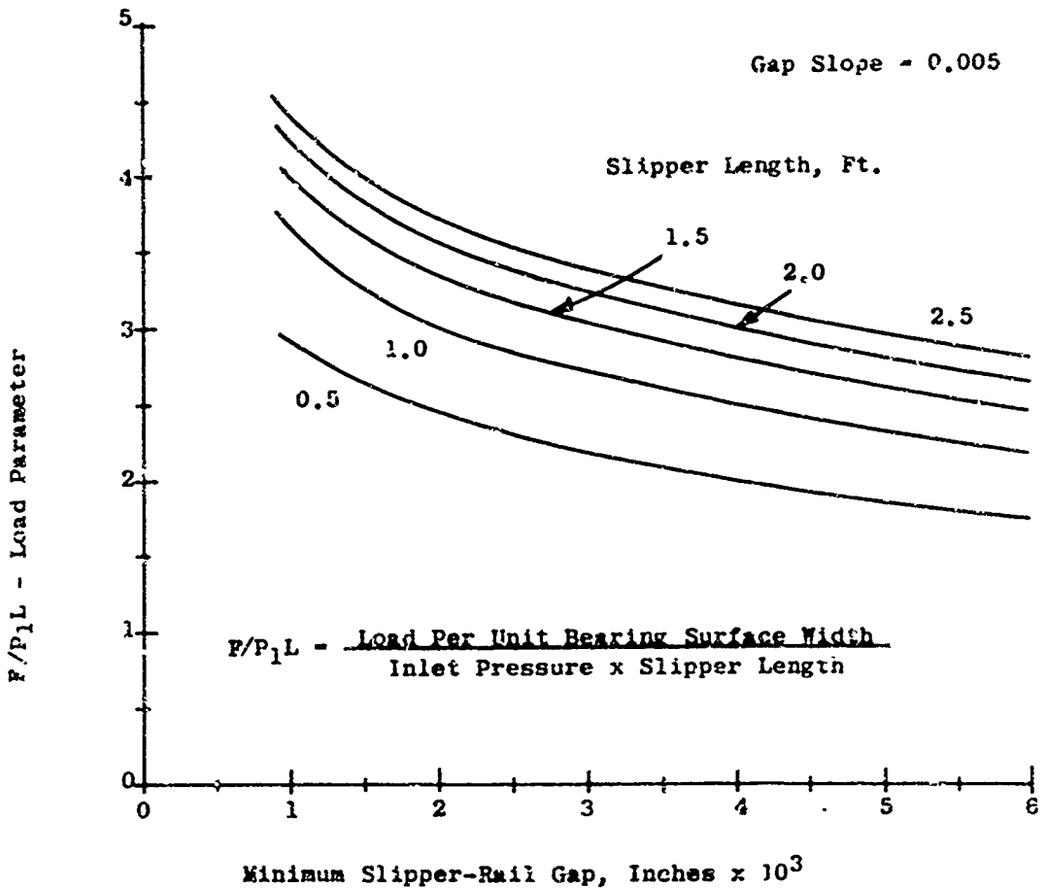

Figure 6. Typical Self-Acting Slipper Bearing Performance

3.3 Self-Acting Slipper Bearing Performance

The results of the analysis are shown in their most useful form in Figure 6. This figure gives the nondimensionalized bearing load per unit width of surface as a function of slipper length and minimum slipper-rail gap, for a slipper slope of 0.005. Slipper bearing performance for other slopes, including center of pressure data, are given in Appendix I.

The load carrying capability of the slipper is given in nondimensionalized form for convenience. The load per unit width of surface (the width of the rail face reacting the load) is divided by the bearing inlet pressure and length. For the results shown in Figure 6, the bearing inlet pressure was assumed to be the static pressure behind a normal shock at the sled Mach number. If this pressure is used, the data in Figure 6 applies for any velocity between Mach 1 and Mach 6. This convenient result is due to the combination of, (1) the form of the lubrication equation and, (2) the equilibrium air properties behind a normal shock. The effect of Mach number enters only through the inlet pressure. Actually, slight differences were found between different Mach numbers but, these differences are very small and may be ignored.

3.4 Factors Affecting Self-Acting Slipper Bearing Design

3.4.1 Effect of the Average Slipper-Rail Gap

Aside from the basic considerations of slipper bearing length and minimum slipper-rail gap, two important factors peculiar to a rocket sled application must be considered in a typical design.

The first factor is the effect of the average slipper-rail gap on overall bearing performance. The schematic shown in Figure 1 for the self-acting slipper bearing depicts the slipper supporting a download. The picture shows that the load is supported by the upper surface of the slipper with a small clearance between the rail and slipper surfaces. However, since the slipper must also react uploads, the lower lip of the slipper is shaped so that it may act as a bearing under upload conditions. If the minimum slipper-rail gap on the lower side of the slipper is approximately the same as on the upper side, the two sides of the slipper will develop opposing forces. These forces will minimize any net load capacity.

The simplest solution to this problem is to provide a sufficiently large average slipper-rail gap so that the force developed by the opposite side of the slipper is minimized. In this case, the slipper bearing would position itself on the rail as shown in Figure 1(a) to support a download with the large gap, between the lower slipper surface and the rail, minimizing the opposing force. To react an upload, the situation would reverse.

The optimum average slipper-rail gap required to minimize the opposing force would be quite large if no limits had to be considered. However, a very large average slipper-rail gap would amplify existing problems of rail induced vibrations and an upper limit is imposed by the track tie-down fixtures. To assess the opposing force, a number of cases were run on the performance program for an average gap corresponding to the present average slipper-rail gap of 1/16 of an inch. The results given in Figure 7, show that the pressure decreases from the inlet value to the exit value for a number of typical cases. In general, this will always be the case if the slipper-rail gap is large. Since the force developed by the opposite side of the slipper is not excessive in these cases, it is recommended that the present 1/16 inch average slipper-rail gap be maintained at the exit of the slipper bearing. Due to the slope of the inner surface, the average slipper-rail clearance will vary over the length of the slipper.

3.4.2 Partial vs Full Slippers

The second design consideration also involves the opposing force discussed above. For the monorail sled, operation at high speed requires the lower lips of the slippers to react the sled lift. If a standard slipper form is used, the upper surface of the slipper, with twice the surface area of the lower lips, will develop a large lift. This will increase the load requirement of the lower lips, thus forcing the slipper to operate with a small slipper-rail gap.

One method of alleviating this problem is to use only a portion of the upper surface as a bearing. A typical configuration would vent half of the upper surface so that no load would be developed in the center section. This type of slipper would resemble the "half" slippers used on some sleds in the past.

The advantage of using a "partial" slipper design was evaluated for the front slipper of the monorail sled at the maximum velocity condition (Mach 6). The minimum slipper-rail gap for full and partial slippers were calculated using the pro-

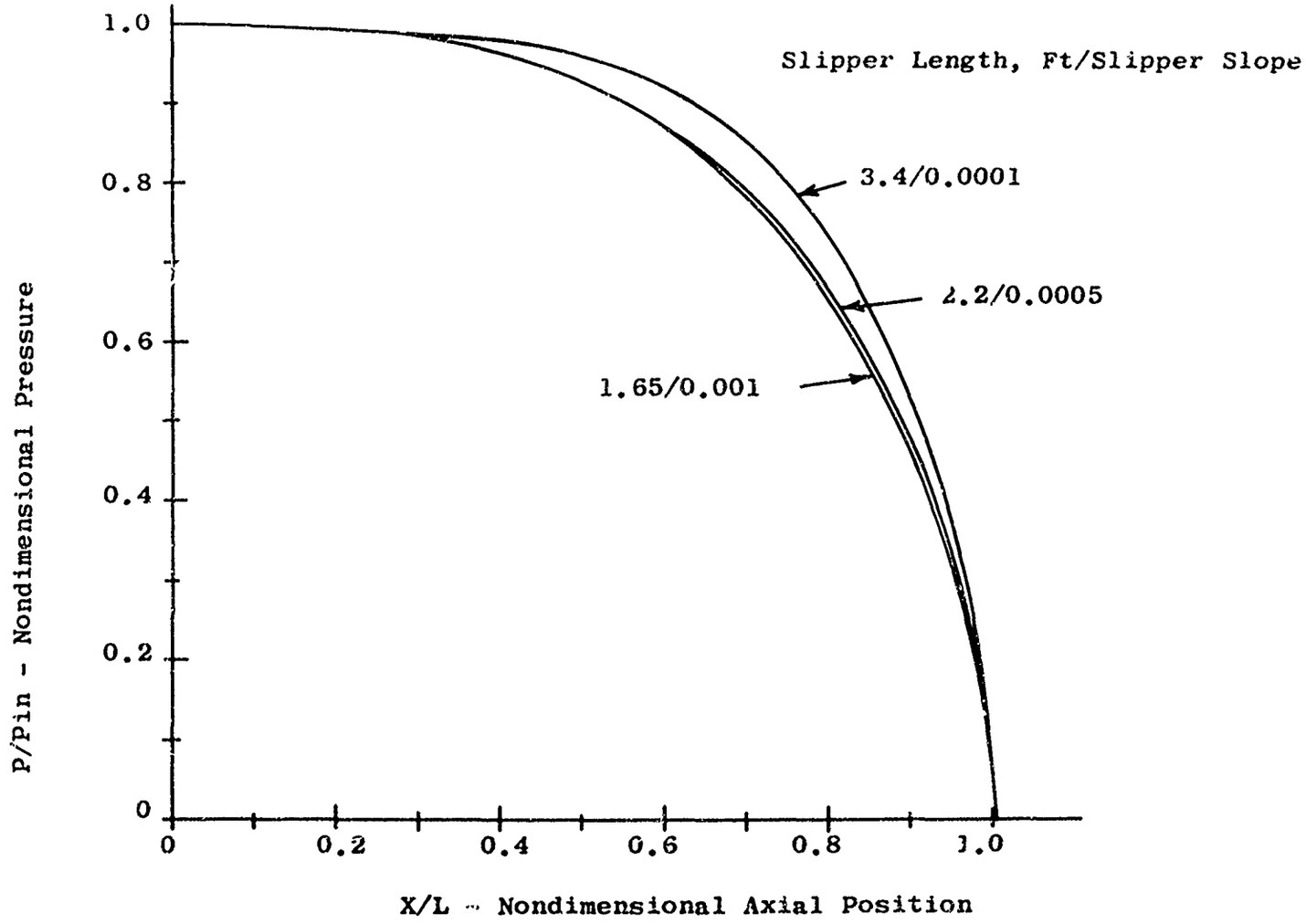

Figure 7. Pressure Distributions in Large Slipper-Rail Gaps

cedure outlined in Appendix II. The results of this calculation are shown in Figure 8, where the partial slipper has 50 percent of its upper surface vented or removed, and the full slipper retains the entire surface. The data shown in Figure 8 illustrates the advantage offered by using a partial slipper. For a given slipper length, the minimum slipper-rail gap is much larger for the partial slipper, than for the full slipper.

An obvious disadvantage of the partial slipper is that the reduced upper surface area reduces the load capacity of that surface. However, this disadvantage occurs only at low speeds (where the slipper load is down) and is outweighed by the advantage gained at high speeds. This is shown in Section 3.5.2.

3.5 Monorail Sled Self-Acting Slipper Bearing

3.5.1 Slipper Design

The choice of a "design point" for the monorail sled slipper bearing is arbitrary, since the slipper operates over large ranges in speed and load. A reasonable point to take as a design point would be the operating condition where the slipper-rail gap is a minimum. Except for very low velocities, where the slipper is bottomed out, the minimum slipper-rail gap occurs at the maximum velocity condition (Mach 6) for the front slipper specified in Figure 2.

With the partial slipper selected as the preferred approach, many combinations of slipper length, minimum gap, and gap slope are possible. The gap slope can be eliminated from consideration since the optimum slope is 0.005 as shown in Appendix II. However, the trade-off between length and gap must consider many parameters each of which are strongly dependent on load, velocity, track conditions, sled geometry and many other factors. For the purposes of a feasibility study, it was decided to select a slipper length that was not unreasonable, but operated with an appreciable gap. For this purpose, a length of 1.5 feet, with a corresponding minimum slipper-rail gap of 0.005 inches, was selected. This corresponds to the design point shown in Figure 8.

A sketch of the slipper with the important dimensions is shown in Figure 9. The dimensions shown on the drawing assume a slipper thickness of 0.38 inches, which has been machined to form a tapered gap. If a constant thickness is required for strength, the form of the slipper would only change in this dimension.

Partial Slipper Has 50 Percent of the
Upper Surface Vented or Removed

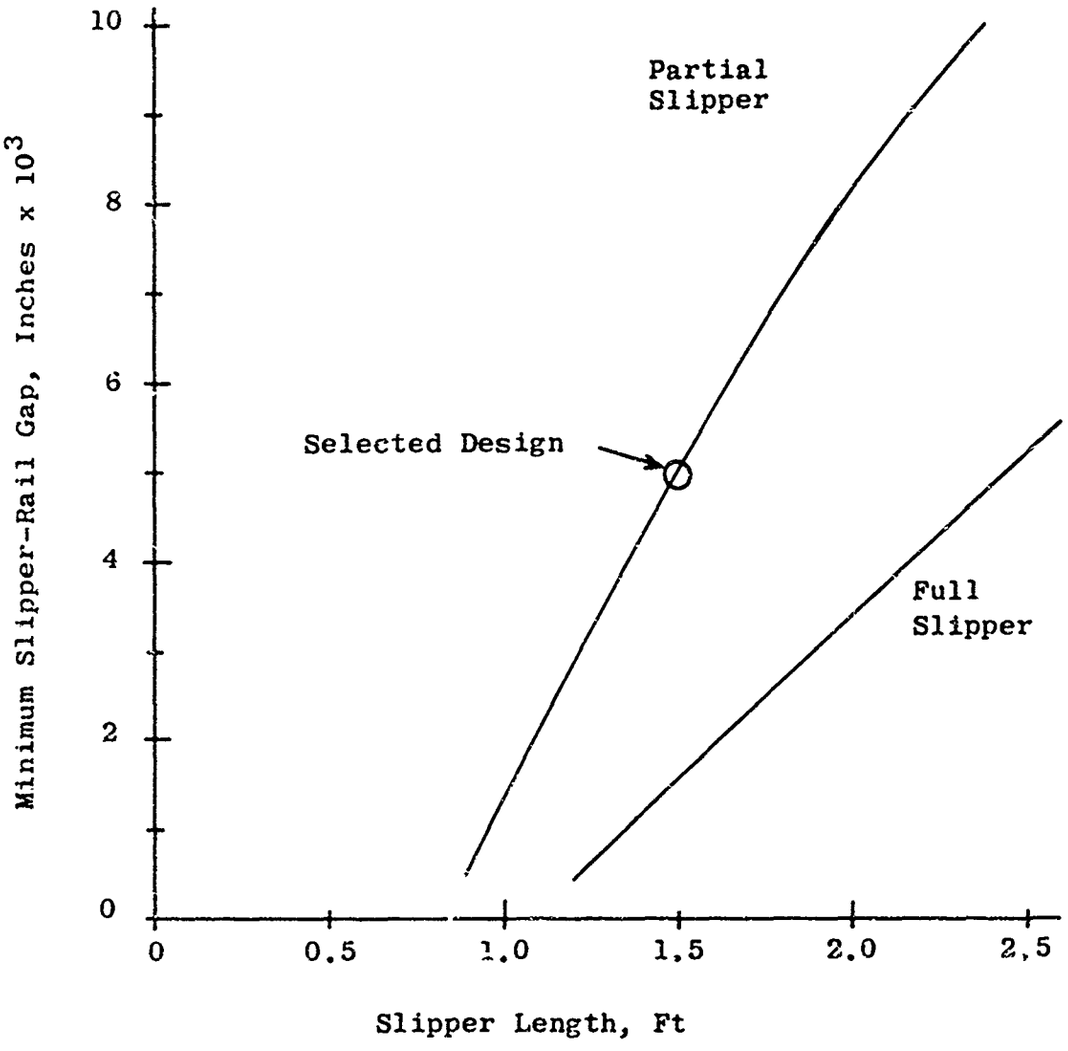

Figure 8. Comparison of Full and Partial Monorail Slippers at Mach 6

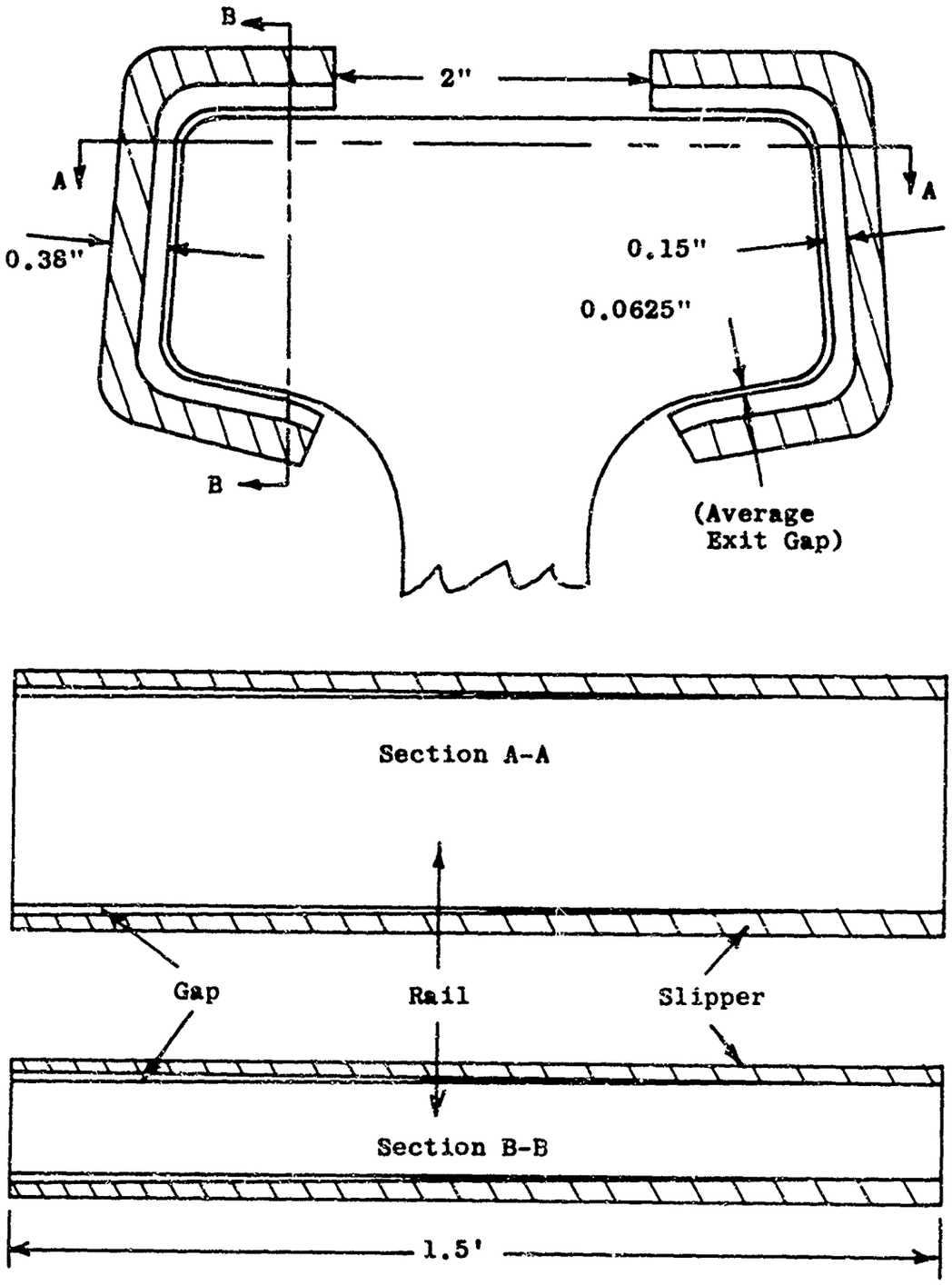

Figure 9. Monorail Self-Acting Slipper Bearing

The same slipper design can be used for the rear slipper, since the loading on the rear slipper is not as severe as on the front slipper. The rear slipper would operate with a larger gap than the forward slipper due to the lower loading.

3.5.2 Variation of the Minimum Slipper-Rail Gap During a Run

The variation of the minimum slipper-rail gap during a typical run is shown in Figure 10. Only the accelerating portion of the run is shown, since the decelerating portion would be quite similar. The data shown in the figure are for the front slipper with the load-velocity relation defined by Figure 2.

The results show that the minimum slipper-rail gap between the lower lip and the rail varies from 0.125 inches (the maximum value) at low speeds, down to 0.005 inches at Mach 6. The minimum slipper-rail gap between the upper slipper surface and rail is zero (bottomed out) until approximately Mach 1.5 and increases to 0.12 inches at Mach 6. The "bottomed out" portion is very dependent on velocity so that lowering the applied loading does not appreciably alter these results.

A similar analysis was performed for a comparable "full" slipper design in the low velocity range of the sled. As mentioned in Section 3.4.2, a full slipper would have better low speed performance than a partial slipper, due to the larger bearing area available on the upper surface. It was found that a 1.5 feet long full slipper would bottom out at approximately Mach 1.1, only 400 ft/sec lower than the partial slipper. Considering the large high speed advantage offered by the partial slipper, the additional velocity capability of the full slipper is not considered an advantage.

The results presented in this section were obtained by applying steady-state slipper performance to highly transient operating conditions. The validity of this approach is demonstrated in Appendix II.

3.5.3 Slipper Attachment Mechanism

The performance of the slipper during a typical run is strongly influenced by the gap slope. For the monorail sled, it was found that if the slipper was pin connected to the support mount, questionable static stability occurred. As shown in Appendix I, the center of pressure of the slipper bearing can vary over a large range, depending on the load imposed on the slipper. Due to the highly variable slipper loading, no stable configuration could be found for "off-design" operation.

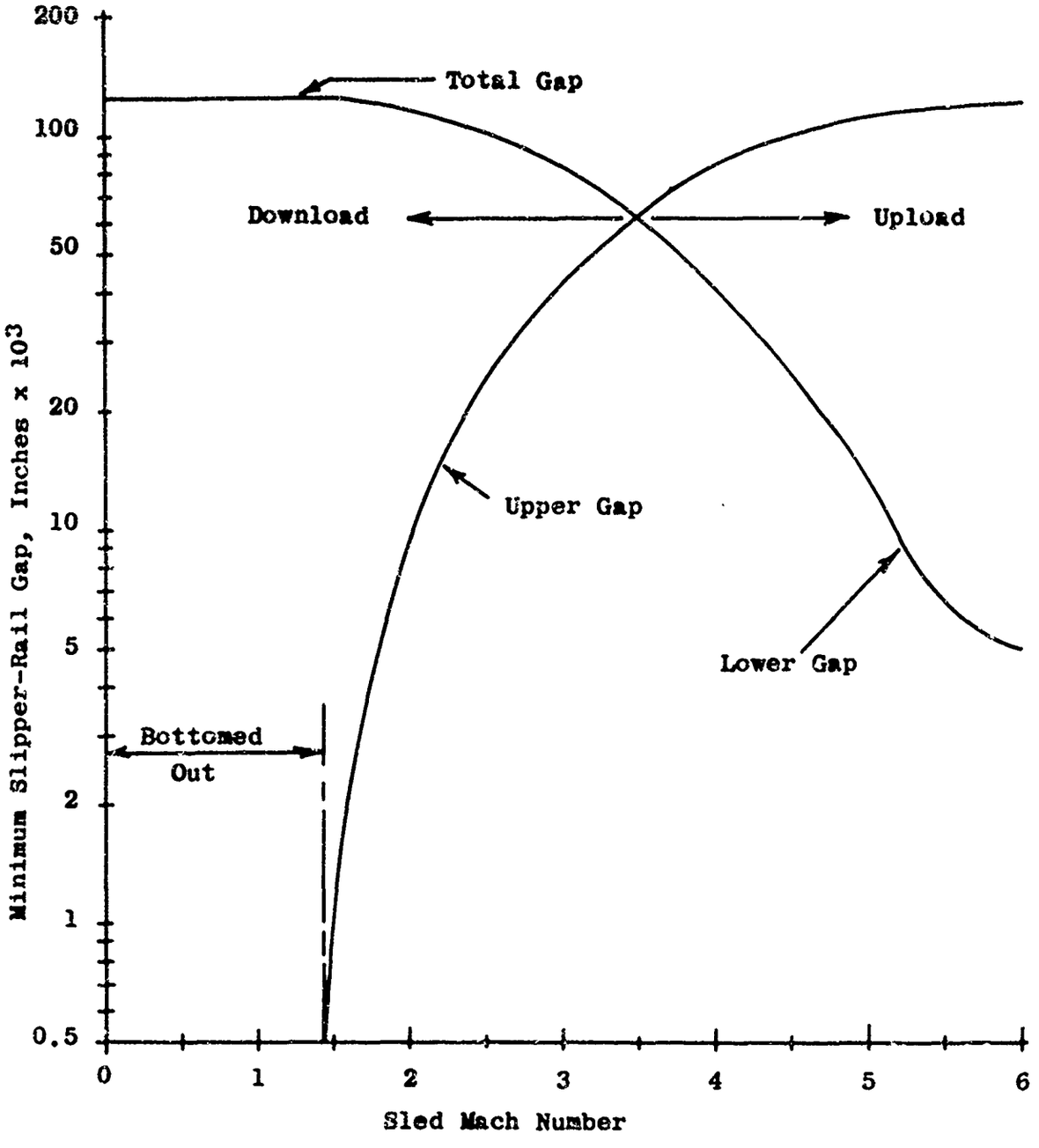

Figure 10. Variation of Minimum Slipper-Rail Gap During Monorail Sled Acceleration Run

This problem arises frequently in bearing operation. However, it does not prove to be a problem since the "pin point" can be placed at a variety of locations and the bearing continues to operate satisfactorily. For the slipper bearing, the load variations are very large and the results obtained in practice for conventional bearings may not be applicable.

The chief difference between conventional bearings and a rocket sled slipper bearing, which has a direct effect on this problem, is the magnitude of the gap slope. The slipper bearing has a gap slope an order of magnitude greater than conventional bearings. This permits a fixed slipper arrangement without sacrificing bearing performance. To illustrate this characteristic, Figure 11 shows the variation of slipper slope due to changes in sled loading. A typical slipper separation distance of 3.3 feet was chosen, corresponding to current monorail test sleds. As shown in the figure, the gap slope varies ± 0.003 during the monorail sled run. For this reason, the geometric slope of the interior slipper surface is 0.008, as shown in Figure 9, but the operating slope of the bearing gap is 0.005 during most of the run. Portions of the run where the slope of the bearing gap is not 0.005, and therefore not optimum, occur where the minimum slipper-rail gap is large. In these cases, the slope of the gap is not critical and does not seriously affect performance.

3.5.4 Lateral Load Capacity

The lateral load capacity of an air bearing slipper is determined by the same considerations as the vertical load capacity. For the slipper shown in Figure 9, the side surfaces of the slipper are shaped the same as the top and bottom surfaces. Under the action of a lateral force, the slipper will shift in the direction of the force until the side of the slipper develops sufficient force to react the load. When no lateral force is present, the slipper will center itself relative to the vertical axis of the rail, due to the equal forces generated by both sides of the slipper.

The method of calculating the lateral load capacity of the slipper is identical to the method used to calculate the vertical capacity. The results of the calculation are shown in Figure 12, where the lateral load capacity of the slipper is given as a function of Mach number and minimum slipper-rail gap. As shown in the figure, the lateral load capacity of the slipper is quite large.

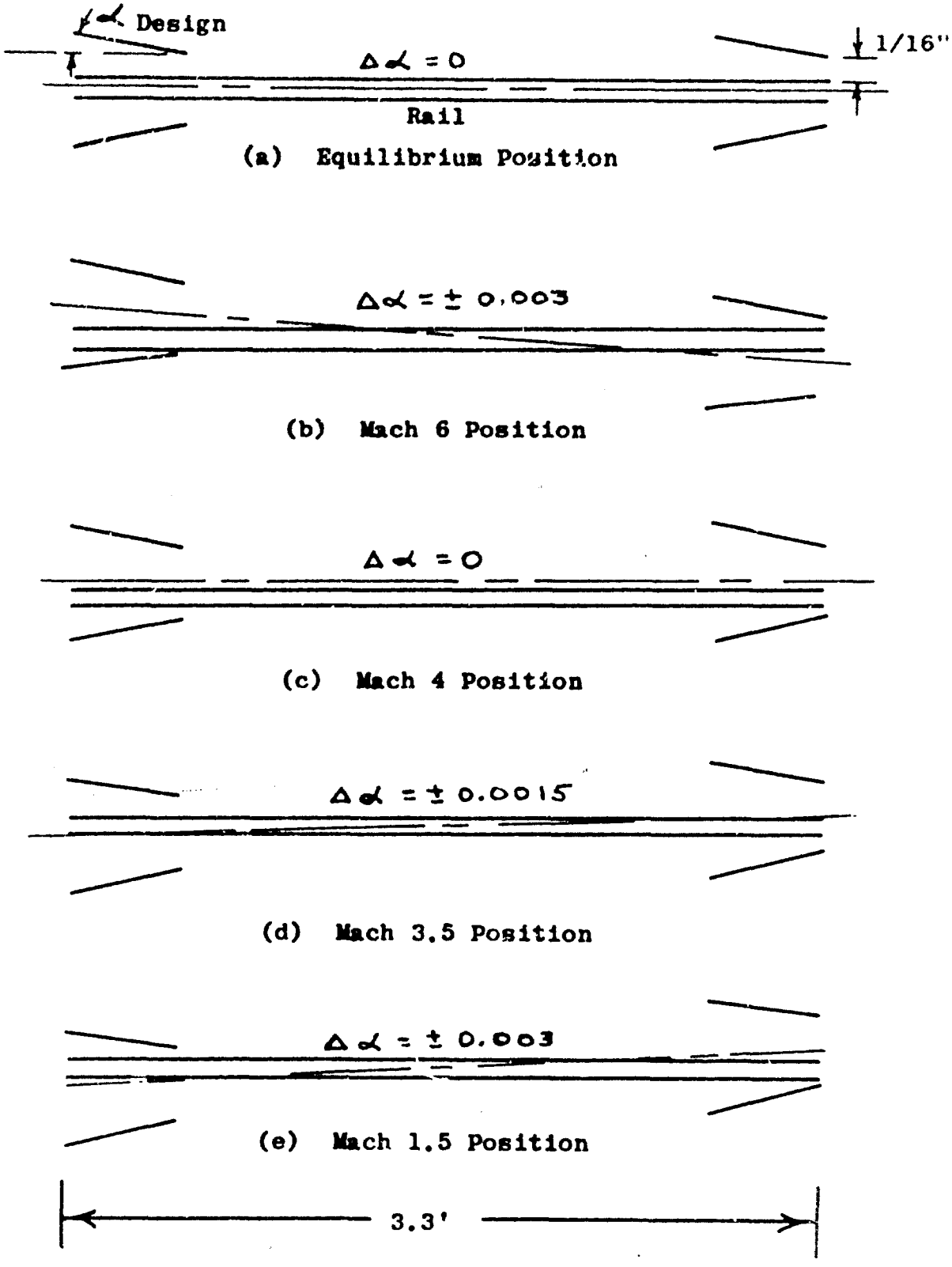

Figure 11. Effect of Sled Loading on Slipper Slope

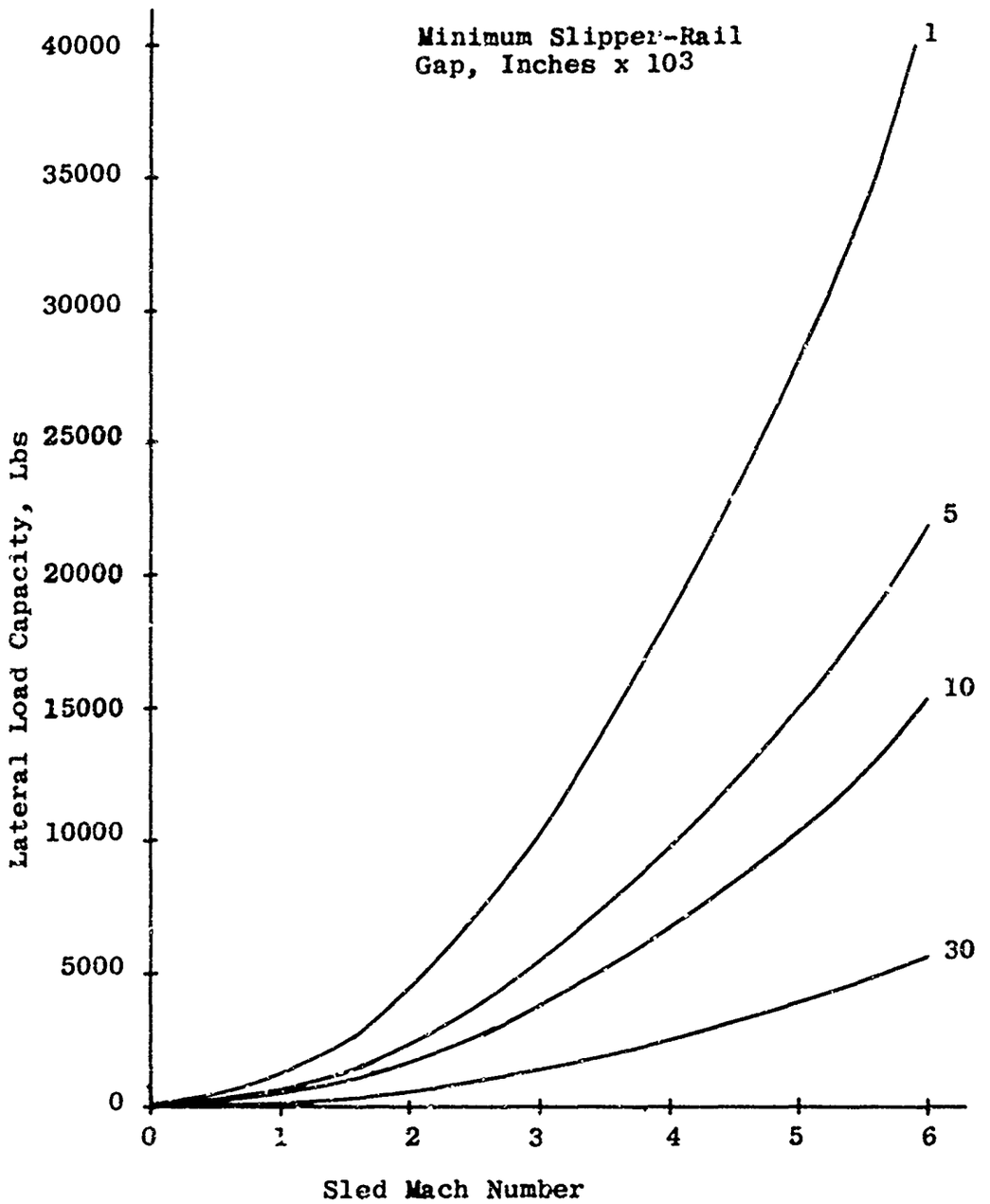

Figure 12. Lateral Load Capacity of Self-Acting Monorail Sled Slipper Bearing

3.5.5 Moment Capability

The moment capability of a monorail slipper bearing is limited by the inherent arrangement of the sled. Unless an outrigger system, which utilizes another slipper on the other rail of the track, is used, any rolling moments imposed on the slipper must be reacted by pure twisting of the slipper on the rail. The situation which occurs is shown in Figure 13, with the actual slipper-rail gaps exaggerated for illustrative purposes.

This illustration is for an upload condition where the smallest slipper-rail gaps occur between the lower lips of the slipper and the rail. Due to the applied load, the sum of the forces generated by the left and right hand lips must remain a constant. However, twisting of the slipper permits one side, in this case the left side, to develop more force than the right side. The differential loading produces a moment opposing the moment which originally caused the rotation.

Even under small rotations the gap varies by an appreciable amount over either of the lips. For the case shown in Figure 13, the minimum slipper-rail gap occurs at the extreme left side of the slipper lower left lip. The gap on the other end of the lip may be a few thousandths of an inch higher, but due to the sensitivity of load to gap dimensions, the "effective" or average gap will be significantly larger than the minimum gap.

To assess the moment capability of the monorail sled slipper, moments were calculated for various minimum slipper-rail gaps at selected sled speeds. The results are shown in Figure 14. The figure shows the moment capability of the slipper as a function of sled Mach number and minimum slipper-rail gap with the moments referenced to the point shown in Figure 13. The intersection of a line of constant minimum slipper-rail gap with the horizontal axis (no moment), yields the gap corresponding to Figure 10 at the same Mach number. For example, the 0.005 in. gap line intersects the horizontal axis at Mach 6. This is the operating gap at Mach 6 with no applied moment. If a moment is to be reacted at this condition, the minimum slipper-rail gap must decrease.

3.5.6 Slipper Drag

With sliding contact between the rail and slipper eliminated by the lubricating air film, the drag of a slipper bearing will be much lower than the drag of conventional slipper. However, there will be an increase in the aerodynamic drag of the slipper bearing compared to a standard slipper due to both increased viscous and pressure forces.

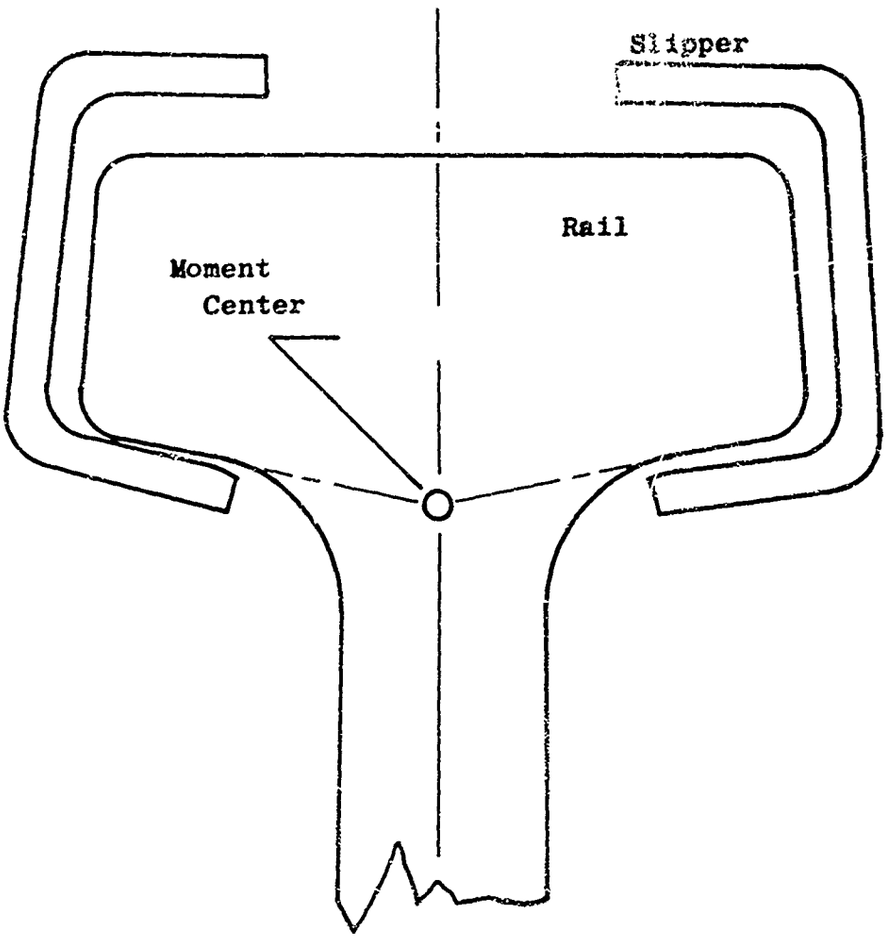

Figure 13. Monorail Sled Slipper Position When Reacting an Applied Rolling Moment

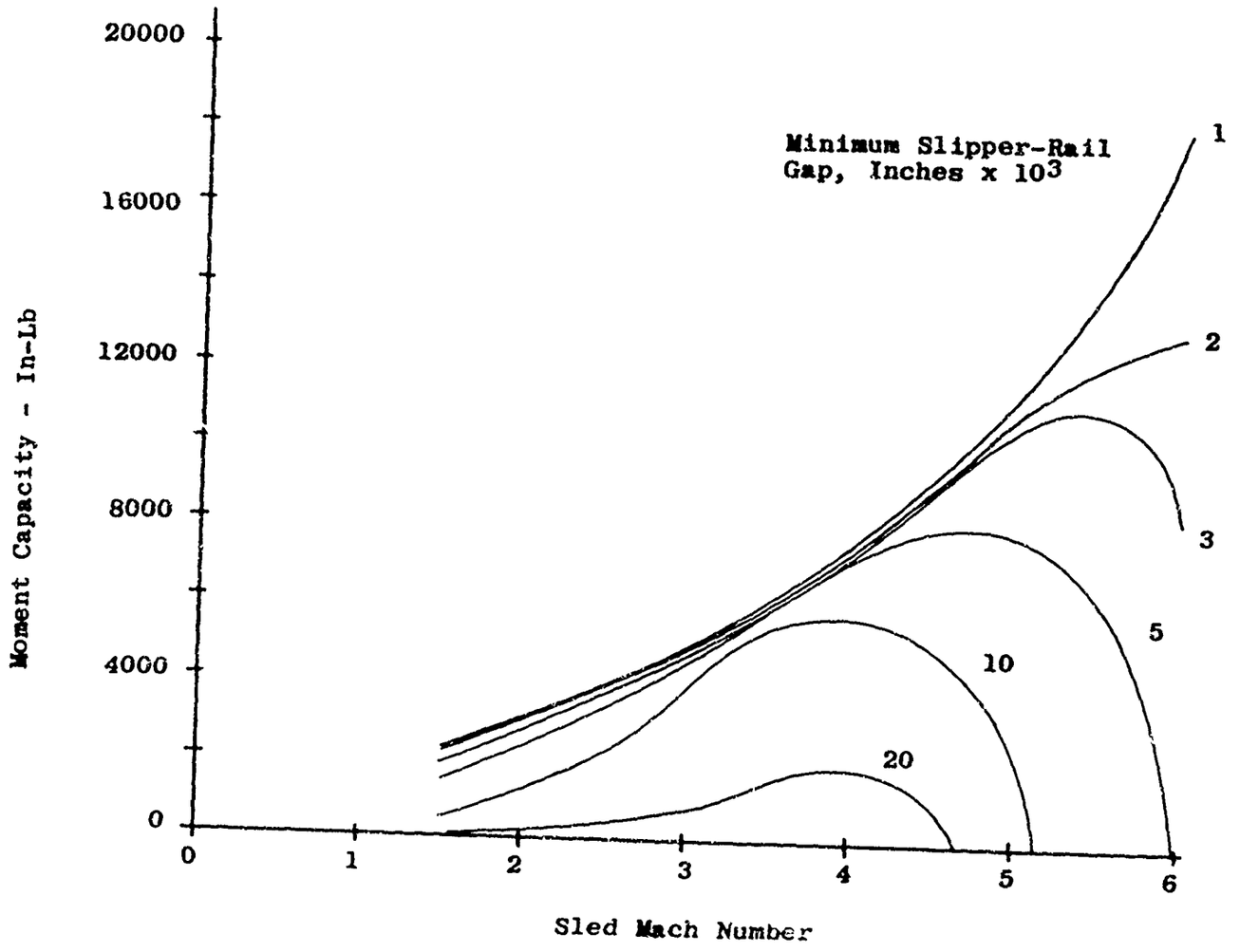

Figure 14. Monorail Self-Acting Slipper Bearing Moment Capacity

To determine the drag of a self-acting slipper bearing, the design shown in Figure 9 was analyzed during the acceleration phase of the monorail sled run specified in Figure 2. The slipper drag is a function of the loading and speed and therefore is dependent on the run profile. Only the front slipper drag was calculated, but the drag of the rear slipper would be similar, although lower. The results are presented in Figure 15 as a function of sled Mach number. The two curves shown in Figure 15 give the net increase in the aerodynamic drag of an air lubricated slipper over that of a standard slipper. The lower curve represents the net aerodynamic drag increase of the slipper shown in Figure 9. The upper curve gives the net drag increase for a slipper which has a constant thickness. The data are presented in this form to eliminate any dependence on slipper thickness.

A large portion of the aerodynamic drag increase is caused by the pressure within the slipper gap. Due to the relatively large gap slope (compared to a conventional bearing), the pressure within the gap exerts an axial (drag) force.

3.5.7 Effect of Wear On Slipper Performance

For a self-acting slipper bearing, the effect of surface wear on slipper performance may be negligible. The results of the studies given in previous sections indicate the preferred slipper design is one resembling the form shown in Figure 9, rigidly attached to the sled. If some wear of the slipper occurs due to occasional contact with the rail or if for operational purposes it is necessary to tow the sled at very low speeds, the rear section of the slipper will be the only portion suffering any damage. Removal of some of the slipper material will result in an interior gap shape similar to the taper-flat slipper bearing shown in Figure 4(b). Unless a large amount of slipper material is removed, the length of the slipper will not change. Since the taper-flat bearing does not have a significantly different load capacity than the plane tapered bearing (it may be higher or lower depending on the slope and relative proportions of the taper and flat sections), the slipper will operate at approximately the same minimum slipper-rail gap at a given sled speed and load.

The entire question of the effect of surface wear may be obviated when additions to the slipper required for operational purposes are made. These are discussed more fully in Section 7.1.

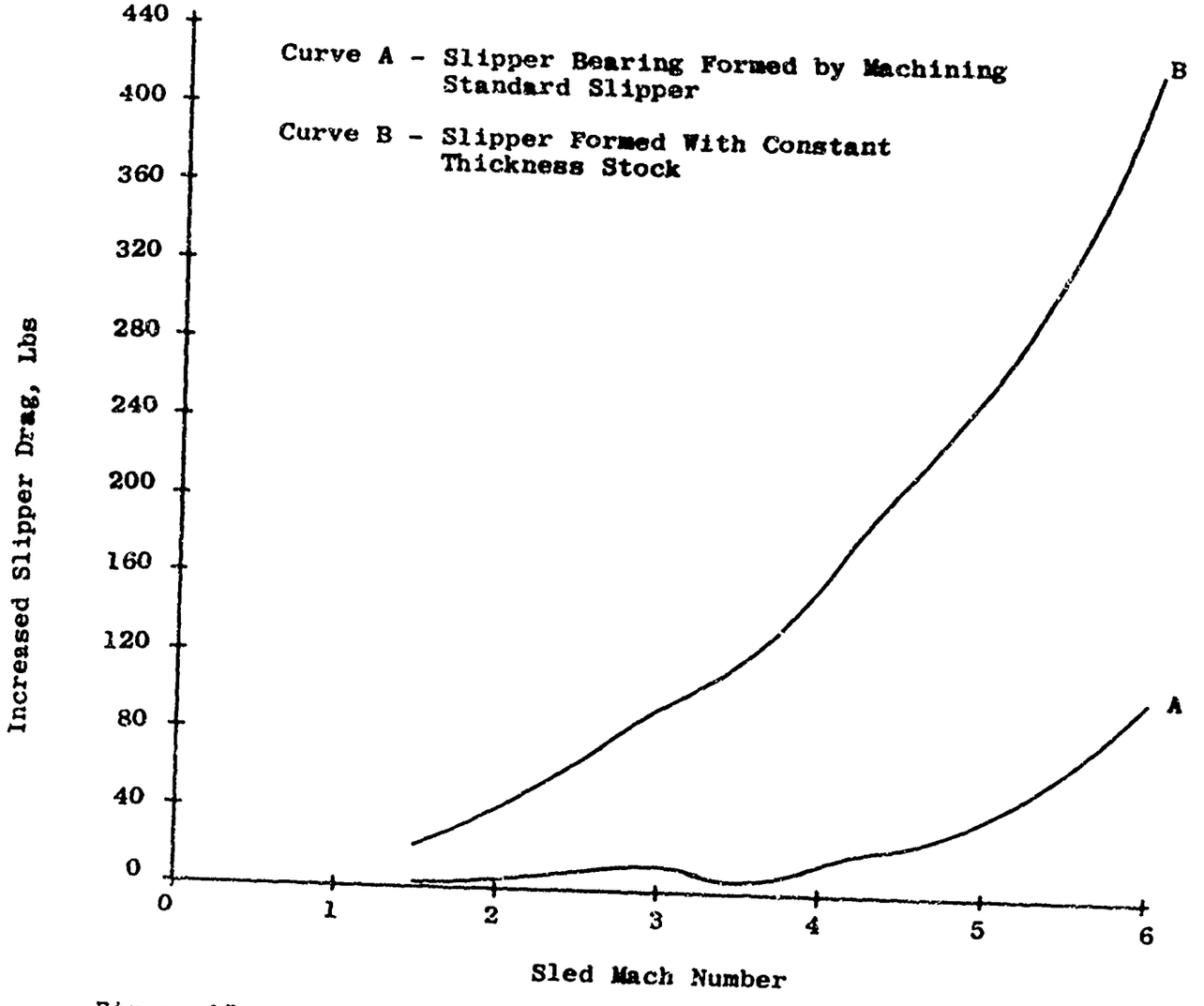

Figure 15. Net Increase in Slipper Aerodynamic Drag Over Standard Slipper

3.6 Dual Rail Sled Self-Acting Slipper Bearing

An analysis similar to that conducted for the monorail sled was attempted for the dual rail sled requirements given in Figure 3. However, due to the combination of low speeds (less than Mach 2) and high slipper loads, the required slipper lengths and minimum slipper-rail gaps were deemed not feasible for any portion of the run. To satisfy low speed requirements, dual rail slipper loads would have to be reduced to values less than that of the monorail sled.

The main reason for this result lies in the levels of available inlet pressure for a self-acting bearing. Under ideal conditions, where the free stream air could be isentropically diffused before entering the slipper gap, it might be possible to satisfy very low loads at speeds greater than Mach 1. However at lower speeds, the slipper bearing load capacity for reasonable slipper lengths and gaps can be best classified as negligible. These results clearly indicate the need for externally pressurized slipper bearings for low speed operation, especially for typical dual rail sled requirements.

The use of a sophisticated inlet system to efficiently diffuse the ram air before introducing it into the slipper gap appears to offer no advantages. As mentioned above, such a system does not significantly improve the feasibility of the slipper bearing at low speed. At high speeds it is unnecessary.

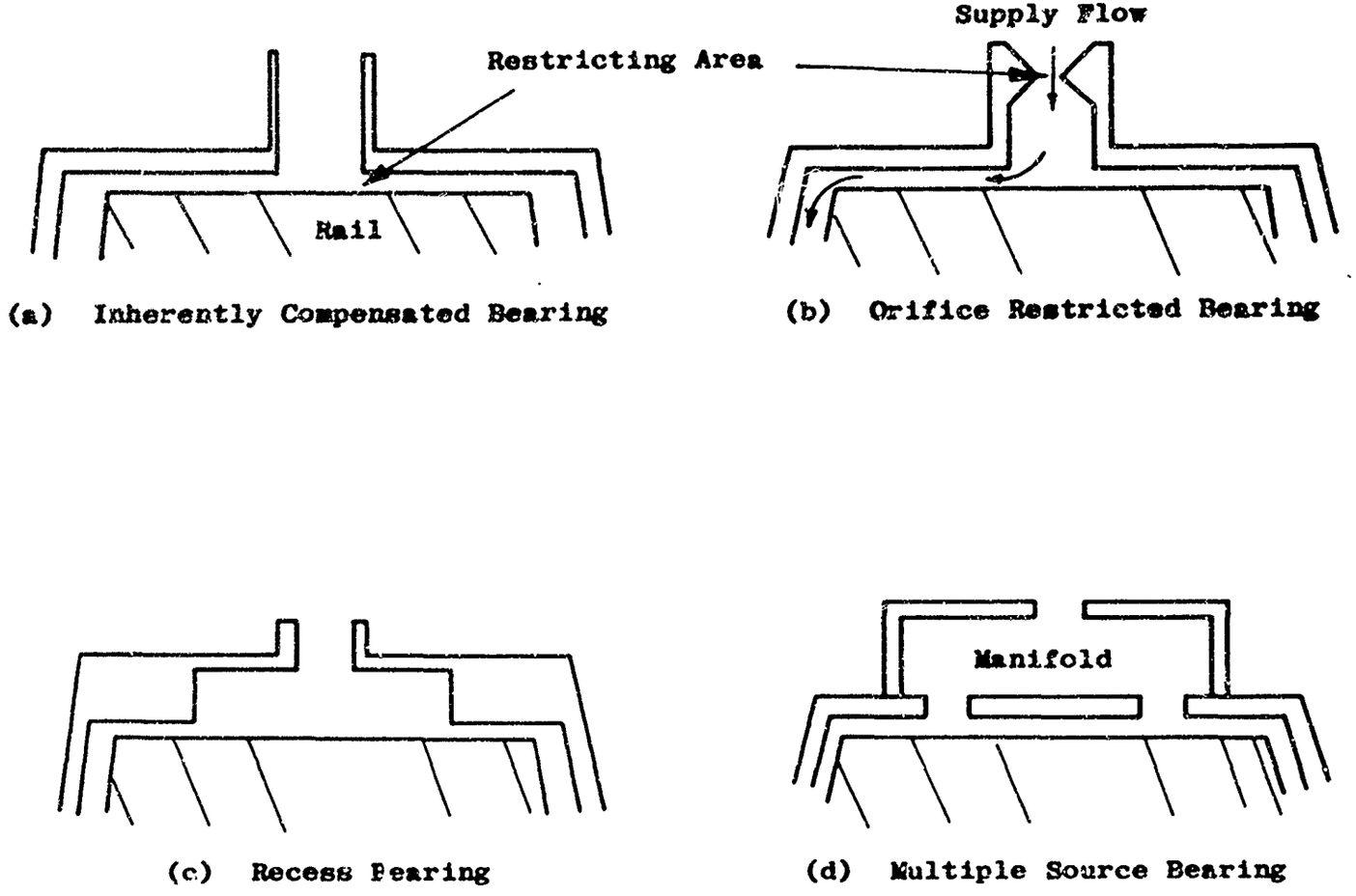

(a) Inherently Compensated Bearing

(b) Orifice Restricted Bearing

(c) Recess Bearing

(d) Multiple Source Bearing

Figure 16. Types of Externally Pressurized Air Bearings

SECTION IV

EXTERNALLY PRESSURIZED SLIPPER BEARINGS

4.1 General Considerations

The results of the studies on self-acting slipper bearings indicate that an externally pressurized slipper is required for a typical monorail sled below Mach 1.5, and over the entire speed range of a typical dual rail sled, if all contact with the rail is to be avoided. Since the support equipment weight and volume of an externally pressurized slipper are the most important considerations of the system, the primary effort of this phase of the study was directed at determining their penalties.

Compared to self-acting bearings, externally pressurized bearings require considerably greater effort to evolve workable systems. The flow within the bearing gap is complicated, and when coupled to a supply system, the overall analysis of the bearing must utilize many assumptions and approximations. Some of the inherent problems of externally pressurized bearings and those peculiar to a rocket sled application are discussed in the following sections. For a comprehensive discussion of these bearings, including the available analyses, the reader is referred to Reference (2).

4.1.1 Bearing Geometry

As in the case of self-acting slipper bearings, many types of externally pressurized bearings can be considered for use on the Holloman Test Track. A common characteristic of many externally pressurized bearings is that they usually incorporate some type of flow restriction mechanism to limit the amount of flow that the bearing will pass. This is necessary to prevent a large flow consumption when the bearing is unloaded or, as in the case of a slipper bearing, the load is reversed.

The major categories of externally pressurized bearings consist of the inherently compensated bearing and the orifice or capillary restricted bearing. The primary difference between these major types is the nature of the flow controlling area. For the former bearing, the controlling area is the inlet to the gap, as shown in Figure 16(a), and for the latter, it is an external device, such as an orifice, as shown in Figure 16(b). Various bearing surface configurations are

applicable, depending on the bearing characteristics required. Two configurations which are used often are shown in Figures 16(c) and 16(d). The type shown in Figure 16(c) has a recess near the inlet source and the scheme shown in Figure 16(d) is an example of a bearing with multiple sources. Each of the types shown in Figure 16 has advantages and disadvantages. The recess type (Figure 16(c)) tends to have a higher load capacity than the others, but due to the compressibility of the air in the recess, this type is more prone to instabilities. Also, the larger the recess, the less area with a small gap is available for developing squeeze film damping, a characteristic which is important when considering the reaction of a bearing to varying loads. A more complete discussion of various types and configurations of externally pressurized bearings may be found in Reference (2).

Since the primary purpose of this phase of the study was to determine the weight and volume penalties of an externally pressurized bearing for a rocket sled application, a typical configuration was chosen for analysis. This design is the one shown in Figure 16(b). The slipper is actually composed of five separate bearings, one for each rail surface. A load in any direction is reacted by the bearing(s) normal to the load direction. Air is supplied to manifolds, which act as reservoirs, flows through the restricting orifice into the small recess formed by the supply tube, and then enters the bearing gap. The air leaving the gap then flows into adjoining gaps and out the bottom and ends of the bearing. Again, the purpose of the orifices is to restrict the flow of the bearings which are not producing a load, thereby minimizing the total flow requirements.

4.1.2 Effect of Linear Motion on Externally Pressurized Bearings

One of the most complicating factors involved in the design of an externally pressurized slipper bearing is the effect of linear motion. At rest, the bearing would operate as described above. Except for leakage at the ends of the slipper, the flow would follow the path shown in Figure 16(b). With linear motion normal to the rail cross-section, the air entering the bearing will be swept downstream. If one source at the front of the slipper is supplying air to the slipper gap, the axial pressure profile within the slipper gap would be very similar to the profile shown in Figure 7 for the self-acting slipper bearing. In this case, the inlet pressure would be the supply

pressure. This pressure profile would occur only near the lateral position of the source, since the air pressure level at lateral stations further away would be lower.

The conflicting design features of slipper bearings operating at rest and at high speeds are schematically shown in Figure 17. At rest, a typical design would resemble Figure 17(a). The supply line would feed a manifold and the air would flow into the slipper-rail gap through an axial slot in the bearing surface. At high speed, a typical design would take advantage of the self-action of the bearing by forming a wedge-shaped gap, as in Figure 17(b). Air would be injected into the gap at the front of the slipper through a lateral slot across the face of the bearing.

Although compromises incorporating features of both systems are possible, the two schemes shown in Figure 17 are basically incompatible. First, to form a wedge-shaped gap, a mechanism to tilt the slipper as linear speed increases is necessary. If a wedge-shaped gap is built in, the flow requirements at rest will be quite high due to the relatively large gap at the front of the slipper. Second, at high speed the self-action of the bearing will produce pressures near the end of the slipper much higher than those near the front. If air is supplied to all sections of the slipper from a common source, the higher pressure at the rear of the slipper will cause the supply slot to act as a bleed. This will reduce any performance benefits due to bearing self-action. Finally, to conserve the air supply the rear sections of the slipper should be sealed when operating at high speed, since this air would not be necessary for operation. The last two problems can be solved by providing individual ports, rather than an axial slot, along the slipper. Each port may be valved off at the proper speed. However, this approach involves a complicated valve and control mechanism, which would have varying design requirements depending on sled velocity and loading.

4.1.3 Effect of Inlet and Exit Pressures

The effects of the external flow field pressure on the performance of an externally pressurized slipper bearing are much smaller than in the case of the self-acting slipper bearing. With the air in the slipper gap supplied from an external source, the major effect of the pressure at the front of the slipper is to alter the flow pattern in the immediate

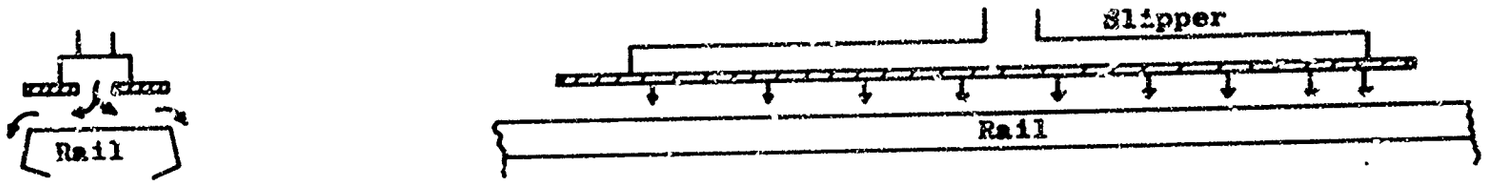

(a) Preferred Arrangement at Rest

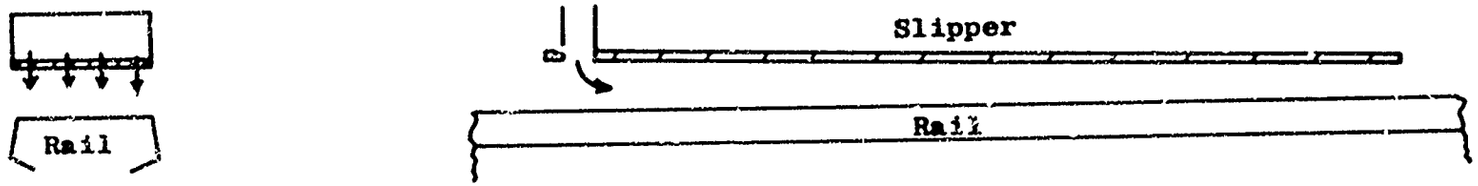

(b) Preferred Arrangement at High Speed

Figure 17. Preferred Design Features for Externally Pressurized Slippers

vicinity of the slipper leading edge. A high exterior pressure will reduce the leakage from the front of the slipper, thus reducing the on-board air supply requirements. Hence, no flow deflector should be used. For dual rail sleds, this presents no handicap since low maximum speeds of dual rail sleds do not impose use of such devices.

The exterior pressure at the rear of the slipper has only a small effect on the performance of an externally pressurized slipper bearing. Since this type of slipper bearing operates as a self-acting bearing at high speeds, the effect of the exit pressure is essentially the same, and therefore small.

4.1.4 Flow Within the Gap and Shock Formation

Although high speed operation of an externally pressurized slipper bearing would resemble a comparable self-acting bearing, static or low speed operation of this type of bearing is quite different. For externally pressurized bearings with small operating gaps and low supply pressures, the air will flow from the supply line into the gap at essentially constant pressure. Upon entering the gap, the pressure will drop off rapidly, due to the expansion, and then gradually decrease to the ambient pressure as it flows through the gap from the inlet to the exit. At the inlet to the gap, the air viscosity does not appreciably affect the flow, because the boundary layers on the surfaces have not built up yet. Further into the gap these forces play an increasingly important role, until finally they completely dominate the flow.

If the supply pressure is high, the expansion will be accompanied by an oblique shock system located in the region denoted by "restricting area" in Figure 16(a). Often, a normal shock will be present. In some cases frictional choking will occur in the gap, and if the gap is large enough, the Bernoulli effect will cause an attractive, rather than a repulsive, force between the two surfaces.

4.2 Bearing Analysis

The slipper bearing configuration chosen for analysis is shown in Figure 18. For the purpose of the study, the bearing layout was assumed to correspond to Figure 17(a) with no provision for either tilting the slipper or valving off flow to the rear section of the slipper as sled speed increases.

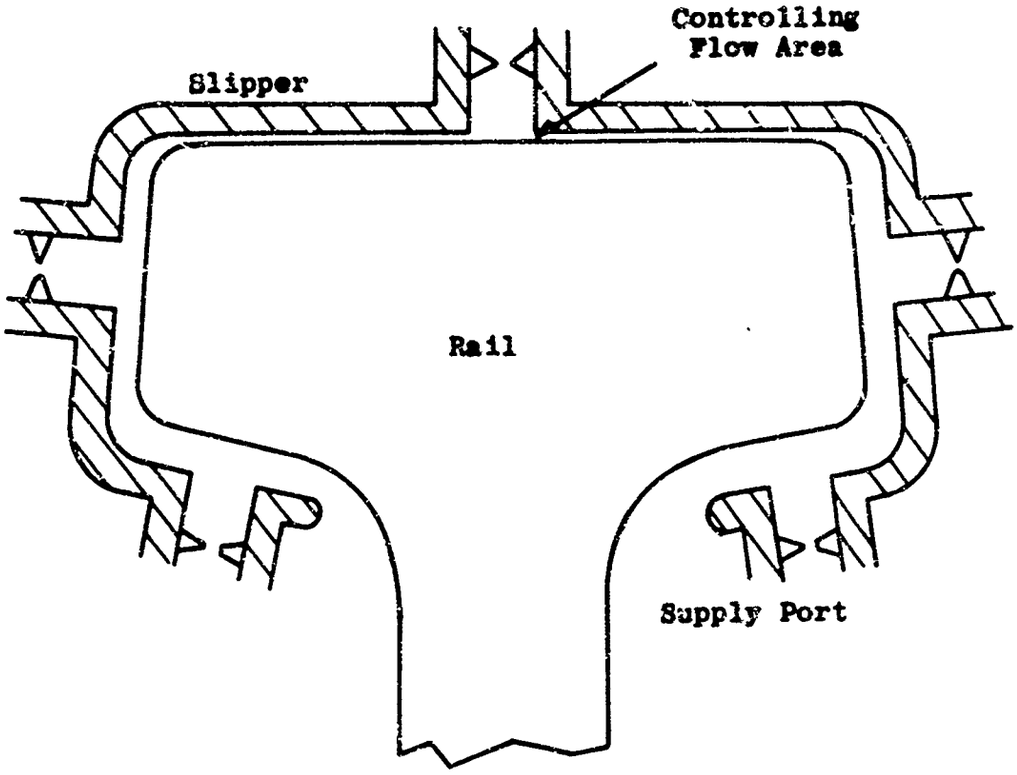

Figure 18. Externally Pressurized Slipper Bearing Design

The basic bearing analysis was taken directly from Reference (2). This analysis does not include the effect of relative surface motion but, as shown later, the basic conclusions reached in this study do not require a solution to this problem. In the analysis, the flow in the gap is assumed isothermal and laminar. Although the former assumption is reasonable, some of the cases involving large slipper-rail gaps would require a turbulent film analysis. However, the results obtained using the laminar assumption have sufficient accuracy to determine the penalties associated with externally pressurized slipper bearing.

4.3 Factors Affecting Externally Pressurized Slipper Bearing Design

4.3.1 Pressurization Requirements

The reason the laminar analysis mentioned above is sufficient to determine the support system penalties involves a consideration peculiar to a rocket sled application. Since the slipper must react loads in all directions normal to the rail surface, air must be supplied to all five surfaces of the slipper. In Figure 18, the slipper is shown in the position it would assume when at rest. The upper surface of the slipper and rail act as the bearing with a small clearance between the two surfaces. As shown in the figure, the controlling flow area is the inlet to the gap. Once the slipper-rail gap is selected, the orifice area is made only slightly larger than the gap inlet area, to limit the flow when the surface is unloaded and the gap increases.

During a typical sled run, slipper loading is highly transient. If flow is not constantly supplied to all sides of the slipper bearing, a complex sensing system, coupled with a valving mechanism, would be needed to supply air to the surface required to react the applied load. The sensing system would be required to detect a change in loading (probably by measuring changes in slipper-rail gap), open the supply valve to the appropriate surface, and close the supply valve to the surface becoming unloaded. Even if such a sensing and valve system were practical, the inherent pneumatic lag of the supply system would probably limit the allowable loading variation to very low levels.

For this reason, all sides of the slipper should be pressurized during the entire run. Since the flow through the load-reacting side of the bearing is a small portion of the total flow, departures from laminar flow in the gap do not seriously affect the support system requirements calculated using this assumption.

4.3.2 Effect of the Average Slipper-Rail Gap

Due to the orifice in the supply line, the effect of the average slipper-rail gap on overall bearing performance is small. If the average slipper-rail gap is very small (less than 0.005 inches), all sides of the slipper would develop appreciable loads and little net loading capacity would exist. This situation is similar to the case of the self-acting slipper bearing. However, due to the orifice, if the gap increases to a value only slightly larger than the design value, the flow is limited and the pressure in the gap drops off sharply. Thus, if the gap is over an order of magnitude larger than the design gap (0.005 - 0.001 inches), the load developed is negligible. Therefore, the present average slipper-rail gap of 1/16 of an inch can be retained for the externally pressurized slipper bearing, and a larger value is allowable.

4.4 Dual Rail Sled Externally Pressurized Slipper Bearing

4.4.1 Typical Slipper Bearing Design

The requirements of an externally pressurized slipper bearing for the dual rail sled loading given in Figure 3, are shown in Figure 19. This slipper is designed for the load requirements at the beginning of the run and is given here to illustrate the minimum penalties associated with externally pressurized slipper bearings. The schematics shown in Figure 19 are for a bottle fed system, where the air is stored in tanks at 60 degrees F, and for a compressor fed system, where the air is supplied at the compressor exit temperature. The compressor efficiency was assumed at 100 percent for simplicity.

For these requirements, the slipper-rail gap was selected at 0.002 inches and the slipper length was set at 15 inches. Increasing the slipper length would lower the pressure requirements but increase the flow requirements. As shown in the figure, air from a supply line at approximately 100 psia flows

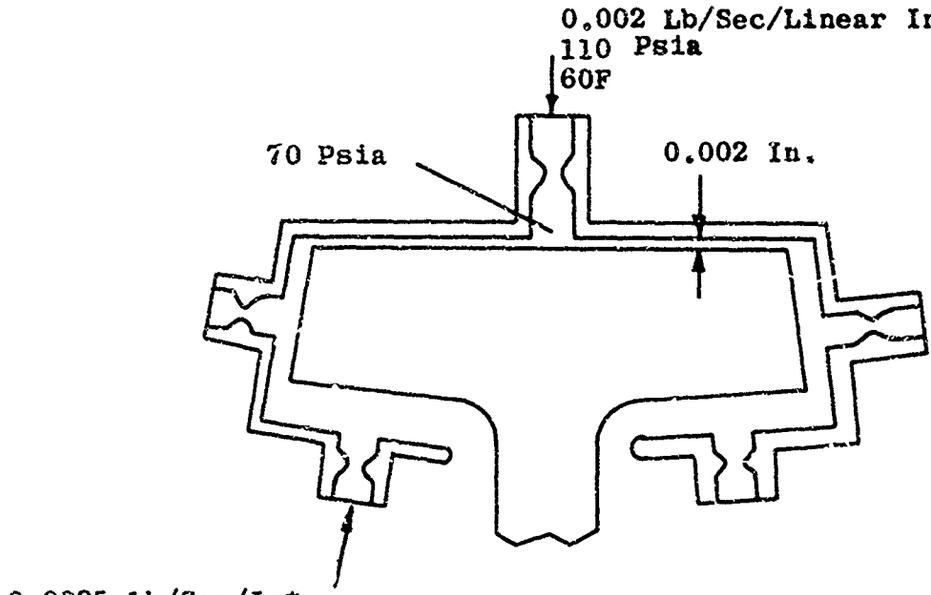

(a) Bottle Fed Bearing

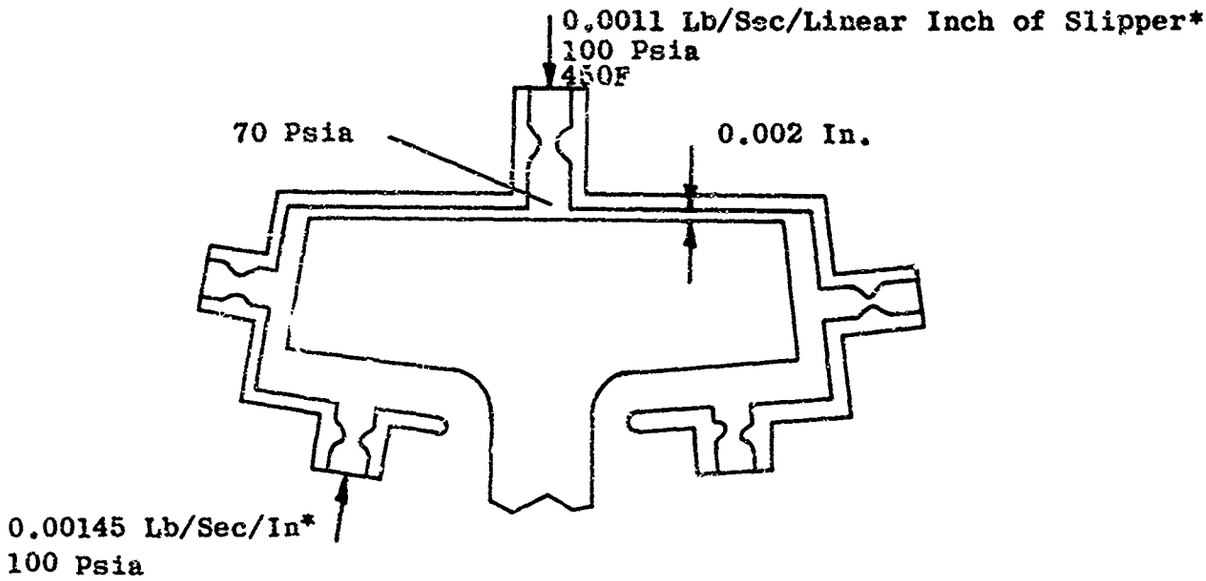

(b) Compressor Fed System

*Flow at Center of Slipper. Flow at Ends Higher Due to Leakage

Figure 19. Dual Rail Sled Externally Pressurized Slipper Requirements

through the orifice in the top surface and is throttled to 70 psia before entering the gap. The flow leaving the gap mixes with the flow coming from the sides and bottom surfaces and exits to the atmosphere. The pressure in the side and bottom gaps is very close to ambient (12.7 psia for the Holloman Test Track) due to the low flow rate and large gaps relative to the upper surface gap.

4.4.2 Effect of the Supply Pressure

A trade-off exists between the supply pressure and total bearing flow which are inversely proportional. The trade-off is obtained by first establishing the gap inlet pressure, in this case 70 psia, to satisfy the load requirement. This pressure then determines the flow rate in the gap. Once the flow rate is established, various supply pressures may be selected, and with each supply pressure the size of the orifice is determined. Assuming the same orifice size for each side of the bearing then determines the total bearing flow. For the slipper conditions shown in Figure 19, the trade between supply pressure and total flow rate is shown in Figure 20. To assess the trade between pressure and flow rate, the total tank volume per minute of operation and the compressor power are plotted in Figure 21 as functions of supply pressure.

These data show that the optimum supply pressure for the compressor fed system is approximately 100 psia and for the bottle fed system, a supply pressure over 110 psia does not result in a significant volume saving. This result (supply pressure/gap inlet pressure = 1.5) was found to be approximately optimum for the other cases investigated and was used throughout the remaining studies to size the orifice.

4.4.3 Effect of the Slipper-Rail Gap

Following the same procedure used to calculate the slipper pressure and flow requirements for a gap of 0.002 inches, a number of cases for different slipper-rail gaps were calculated and the total weight and volume penalties at each gap were established. The results are shown in Figure 22 where the weight and volume of a tank storage system are shown as functions of the slipper-rail gap. These results are for the slipper designed for the dual rail sled at the beginning of the sled run, with a 60-second operating time as specified in Reference (1).

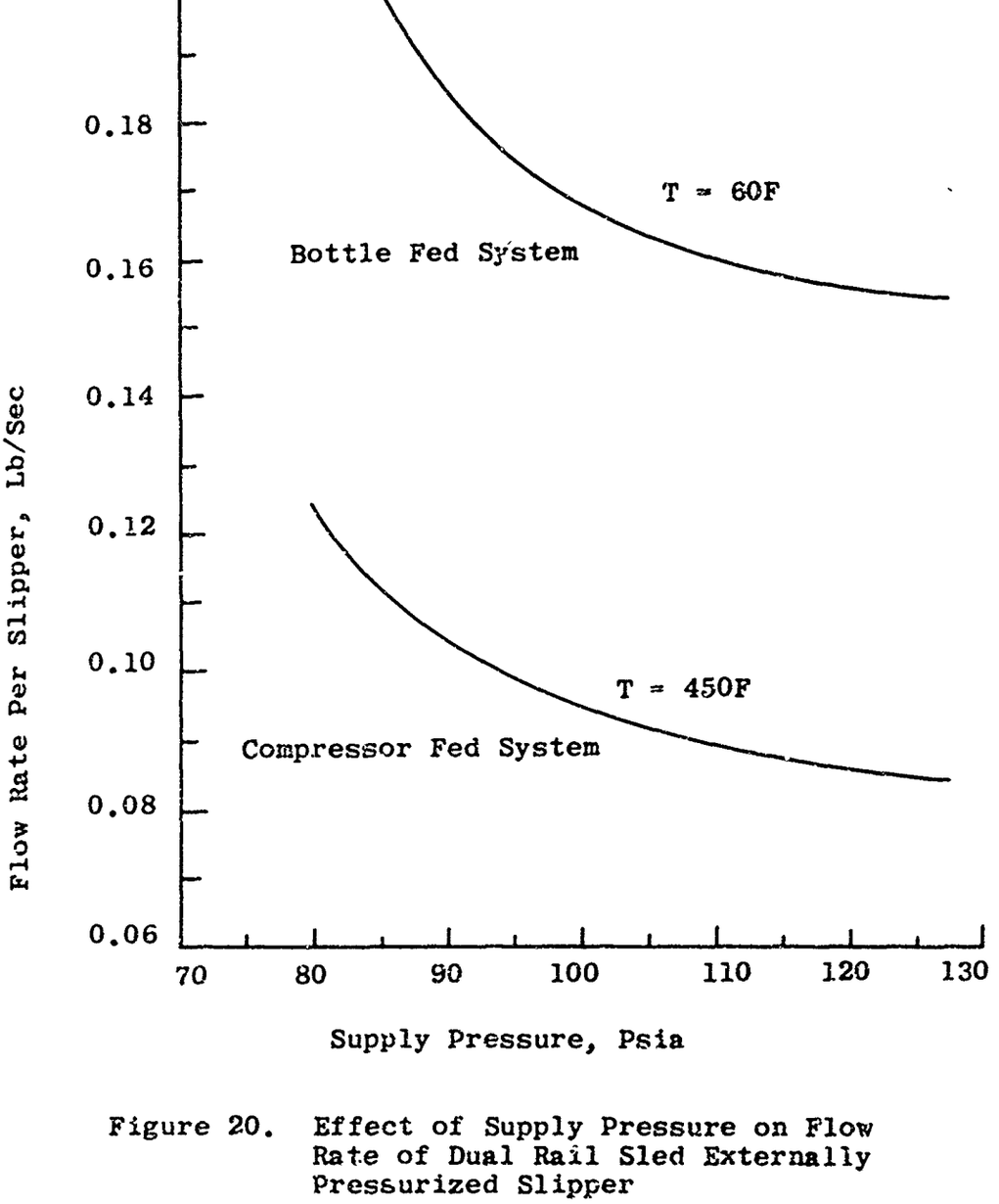

Figure 20. Effect of Supply Pressure on Flow Rate of Dual Rail Sled Externally Pressurized Slipper

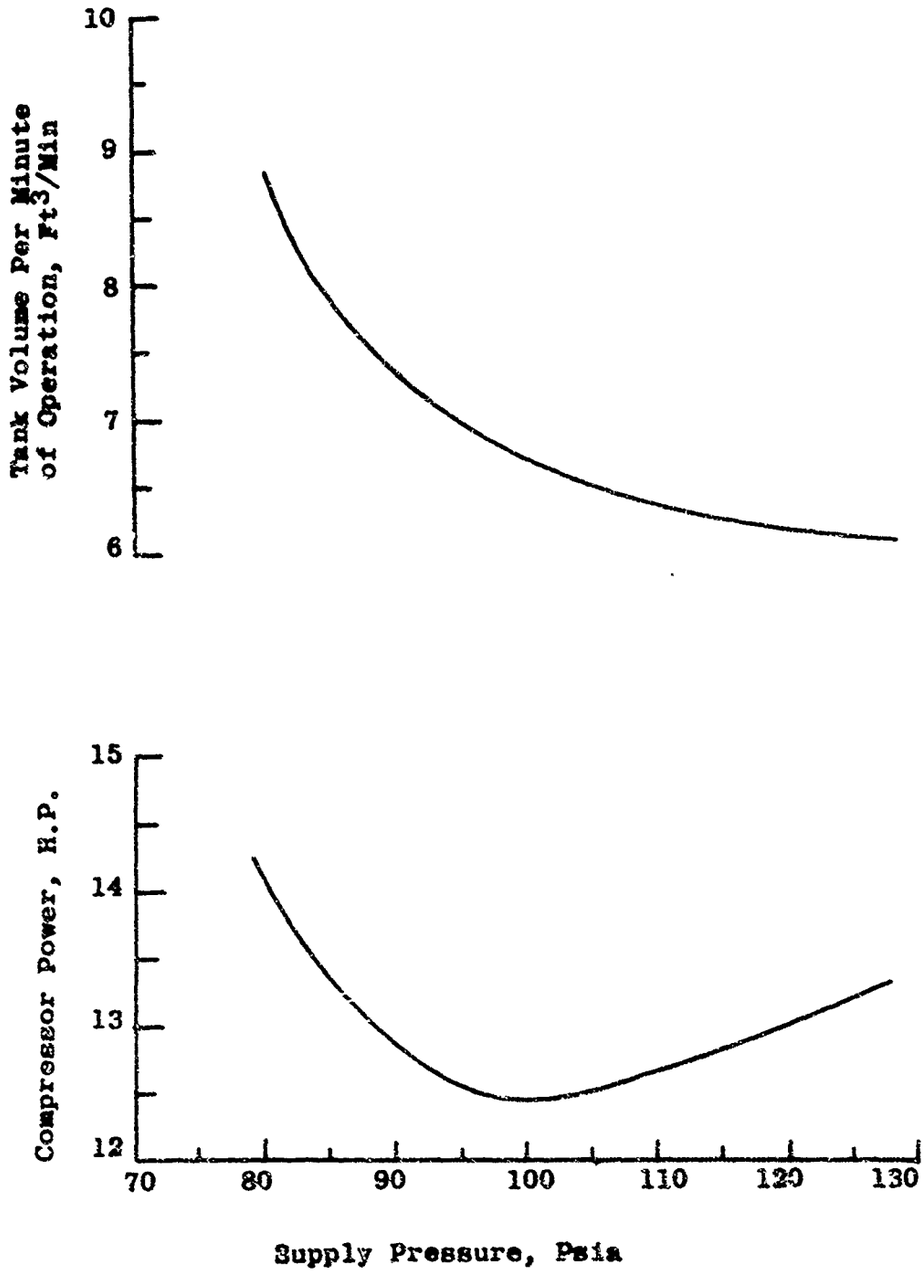

Figure 21. Tank Volume and Compressor Power For Dual Rail Sled Externally Pressurized Slipper

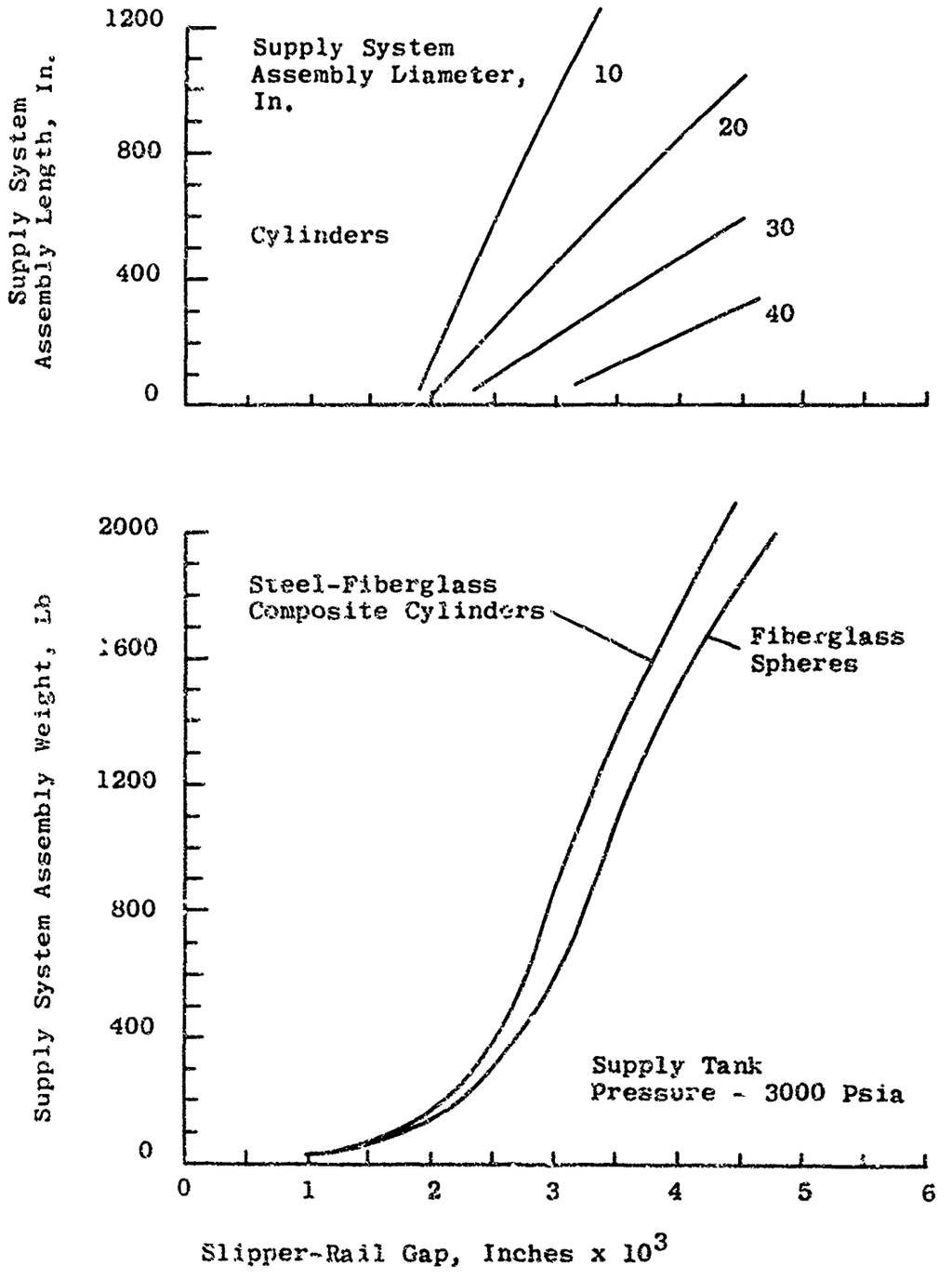

Figure 22. Effect of Slipper-Rail Gap on Dual Rail Sled Externally Pressurized Slipper Penalties

The data shown in Figure 22 indicate that the support system weight and volume increase drastically with slipper-rail gap. If a gap comparable to the self-acting minimum slipper-rail gap is required (0.005 inches), the penalty is enormous.

The weight and volumes shown in Figure 22 were obtained using the data available on aircraft high pressure air cylinders and spheres conforming to military specifications (without gunfire requirements which dictate wire wound vessels). These data represent the lightest available vessels and were obtained from literature on Walter Kidde and Company equipment. Unfortunately, no existing compressors could be found with both the pressure and flow rate ranges required by the slippers. However, rough estimates of suitable compressors, extrapolated from existing hardware, indicated compressor fed systems would have much higher weight penalties than bottle fed systems. The primary reason for this is the relatively short (60 second) operating time required. The fixed weight of the compressor is unsuited to this short an operating time.

4.4.4 High Speed Slipper Design

The slipper requirements for the dual rail sled were investigated at the maximum load condition specified in Figure 3, with the same analysis and weight data used for the cases discussed above. For this case, a slipper-rail gap of 0.002 inches and a slipper length of three feet were selected. However, due to the very high upload and relatively low download requirements of the slipper, two different supply pressures were selected. To satisfy the maximum load condition (upload), a supply pressure of 1200 psia was found necessary for the lower lips of the slipper. However, a supply pressure of 105 psia was found adequate for the upper surface, and the same pressure was used for the sides of the slipper.

The weight and volume penalties for this slipper system are shown in Figure 23 as functions of operating time. If a full 60-second operating time is required, the weight and volume of the support system are quite large. However, a significant weight saving can be realized if the portion of the run experiencing loading in only one direction is known. For the dual rail sled loading specified in Figure 3, it appears that after the initial eight seconds of the run, the slippers are subjected only to downloads. If this is the case, the weight penalty for the slipper design discussed above could be reduced to approxi-

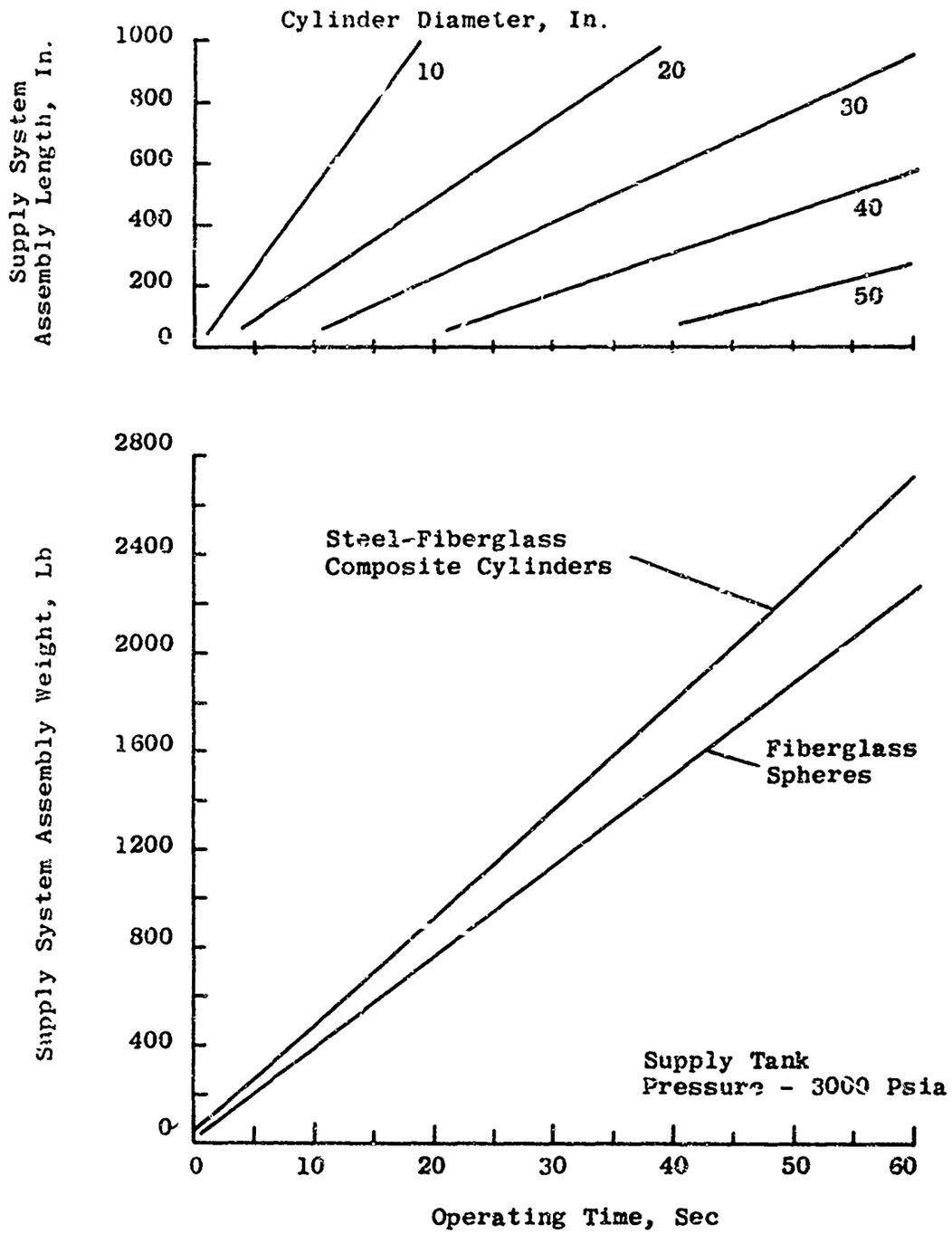

Figure 23. Weight and Volume Penalties of Dual Rail Sled Externally Pressurized Slipper

mately 500 pounds and the tankage volume would be equivalent to a 2½-feet diameter sphere. The 1200 psia tank supplying the lower lips of the slipper would be designed for about eight seconds of operation. At the end of this time the tank would be empty. However, this approach would not allow for incidental load and moment capability or unusual loading conditions at the end of the run, such as during a water braking operation.

To significantly reduce the weight and volume penalties of an externally pressurized slipper, large reductions in slipper loads are required. Although this may be possible at high speeds by aerodynamic load control, low speed loading, which is due to inherent sled design features, would still be high and the support system penalties would remain large.

4.4.5 Lateral Load Capacity

The lateral load capability of the dual rail sled slipper discussed in the previous section depends on the pressure level of its supply. In the absence of any specific requirements, this supply pressure was set at 105 psia, the same level required for the upper surface.

The lateral load capacity of each of the dual rail sled slippers is shown in Figure 24 as a function of sled velocity and the gap between the side of the slipper and the rail. This figure shows the lateral load capacity is constant up to Mach 1 and then drops off as the sled velocity increases. The principal reason for this characteristic involves the opposing force developed by the opposite side of the slipper. At speeds less than Mach 1, it was assumed that the air entering the gap between the opposite side of the slipper and the rail was essentially at ambient pressure. However, above Mach 1, the normal shock standing in front of the slipper lip will produce gap inlet static pressures higher than ambient. At these speeds, the pressure profile within this gap will be similar to that shown in Figure 7, and an appreciable opposing load will be developed. This opposing load will increase with velocity until it reduces the net load capacity to very low values.

4.4.6 Moment Capability

The moment capability of the dual rail sled is related to the allowable minimum slipper-rail gap. At a given sled speed, the slipper will operate with the slipper-rail gap required to

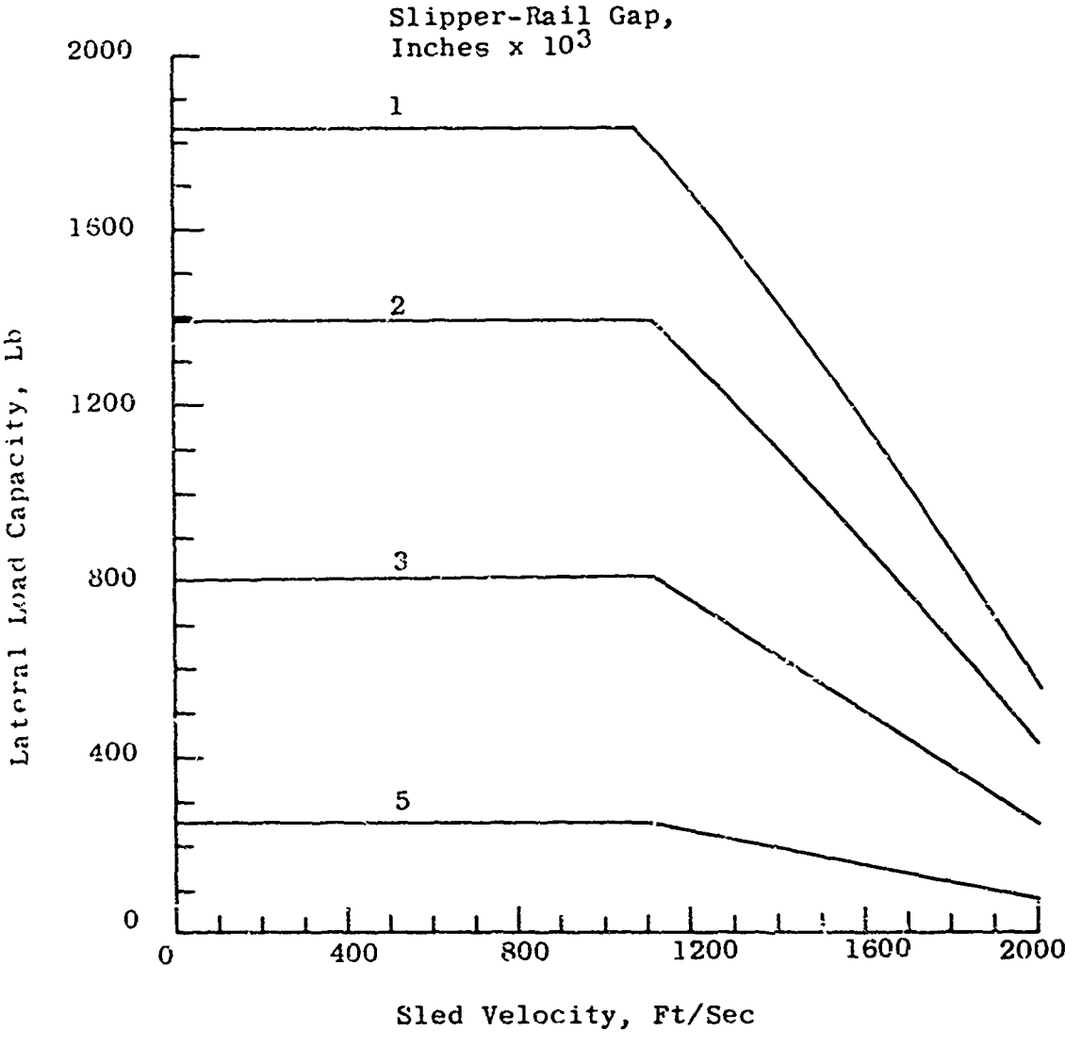

Figure 24. Lateral Load Capacity of Dual Rail Sled Externally Pressurized Slipper

react the applied slipper loading. Under the action of a rolling moment one slipper will deflect to decrease this gap, thereby increasing the developed load, and the other slipper will move so as to increase the gap and thereby decrease the developed load. The differential loading will then produce a moment opposing the applied moment.

Since the slippers on a dual rail sled are separated by seven feet, the small sled rotation due to differential loading does not cause any appreciable variation of the gap across the slipper. For this reason, it is convenient to express the increase or decrease of vertical slipper force with slipper-rail gap. In this form, the data can be used to determine moments and calculate impulsive force and asymmetric loading capacities as functions of slipper-rail gap.

These data are shown in Figure 25 for the dual rail sled at various velocities. At a given velocity, the slipper-rail gap corresponding to zero excess slipper force is the equilibrium gap the slipper operates at under the applied loading given in Figure 3.

4.4.7 Slipper Drag

The drag of the externally pressurized slipper bearing designed for the dual rail sled is of little consequence when compared to the thrust penalties of the added support system weight and drag. For estimating purposes, the increased aerodynamic drag of the externally pressurized slipper over a standard slipper can be taken as shown in Figure 15 for the self-acting slipper (although it would actually be lower). Thus, for the dual rail sled run specified in Figure 3, the slipper drag would amount to no more than 40 pounds per slipper at the maximum velocity condition. Of course, the drag saving realized by eliminating contact with the rail will result in a net decrease in slipper drag.

The drag penalty associated with the support system may be minimized by proper sled arrangement. By locating the air tanks behind a sled forebody, the drag penalty of the support system would be minimized. The actual penalty would be strongly influenced by sled arrangement and forebody geometry and an estimate of this drag requires a design study of an overall sled system.

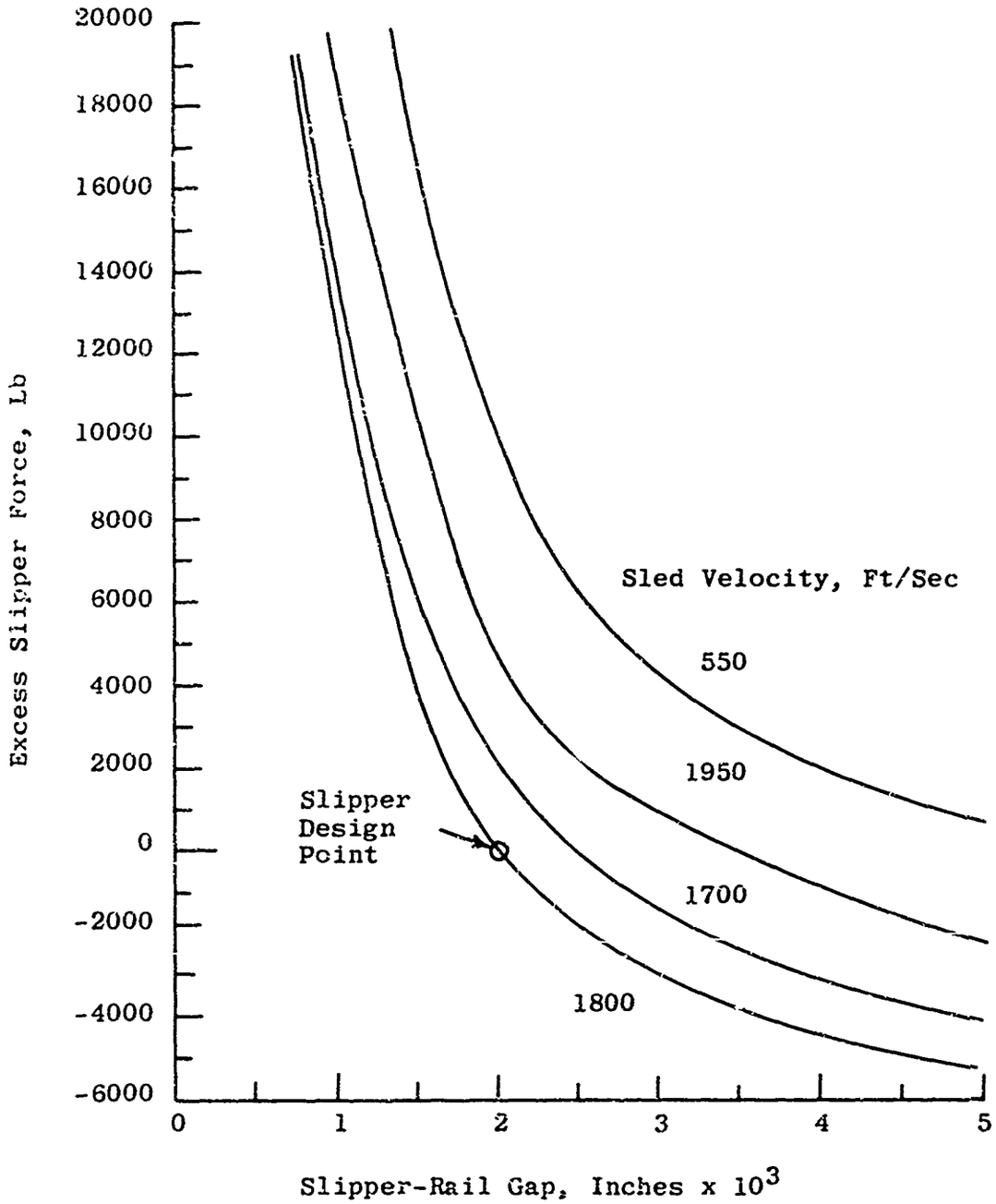

Figure 25. Excess Force of Dual Rail Sled Externally Pressurized Slipper

4.4.8 Effect of Wear on Slipper Performance

The effect of wear on the performance of an externally pressurized slipper bearing mainly involves consideration of the type of wear. As in the case of the self-acting slipper bearing, a typical externally pressurized slipper may be tilted when operating at high speeds. In this event, since it would be operating as a self-acting bearing, the discussion of the effect of wear on the performance of self-acting slippers would apply to the externally pressurized type as well. However, if the slipper is not tilted, occasional contact with the rail may result in damage to the entire slipper surface.

If the damage is severe, with either large distortions in surface profile or large amounts of material loss, the load carrying capability of the slipper would be reduced. However, slight wear, in the form of increased roughness, would actually be beneficial to bearing performance. Slight increases in roughness (where the mean roughness height is small compared to the slipper-rail gap) serve to inhibit air flow. For a given slipper rail gap, this effect will reduce the lubricant flow and therefore the support system penalties.

4.5 Monorail Sled Externally Pressurized Slipper Bearing

4.5.1 Support System Penalties

The support equipment penalties for a monorail sled using a supply tank air source are shown in Figure 26 as a function of operating time. The slipper for the monorail sled would be 30 inches long and operate with a slipper-rail gap of 0.002 inches. The same analysis and support equipment data used for the dual rail sled was employed to obtain the data in Figure 26. In this case, the slipper may be sized at the initial (rest) condition, since the slipper loads do not exceed those at rest (even accounting for the differences in bearing areas between the upper and lower slipper surfaces) until the sled has reached a velocity where the slipper bearing can support itself due to self-action. A schematic showing the operation of this slipper is given in Figure 27.

4.5.2 Combined Self-Acting and Externally Pressurized Slipper Bearing

The possibility of using an externally pressurized slipper bearing only for the low speed portion of the monorail

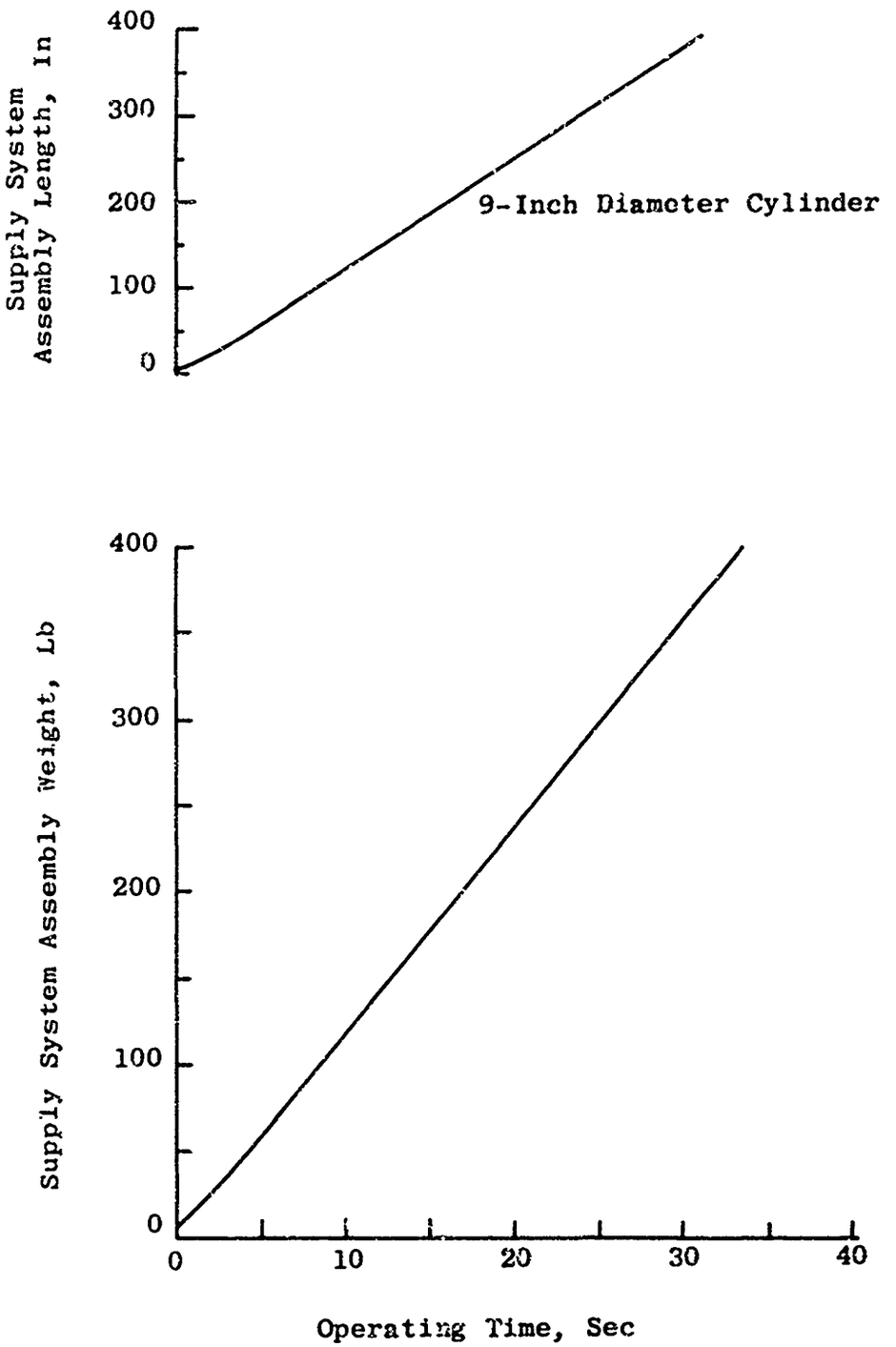

Figure 26. Weight and Volume Penalties of Monorail Sled Externally Pressurized Slipper

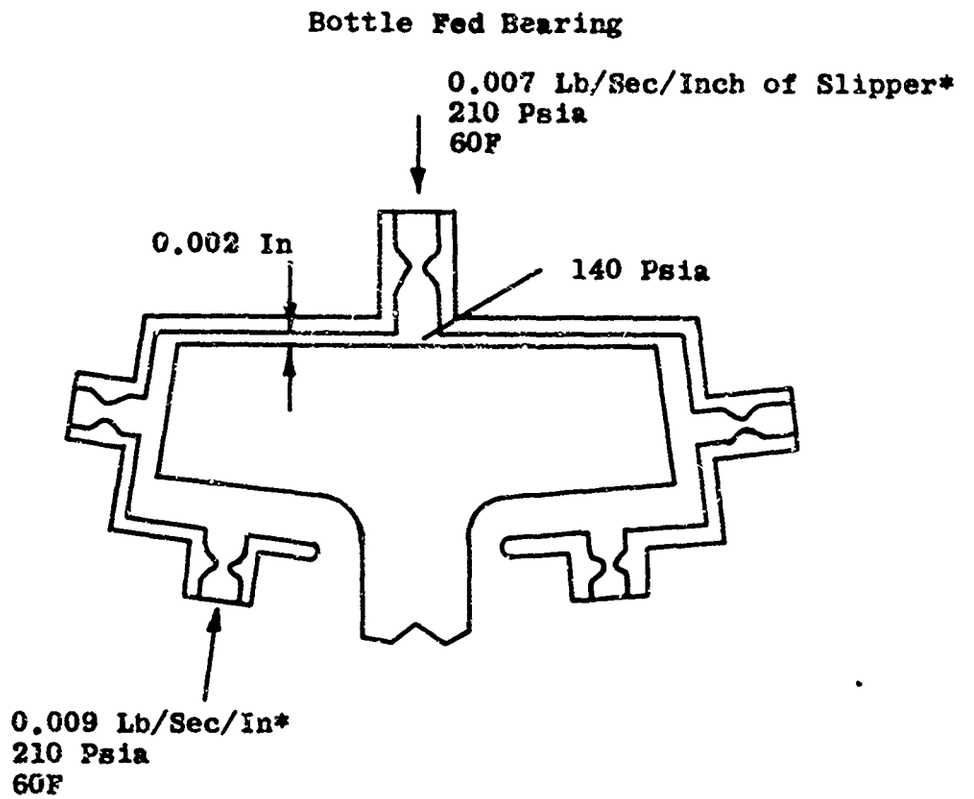

Figure 27. Monorail Sled Externally Pressurized Slipper Requirements

run would result in a compromise in the performance of the self-acting slipper. The addition of supply ports, especially on the lower lips of the slipper, would reduce the effective bearing area. In this case, the slipper length would have to be increased, probably to about 2.5 feet, to compensate for this loss. The problem of providing a constant gap during operation as an externally pressurized bearing and then tilting the slipper to form a wedge-shaped gap at high speeds might be solved using a spring loaded mechanism triggered by command or at a particular track station.

However, the weight penalties associated with this approach, although small compared to the dual rail sled, are prohibitive. As shown before, a self-acting monorail slipper bearing can operate at a speed over Mach 1.5. This speed is attained after the first four to five seconds of the monorail sled run specified in Figure 2. If the supply system is sized for this operating time, the weight penalty would be approximately 50 pounds, a sizable percentage of a typical high speed monorail sled weight. Even more significant is the volume penalty. If a 9-inch diameter monorail sled is selected, the supply tank would require a carriage approximately four feet long. The weight of the sled structure alone would probably double the 50-pound weight penalty. These penalties are associated with a system providing external pressurization only during the acceleration phase of the monorail sled. Additional weight and volume would be required for a system which would operate during the low speed portion of the deceleration phase.

4.5.3 Lateral Load Capacity

The lateral load capacity of the monorail sled externally pressurized slipper bearing shown in Figure 27 is given in Figure 28. The data shown in the figure were prepared using the same analysis and assumptions used for the dual rail sled slipper. These data only extend to a velocity of 2000 feet per second since at higher speeds the slipper should be designed to support itself as a self-acting bearing.

4.5.4 Moment Capability

The reaction of an externally pressurized monorail slipper bearing to a rolling moment is similar to that of the self-acting type described in Section 3.5.5. The slipper will rotate slightly so that the gap on one side of the slipper is

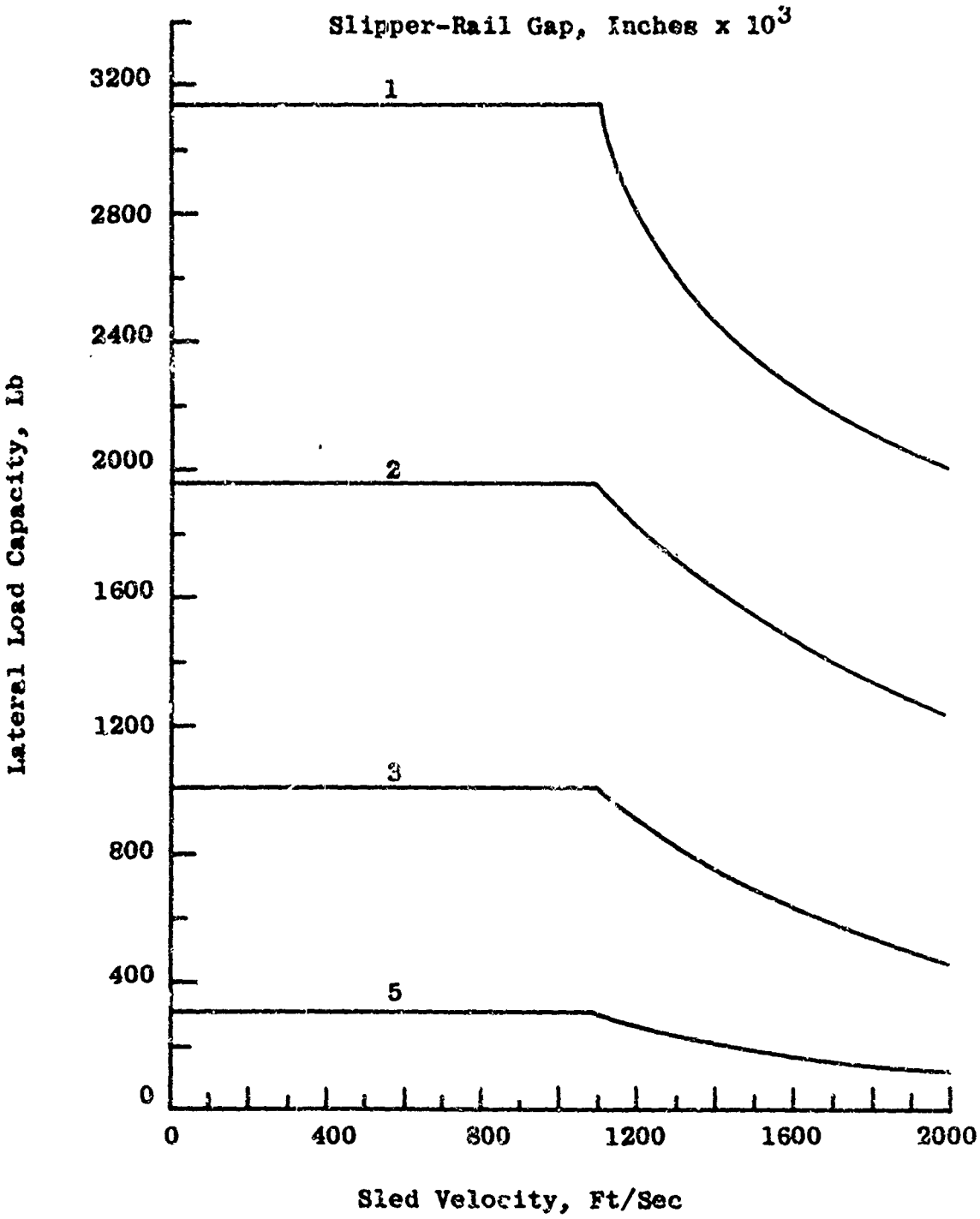

Figure 28. Lateral Load Capacity of Monorail Sled Externally Pressurized Slipper

less than on the other side, as shown in Figure 13. The sum of the forces developed by the left and right sides of the surface reacting the applied load remains constant, but due to the force differential, a moment is produced. This moment then reacts the applied moment.

At rest or low sled speeds, the monorail sled rolling moment problem is more acute than at higher speeds due to the inherent characteristics of the externally pressurized slipper bearing. The use of orifices, although necessary to minimize support system penalties, limits the total flow available to the bearing. When the slipper rotates, most of the flow will pass through the side of the bearing with the larger gap. If this gap becomes large enough the limited flow and increased flow area will result in a reduced pressure entering the slipper-rail gap. As this pressure drops, the load reduces and the slipper is likely to bottom out.

Another problem involves the magnitude of the slipper-rail gap. As shown in previous sections, small gaps are required to minimize support system weight. With a small slipper-rail gap, the allowable slipper rotation, and therefore moment capability, is limited by bottoming out of the slipper.

The actual moment capability of the monorail sle xtern-ally pressurized slipper bearing was calculated for t operating condition at the beginning of the run when e slipper-rail gap is a minimum (0.002 inches). The results are shown in Figure 29 with the moments referenced to the point shown in Figure 13. As shown in Figure 29, the rolling moment capability of the slipper is quite low.

4.5.5 Slipper Drag and the Effect of Wear on Slipper Performance

The discussion presented in Sections 4.4.7 and 4.4.8 for the dual rail sled externally pressurized slipper also applies to the monorail sled slipper. However, the drag penalty caused by the support system air tanks would be much more severe for the monorail sled than for the dual rail sled due to the small diameter forebody on most high speed monorail sleds.

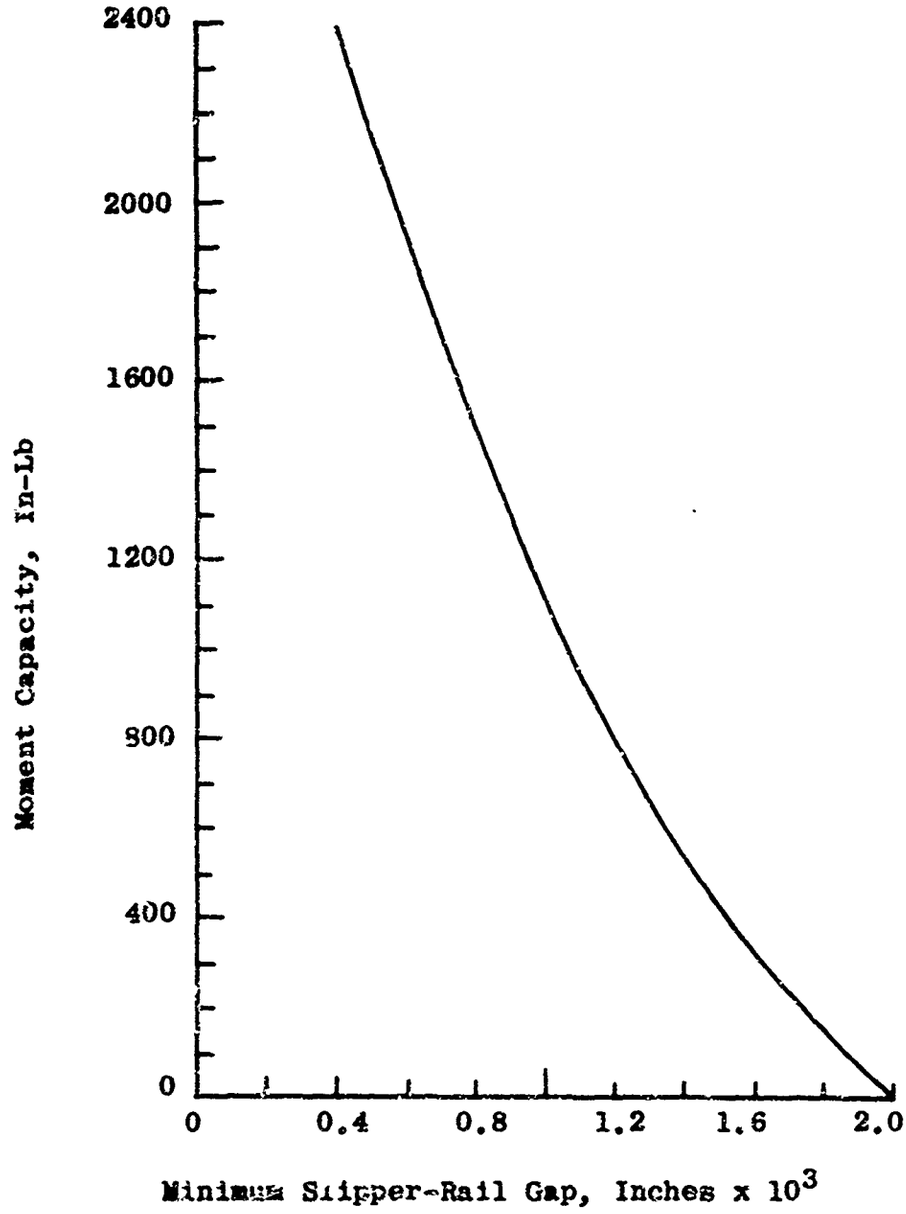

Figure 29. Moment Capacity of Monorail Sled Externally Pressurized Slipper at Rest

SECTION V

EFFECT OF TRACK CONDITIONS

The results of the performance studies on self-acting and externally pressurized slipper bearings, presented in Sections III and IV, have not included the effect of track conditions on overall slipper operation. The effects of rail alignment and dimensional variations, track roughness, and foreign material in the gap are examined in this section. As shown below, the most critical of these items is the effect of rail alignment and dimensional variations.

5.1 Effect of Rail Alignment and Dimensional Variations

5.1.1 Motion of the Slipper

As an air lubricated slipper travels down the test track, the force developed by the slipper tends to cause it to follow the rail. The motion of a slipper entering a section of rail where either the alignment of the rail or its dimensions are varying is depicted in Figure 30. The variation in alignment or dimension is shown as a linear ramp, which the slipper approaches from a section of track where the slipper motion is steady. Before entering the ramp section the slipper is in equilibrium. The force developed by the slipper bearing is balanced by the applied load. Due to the inertia of the sled, the slipper will tend to follow its original trajectory as it enters the ramp section. The slipper-rail gap will decrease as the slipper proceeds into the ramp and this smaller gap will cause a higher force to be developed by the slipper. The excess force on the slipper (the difference between the developed force and the applied load) will cause a vertical acceleration of the slipper away from the rail. If the excess force is large enough, the slipper will not bottom out and will follow the path shown in Figure 30.

5.1.2 Analysis of Slipper Motion

To analyze the motion of the slipper due to rail alignment and dimensional variations, the linear ramp model shown in Figure 30 was used. Since it was required to determine the maximum allowable variations, a conservative performance model was used at the most critical operating condition.

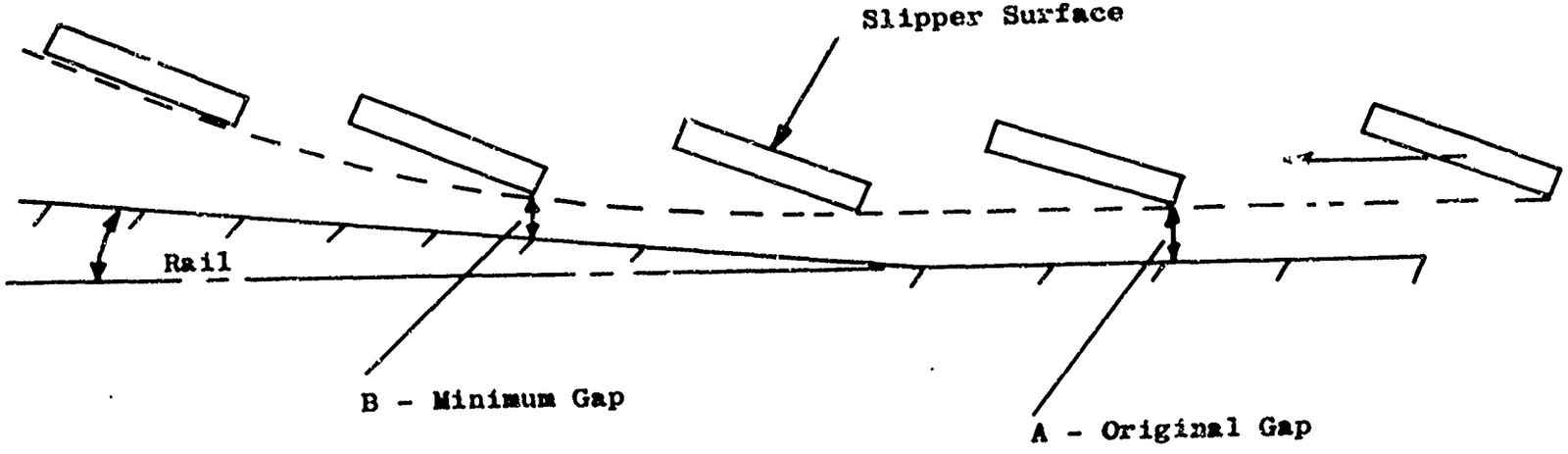

Figure 30. Motion of Slipper Due to Variation in Rail Alignment or Dimensions

The four primary factors affecting the motion of the slipper are: (1) the slipper-rail gap, (2) the sled velocity, (3) the ramp slope and (4) the sled mass. The first factor is obviously important, since a slipper operating with a small gap before entering the ramp will tend to bottom out more easily. The second parameter determines how rapidly the slipper proceeds up the ramp. If the velocity is high, only a short period of time is available for the excess slipper force to accelerate the slipper away from the rail. The third factor is of equal importance, since a very high ramp slope will cause the gap between the slipper and rail to decrease rapidly. Finally, the sled mass will determine the vertical acceleration of the sled due to the excess force.

For the monorail sled, the combination of highest velocity and minimum slipper-rail gap occurs at the Mach 6 operating condition. At this point, the minimum gap is between the lower slipper lips and the rail. For the schematic shown in Figure 30, the lower lip is the slipper surface and the rail is the lower surface of the head. Therefore the vertical alignment or dimensional variations of the rail are the most critical.

The vertical motion of the sled was analyzed by assuming various ramp slopes and calculating the variation of the slipper-rail gap over the ramp. The initial conditions (before entering the ramp) were taken at a velocity of Mach 6, with a corresponding minimum gap of 0.005 inches (Figure 10). A typical monorail sled weight at this condition would be less than 200 pounds, and it was assumed that the front slipper share would be 100 pounds. The actual calculation procedure consisted of a step-by-step quasi-steady analysis using the load-gap relation given in Figure 6. This approach does not include the squeeze film damping of the air film. In addition, no sled structural damping was included in the analysis. By ignoring both of these effects, conservative estimates of the allowable rail alignment and dimensional variations are obtained.

5.1.3 Results of the Analysis

When the slipper enters the ramp section, the motion of the slipper causes the slipper-rail gap to decrease to some minimum value and then to increase again. The minimum slipper-rail gap during this phase is shown in Figure 31 as a function of a parameter τ. This parameter expresses a characteristic period, and is the length of the slipper divided by the product of the ramp slope and sled velocity. As discussed in the previous section, the greater the ramp slope and sled velocity and the smaller the initial slipper-rail gap, the greater is the possibility that the slipper will bottom out on the ramp.

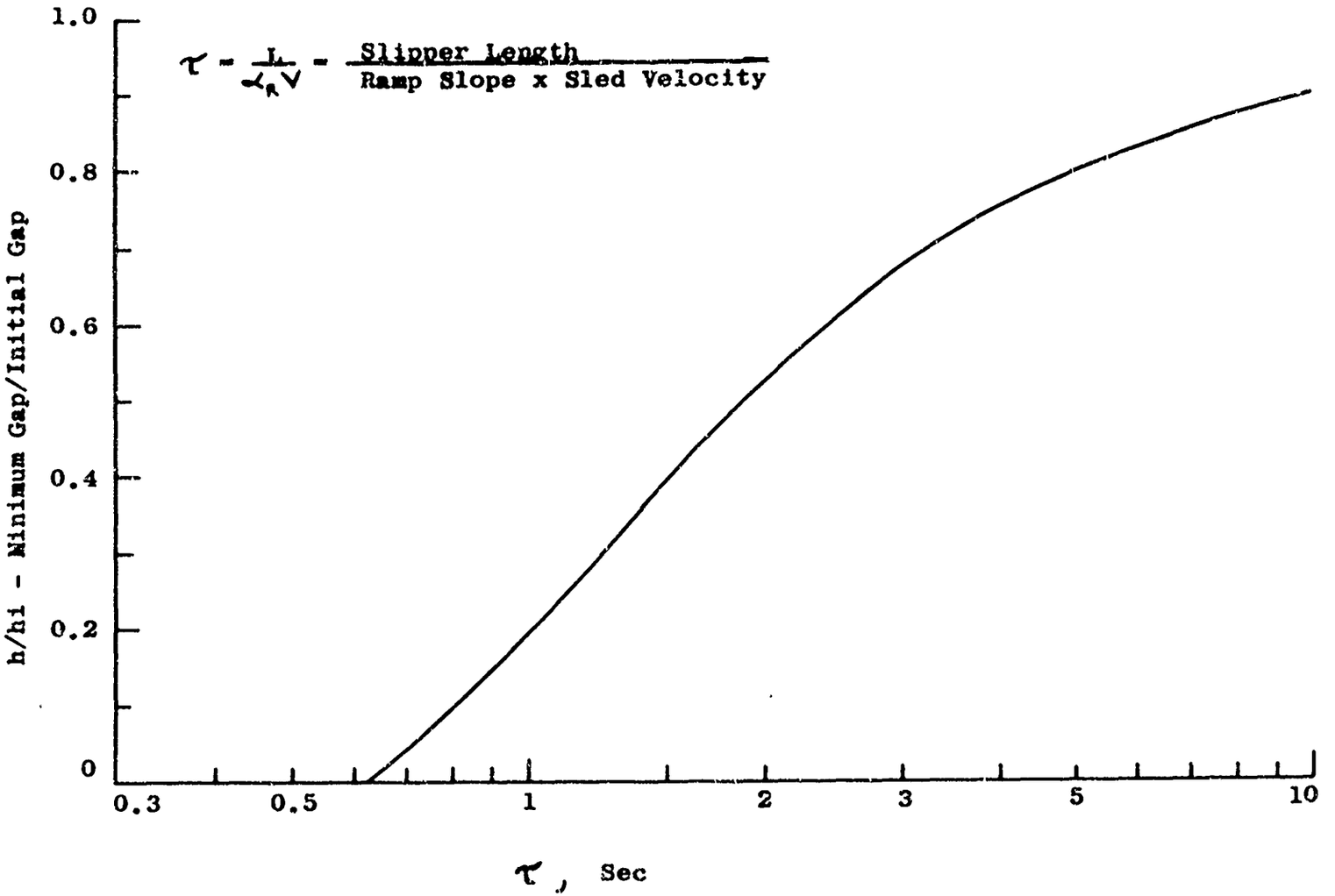

Figure 31. Minimum Slipper-Rail Gap on Initial Section of Ramp

Since the gap is directly related to the slipper length, as shown in Figure 8, the length may be substituted for the gap in this relation. Therefore, the parameter τ combines the most important quantities affecting the motion of the slipper due to variations in rail alignment and dimensions.

The data in Figure 31 shows that the minimum slipper-rail gap attained during the initial portion of the ramp section (Point B in Figure 30) decreases from the initial gap value when $\tau \rightarrow \infty$ (α Rail = 0), to zero when $\tau = 0.63$. Therefore, when the velocity and length of the slipper are known, the maximum allowable ramp slope is specified.

Although the slipper may not bottom out on the initial portion of the ramp, the vertical motion caused by the ramp may result in an unstable oscillation. The air film acts like a spring and may produce unstable vertical motion. This effect is shown in Figure 32, where the variation of the slipper-rail gap over the ramp is shown. This figure illustrates that although the $\tau = 0.75$ case does not bottom out during the initial portion of the ramp, the motion of the slipper after this point is unstable and the slipper will bottom out further down the track. The lower limit of acceptable values of τ occurs at $\tau = 2.25$ where the motion is neutrally stable and continues indefinitely.

If the rail section alignment changes, or if the dimensional variations are modified, the motion of the slipper is altered. This effect is shown in Figure 33, where three cases are illustrated. The first case depicts the variation in slipper-rail gap for a continuous ramp with $\tau = 2.25$. This is the same curve shown in Figure 32. The other two curves show this variation for cases where the ramp ends at different points. For these two cases, the amplitude and wavelength of the curves are different, but as expected, the motion is still neutrally stable.

The results of this study indicate that rail alignment and dimensional variations may be a problem for air lubricated slipper bearings. The model used for the analysis does not include damping effects of either the air film or sled structure, and as such, yields minimum acceptable variations.

5.2 Effects of Roughness on Slipper Bearing Performance

The effect of rail and slipper surface roughness on slipper bearing performance requires an examination of the types of "roughness" involved. For this purpose, the surface condition of the rail is broken down into major categories: holes, spikes, bumps, and uniformly distributed surface roughness.

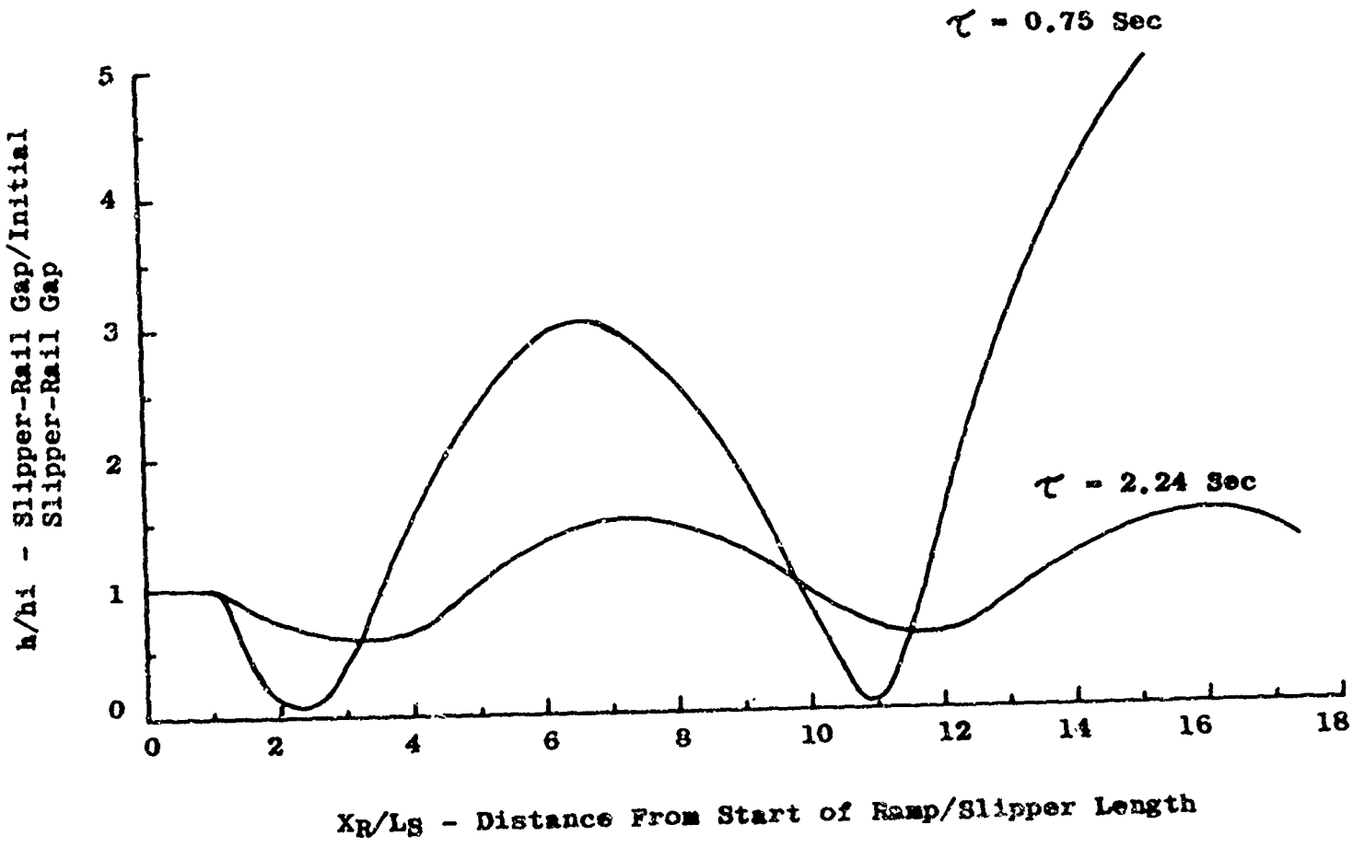

Figure 32. Variation of Slipper-Rail Gap on Ramp

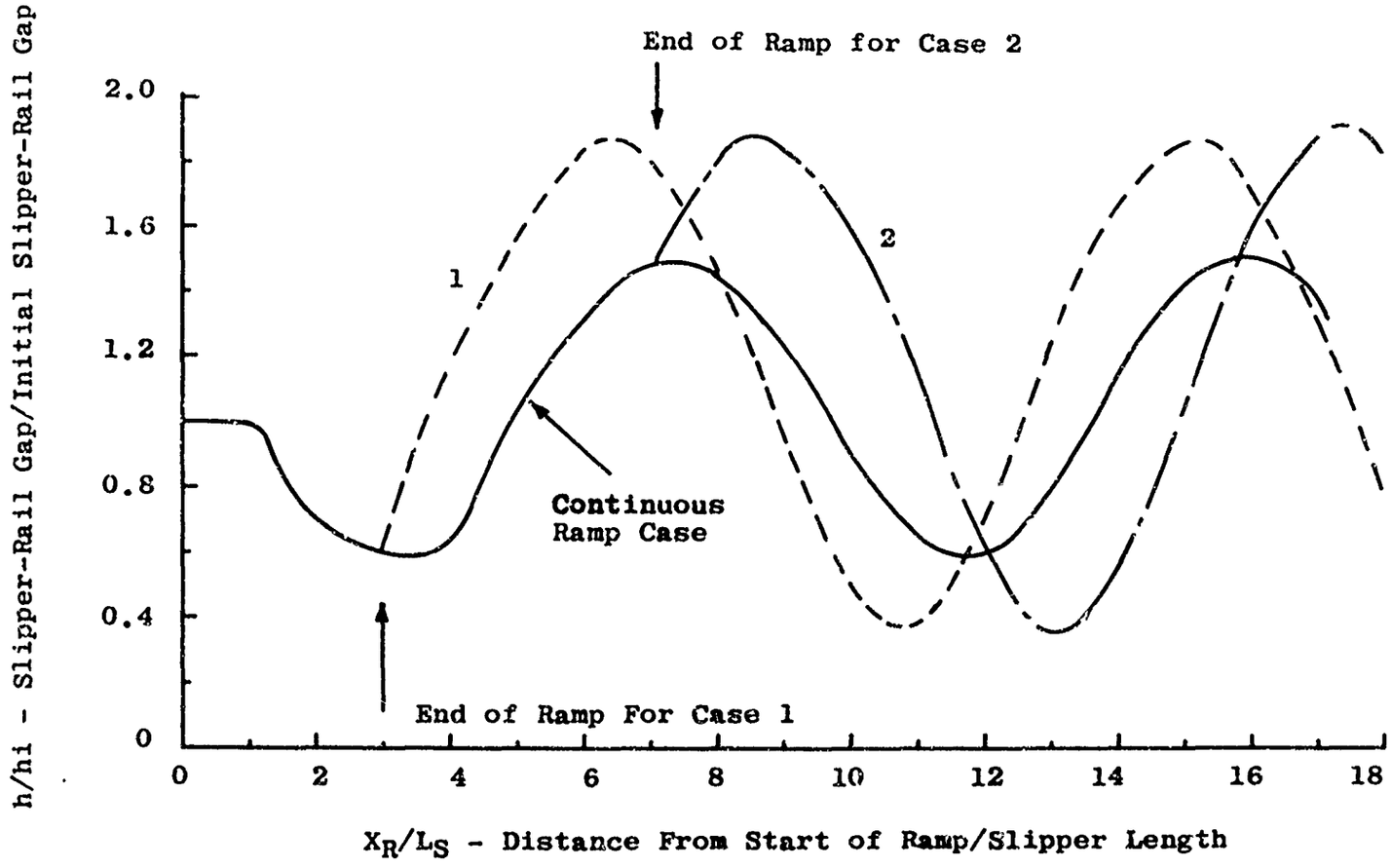

Figure 33. Effect of Ramp Length on Slipper-Rail Gap Variation

5.2.1 Holes

Serious damage to a rail, in the form of holes, may obviously deteriorate slipper bearing performance. Here, a hole is defined as a section of rail surface where a significant amount of material has been removed. Examination of the Holloman Test Track reveals sections of rail where slippers have gouged large amounts of material from the surface. These areas are relatively small compared to the total track surface, and are repaired by filling.

A numerical example of the effect of a hole on slipper bearing performance is discussed here to illustrate that the effect of occasional holes on slipper bearing performance is much less severe than the effect of variations in rail alignment and dimensions. For this purpose, the same analysis and operating condition (Mach 6) used to analyze the effect of rail alignment variations was used. It was assumed that a six-inch section of rail was completely destroyed and the motion of the slipper over the resulting "hole" was calculated. As the slipper enters the missing section, all bearing load generated by slipper self-action ceases and the sled is accelerated in the direction of the applied load. It was found that if the slipper-rail gap on the rail section ahead of the hole is 0.005 inches (the selected design), after passing the hole, the minimum slipper-rail gap on the rail section following the hole is slightly less than 0.001 inches. Thus the slipper can survive an occasional "hole" with less gap variation than a gradual variation in rail alignment.

5.2.2 Spikes

A spike is defined as a small protrusion above the rail surface. If the height of the spike is less than the minimum slipper-rail gap, no surface contact between the rail and slipper occurs and the limited area of the spike will not seriously disturb the flow in the gap. If the spike height is greater than the slipper-rail minimum gap, the slipper will shear the top of the spike and some effect on performance will occur. However, considering the large forces holding the slipper in equilibrium (37000 pounds at Mach 6 where the slipper-rail gap is a minimum), a large number of spikes would be required to seriously affect the immediate slipper performance. The surface damage caused by the spike would increase the roughness of the slipper and deteriorate subsequent performance. The degree of the effect would be small for the definition of a spike given above, unless a great number of spikes were present on the rail. It should be mentioned here that conventional bearings operate quite satisfactorily with occasional asperity contact. A spike on the rail surface is an example of such an asperity.

5.2.3 Bumps

The effect of a rail bump on slipper performance is much more severe than that of a spike. Within this context, a bump is defined as a relatively large amount of material protruding above the rail surface. If the height of the bump is small (less than the minimum slipper-rail gap), very little effect on slipper performance occurs. The exposure time of the slipper to the bump is small and the perturbing force, being limited in duration, will cause a small vertical oscillation in sled motion. The motion would be similar to that described previously for ramp induced sled oscillations, but would have a smaller amplitude.

If the bump height is larger than the slipper-rail gap, impact on the bump near the trailing edge of the slipper will occur. The sudden vertical force on the sled will cause an oscillating motion. If the combination of impact force and structural damping results in a moderate acceleration, the motion of the sled may remain neutrally stable or damp out. However, it is likely that such an impact will result in large accelerations and resemble the jumping action of present slippers.

5.2.4 Uniform Roughness

Within the context of the following discussion, uniform roughness is defined as surface irregularities of small amplitude, more or less uniformly distributed over the surface of the slipper or rail. With this definition, the extensive experimental data available on the effects of roughness on free body drag can be applied to the slipper bearing problem.

In many free body experiments, it has been found that a relatively rough body will have the same drag as a smooth body. This is due to the fact that the surface roughness elements do not protrude above the laminar sublayer of the turbulent boundary layer. It has also been determined that the mixing length used in turbulent boundary layer analysis is not affected by surface roughness. These conclusions are the results of numerous experiments conducted in the past and are summarized in Reference (4).

For the self-acting slipper bearing and the externally pressurized slipper bearing operating at high speeds, the laminar sublayer existing on the slipper and rail may be thick enough to completely contain any surface roughness elements. This is more likely to occur on the slipper surface, rather than on the rail, due to the adverse pressure gradient existing over

most of the slipper length. If the rail roughness elements protrude above the laminar sublayer, the velocity gradient, and therefore the pressure gradient, within the gap will be altered. Unfortunately, the analysis used to predict self-acting slipper bearing performance cannot account for the effect of surface roughness without empirical adjustments to the velocity profiles within the slipper gap. However, if decreases (or increases) in slipper load capacity are caused by surface roughness, small changes in slipper-rail gap can be a compensating mechanism.

These changes in slipper-rail gap do not compensate for increases in slipper drag. This drag, like the drag of a free body, will be significantly affected by surface roughness, even if the load capacity is not altered. To obtain a rough estimate of the increased drag due to surface roughness, a simple channel flow model was analyzed.

First, it was assumed that at each station along the slipper, the flow within the gap could be represented by half of an equivalent channel flow problem, with the rail as the centerline of the flow. The equivalent Reynolds number of the gap flow was then calculated. Next, various mean heights of an equivalent sand roughness were selected and the ratio of the mean height to the equivalent hydraulic diameter of the gap was computed. With this data, the ratio of the friction factor of the rough "channel" compared to a smooth channel was calculated. The friction factor data was obtained from Reference (4). The friction factor ratio multiplied by the "smooth" slipper viscous drag yields the "rough" slipper viscous drag.

The data obtained by this analysis are presented in Figure 34, where the increased slipper drag due to roughness is plotted as a function of Mach number for various roughness conditions. The data are presented only for the front slipper of the monorail sled, although the drag increase of the rear slipper would be very similar. It should be noted here that it was assumed that the roughness elements existed on the slipper, as well as on the rail. Since the slipper surface can be controlled during preparation, the effect of rail roughness would not be as severe as shown in Figure 34.

Surface roughness effects on the performance of externally pressurized slipper bearings have been discussed in Section 4.4.8. In general, they are small. The drag increases due to roughness would be comparable to the self-acting slipper shown in Figure 34. Since externally pressurized slippers are not required for speeds greater than Mach 2, the drag increase due to roughness is negligible.

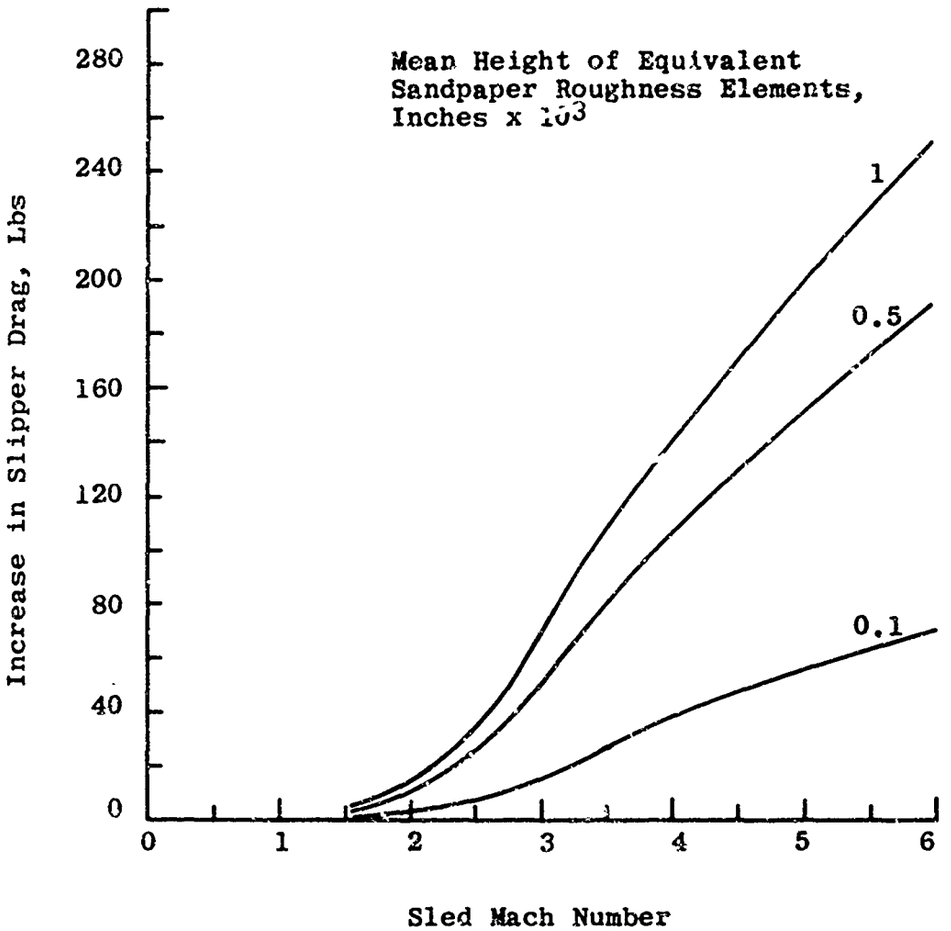

Figure 34. Effect of Roughness on Slipper Drag

5.3 Effects of Foreign Objects on Slipper Performance

During a typical rocket sled run, foreign objects in the vicinity of the rail may be churned up and enter the slipper-rail gap. At high test speeds, erosive oxidation and melting effects can result in the shedding of drops of molten metal, which may also enter the slipper gap. Both of these effects deteriorate slipper performance due to (1) immediate forces caused by the presence of foreign material, and (2) surface damage.

5.3.1 Inert Foreign Particles

Conventional air bearing systems usually require very clean operating environments because of their small operating gaps (usually less than 0.001 inches). Externally pressurized bearings use filters to insure that the supply source does not contaminate the bearing. In the case of rocket sled slipper bearings, the bearing gaps are much larger and the same level of cleanliness is not essential. In addition, any foreign material within the gap will not be recirculated, as is the case for many self-acting journal bearings where the unit is sealed.

If a large amount of foreign material in the form of small (less than the minimum slipper-rail gap) inert particles enters the slipper-rail gap, the air supply will be effectively throttled with an attendent drop in pressure level. This will result in a decrease in load capacity. If the total amount of material is limited, immediate performance is affected for only a short duration of time. Due to the large forces holding the slipper in equilibrium and the inertia of the sled, the effect of the foreign material will not be as severe as the effects due to variations in rail alignment and dimensions. Of course, if the gap is effectively "flooded" with particles over a large stretch of track, the slipper will not operate as an air bearing.

In the event that a limited amount of material, not sufficient to cause immediate failure of the slipper bearing, enters the slipper gap, the surface damage caused by particle impact will deteriorate subsequent performance. Roughening of the slipper surface due to particle impingement will have the same effect as inherent roughness, as discussed in Section 5.2.4.

Large particles entering the slipper gap will become wedged between the surface of the slipper and the rail until the rail wears away enough of the particle material so that it may pass through the slipper. The wearing process, especially at high speeds where the minimum slipper-rail gap is the smallest, will be very rapid. Within the time required to pass a particle wedged near the exit of the slipper, the applied loading would not vary and no vertical motion of the slipper due to load variation is required. The immediate effect on performance would then be the flow distortion caused by the presence of the particle. However, pebble-sized particles, which would wedge between the slipper and rail near the inlet of the slipper, would require a longer time interval to pass. If the interval is long enough, the applied loading will vary and the slipper will move vertically, relative to the rail. Should the slipper surface with the trapped particles be unloaded, the gap will increase, causing the passage of the particle to be more rapid. If the surface loading is increased, the particle will be crushed and severe damage to the slipper surface may occur. In any case, although the number of large particles entering the slipper-rail gap may be much less than the number of small particles, the effect of the larger particles on slipper bearing performance is more pronounced.

5.3.2 Molten Metal Droplets

Due to their plasticity, molten metal droplets within the slipper gap will have less immediate effect on slipper performance than inert particles. Droplets smaller than the slipper gap will be subjected to large shearing forces caused by the steep velocity gradient across the gap. This gradient will produce differential drag forces on the droplet and cause it to elongate and break up. Very large droplets will be directly sheared by the slipper and the rail.

The serious effect of molten metal within the gap will be due to the damage the droplets cause on the slipper surface. Shearing of the metal droplets increases their surface area to volume ratio and hence, the amount of oxides produced. The high oxidation rate, caused by the high pressure and temperature within the gap, combined with the large amount of exposed material, will cause local areas of very high temperatures. This process can be self-propagating and approach a rapid combustion process if the slipper is uncoated steel. With a coating, the effect of molten metal damage can be minimized.

SECTION VI

HIGH SPEED SLIPPER COATINGS

The problem of preventing erosive oxidation and melting of slipper material at high sled speeds is actually the problem of protecting the surface of the slipper. If the surface of the slipper can be insulated and oxidation is prevented, no serious degredation of slipper strength or bearing performance will occur. Current slippers commonly rely on protective flow deflection devices to reduce the air temperature in the vicinity of the slipper. Due to the low pressure regions directly behind them, such devices cannot be used for protecting self-acting slipper bearings. Therefore a protective coating is mandatory for a high speed slipper bearing.

6.1 Candidate Materials

Various coating materials can be used to protect a slipper bearing. The structural requirements of the material are very low since the air film in the slipper gap prevents direct slipper-rail contact. With low structural requirements, ablative and refractory coatings are the best choices. However, it is desirable that the amount of coating loss during a run be as low as possible to minimize the amount of foreign material in the gap and geometric changes of the slipper surface. For these reasons a refractory coating is preferred. In addition, a refractory coating is easy to apply and the low rate of material loss might permit their re-use without extensive refurbishing.

6.2 Current Coating Program

The need to protect critical leading edge sections of hypersonic rocket sleds has already led to a materials program designed to evolve a protective refractory coating. This program, conducted for AFMDC requirements by the Research Institute of the University of Dayton, Ohio, is under the direction of the Air Force Materials Laboratory. The progress of the program is reported in Reference (5). Several plasma sprayed coating systems were applied to the basic 340 stainless steel slipper material and subjected to a plasma torch, simulating a Mach 7 sled run. The coatings consisted of a three layer system; a 10-15 mil oxide coating for thermal insulation, a 6-10 mil oxide-metal layer for thermal mismatch compensation, and a 4 mil metal bonding layer. Two of the combinations tested lost only the exterior oxide coating. Further testing led to the selection of a nickel bonding layer /nickel-Zircon intermediate layer/ Zircon oxide coating composite as the best combination.

A material such as that selected for protecting other parts of the sled is adequate for an air lubricated slipper. If only the 10-15 mil oxide layer is lost during the run, the mass of the layer, compared to the air flow in the gap, is negligable, and the effect of the oxide coating particles on slipper performance may be ignored. Even if the loss is not symmetric, with more material being lost at the front of the slipper than at the rear, the change in slipper slope is small and the effect on performance is negligable. The change in performance due to the increase in average slipper-rail gap is also negligable.

SECTION VII

OPERATIONAL REQUIREMENTS AND DEVELOPMENT EFFORT

The operational requirements of air lubricated slipper bearings, and the development effort required to provide a prototype system are closely related. This is especially the case for externally pressurized slippers, since the weight of the support system is inversely proportional to the complexity of the system and the effort required to develop the various subsystems.

7.1 Self-Acting Slipper Bearing System

The operational requirements of a self-acting slipper bearing involve only the proper alignment of the slipper on the sled. The slipper must be aligned to the sled, so that when operating, the proper gap geometry is obtained. The slope of the inner slipper surface is not extremely critical, so relatively simple alignment tools can be used to adjust the slipper orientation on the sled. A carefully controlled sled fabrication process could eliminate an on-site alignment procedure, but since this procedure is simple, controlling the fabrication process is probably not worth the effort.

The development effort required to provide a prototype self-acting slipper bearing depends to a large extent on the actual load-velocity requirements of the sled. If hypersonic operation is required, the slipper must be coated with a protective material. Since the effort to develop a coating for other portions of the sled is well underway, no special development effort for the slipper is required in this area.

During the low speed portions of a sled run, some mechanism must be provided to support the slipper. If the load-velocity requirements of the monorail sled given in Figure 2 are typical, the slipper must have an auxiliary support mechanism for operation below Mach 1.5. This may take the form of a simple flat section attached to the rear of the slipper. The flat section would be provided with a small wear insert, positioned so that it does not interfere with the flow through the gap.

The actual steps required in the development of a prototype system would consist of; (1) a prototype system design (Phase II efforts), (2) fabrication of the slipper and (3) fabrication of an alignment device. The latter component could consist of a simple feeler gage.

7.2 Externally Pressurized Slipper Bearing System

The operational requirements of an externally pressurized slipper bearing system depend on the complexity of the air supply subsystem. In its simplest form, the system would operate with its pressurization equipment on for the entire run. After mounting the sled on the track, the slipper would be jacked up to establish the gap between the rail and the upper surface of the slipper. This operation is necessary, because if the slipper were to rest on the track, only the small area of the supply port would be pressurized. This small area would not develop sufficient force to lift the sled off the track.

Next, the slipper would be aligned. This procedure would be more involved and require more precise equipment than the comparable operation on a self-acting slipper, since externally pressurized slipper performance is very sensitive to gap variations. Finally, the pressurization system would be turned on, the jacks removed, and the sled fired.

An additional operation might be required due to the jack system. If the jacks are built into the sled and operated automatically, the procedure described above would be followed. However, if the jack system is external to the sled, and manually operated, some time will be required to release the jacks and clear the area after the pressurization system is turned on. If the time required for this operation is long enough, additional on-board storage tanks will be necessary. To minimize on-board weight, a track-side compressor should be used to supply the slippers with air while the sled is at rest. In this case, the compressor feed line would have to be released, and the on-board pressurization turned on, just before the sled is fired.

The development effort required to provide a prototype externally pressurized slipper bearing system can be minimized by using readily available equipment. Aside from the slipper design and fabrication, all of the other components required for the system are available. Some detail design work would be necessary to integrate the tanks, valves, and supply lines with the sled structure. However, if the supply system weight using standard components is excessive, a lighter weight system would require a special development program. The extent and level of this program would depend on the weight reductions required.

The weight savings gained by a supply system development program might not be sufficient for practical use of externally pressurized slipper bearings. In this case, further reductions in supply system weight can only be obtained by reducing its requirements. This may be accomplished by developing special equipment to minimize flow requirements of the slippers. Such devices would selectively pressurize only those portions of the slipper required to react a load, and would adjust the pressure level of the supply to the minimum values required. These functions could be provided by a system comprised of; (1) a device to measure varying slipper loads (probably by measuring changes in slipper-rail gap), (2) an on-board computer to interpret the measurements and actuate a valve control system, and (3) the valve and valve control system. The development effort required to provide a system with these capabilities would be large, and would probably be dominated by the load measuring device.

SECTION VIII

CONCLUSIONS AND RECOMMENDATIONS

The major conclusions reached as a result of this study, and the recommendations for future efforts are given below.

8.1 Conclusions on Self-Acting Slipper Bearings

1. Air film lubrication of a typical monorail rocket sled slipper above Mach 1.5 is feasible and practical, utilizing a simple, self-acting form of air bearing.

2. Simple mechanical systems can be provided to support the sled at low velocities (up to Mach 1.5) where air film lubrication is not necessary.

3. This type of slipper is compatible with the Holloman Test Track. It utilizes impacting air as the lubricant, and requires no additional equipment.

4. The slipper resembles current slippers but has lower drag and a small weight penalty.

5. The problem of erosive oxidation at high speeds can be overcome by providing the slipper with coatings now under development for other critical components of hypersonic rocket sleds.

6. The permissible variations in rail dimensions and vertical alignment are less restrictive for the self-acting slipper bearing than for a standard slipper.

7. Minimal operational complications and development efforts are required for a prototype system.

8. Operation of a slipper as a self-acting air bearing is not feasible below Mach 1.5 for a typical monorail sled, unless large reductions in slipper loads are achieved. This is also true for a typical dual rail sled over its entire speed range.

8.2 Conclusions on Externally Pressurized Slipper Bearings

1. Air film lubrication of typical monorail and dual rail rocket sled slippers is feasible with an externally pressurized slipper. This type of slipper bearing can operate over the entire speed range of both sleds, although external pressurization

is not necessary for a typical monorail sled at speeds over Mach 1.5. However, these systems appear impractical for AFMDC use due to excessive weight and volume penalties.

2. The slipper is compatible with the Holloman Test Track, utilizes an on-board pressurization system, and must operate with a small slipper-rail gap to avoid excessive penalties.

3. The slipper requires an involved fabrication process compared to current slippers, but would not generate large weight and drag penalties. The support equipment for the slipper would be the major contribution to such penalties.

4. If the slipper is required to operate at high speeds, the problem of erosive oxidation can be solved by the same approach used for the self-acting slipper.

5. Vertical alignment and dimensional variations of the test track may be more of a problem with this slipper than with the self-acting type, because of the smaller operating gap between the slipper and rail.

6. Operational complications, compared to the self-acting type of slipper, are greater. The development efforts required to evolve a prototype system are considerably greater.

7. Operation of the externally pressurized slipper bearing is not required at high speeds. However, hybrid designs, utilizing the advantages of both systems for operation over the entire speed range, have all of the disadvantages of the externally pressurized type.

8. Large reductions in monorail and dual rail sled slipper loads are required to appreciably reduce the weight and drag penalties of the externally pressurized slipper support system.

8.3 Recommendations

Based on the results of this study, we believe that a simple self-acting slipper bearing will satisfy AFMDC requirements. It is therefore recommended that AFMDC direct its attention toward this type of air lubricated slipper bearing.

It is also recommended that Phase II of this contract be implemented. This effort will be directed at the design of a simple self-acting slipper bearing which is easily fabricated and readily tested.

To minimize the time and cost required to evaluate the effectiveness of the slipper bearing, the following recommendations are made.

1. Pressure data on the flow within the slipper-rail gap of existing AFMDC test slippers should be obtained. It is believed that existing test slippers and instrumentation can provide data on the pressure levels in the slipper-rail gap. This data would be useful in determining if any modifications to the prototype design are desirable.

2. The prototype slipper should be initially tested at less than hypersonic speeds. Testing at lower speeds will ease fabrication requirements in the prototype stage by eliminating the need for, and concern with, protective coatings.

3. Data obtained from the above tests should be used to evaluate the performance theory. This data would form a sufficient base for evaluating the degree to which the conservative assumptions used in the analysis can be relaxed.

SECTION IX

PHASE II PROPOSALS

A proposal on the recommended effort for Phase II of this contract is outlined below. This proposal is based on the conclusions and recommendations of Phase I studies. It recommends some additional effort beyond the scope of the Phase II tasks outlined in Reference (1). The basic features of the proposed program consist of:

1. Modification of the performance theory program to permit its use as a design and data correlation tool.

2. Design and fabrication of a prototype operational air bearing slipper and a special test slipper to evaluate the performance theory utilized in Phase I studies.

3. A test program to obtain theory evaluation data with the special test slipper and to evaluate the effectiveness of the prototype operational air bearing slipper.

4. Correlation of the test data and incorporation of the results into the performance theory.

9.1 Performance Program Modification

The performance computer program evolved under Phase I efforts was prepared for the purpose of determining the feasibility of an air lubricated slipper bearing. Its use as a design tool, correlating test data, or performing parametric performance studies is inefficient and costly due to the large amounts of output cross-plotting and interpolation required.

It is therefore proposed that the computer program be modified to permit direct calculation of the slipper performance, including the pressure and temperature distributions, load, and center of pressure, by direct input of the geometry of the slipper as well as the basic operating parameters. Additional changes, permitting the calculation of general polytropic processes and parametric studies on the gradient of the mixing length (σ), will also be made.

9.2 Slipper Designs

In addition to the design of a prototype operational air bearing slipper, as required in Reference (1), it is proposed that a special test slipper design be provided under Phase II efforts. This slipper design will be provided with a variable

geometry gap and instrumented so that test data covering the range of operation of an air bearing slipper may be obtained. Both the prototype operational slipper and the special test slipper designs will be based on the results of parametric studies obtained from the performance computer program. The slipper designs will include design layouts, performance data, instrumentation requirements and stress analyses.

9.3 Slipper Fabrication

To facilitate a consistent and continuous program, it is proposed that Kaman Aircraft Corporation fabricate both the prototype operational air bearing slipper and the special test slipper. Fabrication of the slippers will be in accordance with AFMDC practice and recommendations. The materials to be used and the number of spares will be as specified by AFMDC.

9.4 Test Program

A test program recommendation will be supplied with the slipper designs. This program will be designed to obtain the required data for evaluating the performance theory with the special test slipper and to evaluate the effectiveness of the prototype operational air bearing slipper. The test plan will include the number and sequence of tests and will be compatible with AFMDC requirements.

9.5 Test Data Correlation

It is recommended that Kaman Aircraft Corporation assist in the initial data correlation effort. This participation will provide guidance to AFMDC personnel during the initial effort in operating the performance computer program, correlating the test data and planning future tests. This is considered to be the most effective means of transferring the detail knowledge related to the theory and developing AFMDC capability in the design of air bearing slippers.

REFERENCES

1. Technical Exhibit "A", Contract No. AF 29(600)-5516, Air Force Missile Development Center, February 11, 1966.

2. Gross, W.A., Gas Film Lubrication, John Wiley and Sons, 1962.

3. Tipei, N., Theory of Lubrication, Stanford University Press, 1962.

4. Schlicting, H., Boundary Layer Theory, McGraw-Hill Company, 1960.

5. "Monthly Letter Report No. 21 on Contract AF 33(615)-1312", Research Institute, University of Dayton, February 1966.

6. Pinkus, O. and Sternlicht, B., Theory of Hydrodynamic Lubrication, McGraw-Hill Company, 1961.

7. Istracon Handbook, Istracon Report No. 60-1, Air Force Systems Command, December 1961.

8. Tendeland, T., et al, The Flow Field Over Flat Plates and Its Effect on Turbulent Boundary-Layer Growth and Heat Transfer at a Mach Number of 4.7, TND-689, National Aeronautics and Space Administration, February 1961.

9. Rom, J., Near Wake Flow Studies in Supersonic Flow, TAE Report No. 38, Technion Research and Development Foundation, March 1965.

10. Constantinescu, V.N., On Turbulent Lubrication, Proceedings of the Institute of Mechanical Engineers, Volume 173, No. 38, 1959.

11. Constantinescu, V.N., On Gas Lubrication in Turbulent Regime, Trans. of ASME, Journal of Basic Engineering, Series D, September 1964.

APPENDIX I

SELF-ACTING SLIPPER BEARING ANALYSIS AND RESULTS

The analysis summarized below was adopted from that given in Reference (3) with a number of related assumptions. The assumptions, with regard to the slipper bearing problem, are also discussed below and the results of the analysis are included at the end of this section. Details of the analysis and a description of the operation of the performance program are given in Appendix IV.

Analysis

The performance analysis for turbulent, self-acting bearings parallels the analysis of laminar bearings with the basic turbulent flow analysis from boundary layer theory. The approach is to introduce the time-averaged values of the velocities and lubricant properties into the Navier-Stokes equations and then perform standard bearing analysis order of magnitude estimates. The reduced differential equations then contain terms involving the turbulent or apparent stresses which are replaced by suitable expressions derived from the Prandtl mixing length hypothesis.

The turbulent stresses are represented by:

$$\tau = \rho \ell^2 \frac{\partial u}{\partial y}\left|\frac{\partial u}{\partial y}\right| \qquad (1)$$

where ℓ is the mixing length, whose value is determined by experiment. After introducing expressions similar to Equation (1) for the turbulent shear stresses into the reduced Navier-Stokes equations, and integrating the result, the following equation for the pressure gradient within the slipper-rail gap is obtained:

$$\frac{dp}{dx} = \frac{\mu V}{2h^2}\left[12 + 0.14\, R^{*0.725}\left(\frac{\rho h}{\rho_m h_m}\right)^{0.725}\right]\left(1 - \frac{\rho_m h_m}{\rho h}\right) \qquad (2)$$

$$R^* = \frac{\rho_m V h_m \sigma^2}{0.16\,\mu}$$

In Equation (2), the subscript M denotes the fluid and geometric properties of the bearing at the maximum pressure point. This equation was derived assuming that the flow within the gap is isothermal, the mixing length varies linearly from zero on the wall to a maximum at the center of the gap, and the film is two dimensional (no side flow). The term σ represents the mixing length gradient at the walls.

$$\left(\frac{\partial l}{\partial y}\right)_{y=0,h} = \pm \sigma \qquad (3)$$

To obtain the pressure profile within the slipper gap, and therefore determine the load and center of pressure, it is necessary to integrate Equation (2). Even for a simple wedge-shaped gap, the equation is not integrable, and in Reference (3), the author was forced to linearize a portion of the equation to obtain a closed-form solution. The linearization limits the applicability of the equation, and as a result, a computer program was developed to integrate the equation numerically.

Assumptions

1. Isothermal Flow in the Gap

In conventional air bearing analysis, it is usually assumed that the flow in the gap is isothermal. However, for the slipper bearing, this may not be the case. The very high speed of the slipper and the possible use of an insulating coating may cause the flow to be closer to adiabatic conditions. The usual order of magnitude calculations are difficult to apply since the flow is highly turbulent and the effective heat transfer rate must be determined. Since the viscosity of air increases with temperature, air bearing analyses, similar to one given in Reference (5), indicate adiabatic operation results in higher load capacities than isothermal operation. For this reason, the isothermal analysis was chosen to define the lower performance limits of the slipper bearing.

2. Two-Dimensional Film

The assumption of a two-dimensional film is consistent with standard bearing analyses. It has been found in practice that high speed bearing performance can be adequately predicted by assuming no side flow exists.

3. Representation of the Mixing Length

The form chosen to represent the mixing length and the value of the gradient of the mixing length at a solid wall has a direct effect on bearing performance. In Reference (3), the author assumes a linear variation of the mixing length and in subsequent analysis, assumes $\sigma' = 0.4$. This is consistent with boundary layer analysis, verified by experiment. For a free turbulent boundary layer, the mixing length does vary linearly with a gradient of 0.4 in the region of the surface. This is shown in Reference (4). In the case of a turbulent lubricating film, the distance from the surface (rail or slipper) to the center of the gap falls well within the region where this relation holds.

4. Inlet Pressure

The inlet pressure of a self-acting air bearing has a direct influence on its load capacity. For this reason, it was assumed that the inlet pressure of the self-acting slipper bearing was the static pressure behind a normal shock standing at the front lip of the slipper. Unless the slipper is placed in a base flow region (shielded by the sled or a flow deflection device), this would be the minimum available inlet pressure that the slipper would operate with. This assumption is especially valid for the lower lips of the slipper since this lip is protected by the rail head.

5. Development of the Lubricating Film

In the analysis of conventional air bearings, the inlet and exit effects on overall performance are usually ignored. Although the exit effects of a self-acting rocket sled slipper bearing may be ignored, in some cases it is necessary to examine the development of the lubricating layer in the inlet region. The schematic shown in Figure 35 illustrates the flow situation in the forward portion of the slipper-rail gap for a typical case. The case selected corresponds to the monorail front slipper operating at Mach 6. Representative velocity profiles in this region of the gap are shown in Figure 36.

The schematic in Figure 35, which is drawn approximately to scale, shows the boundary layers which build up on the rail and slipper do not completely fill the gap until a position approximately two to three inches from the inlet is reached. For an eighteen-inch slipper, this amounts to ten to fifteen percent of the entire slipper where the lubrication analysis does not completely apply. In this case, the total error is not very great since the pressure increase in this region, as predicted by the theory, is not large. However for very

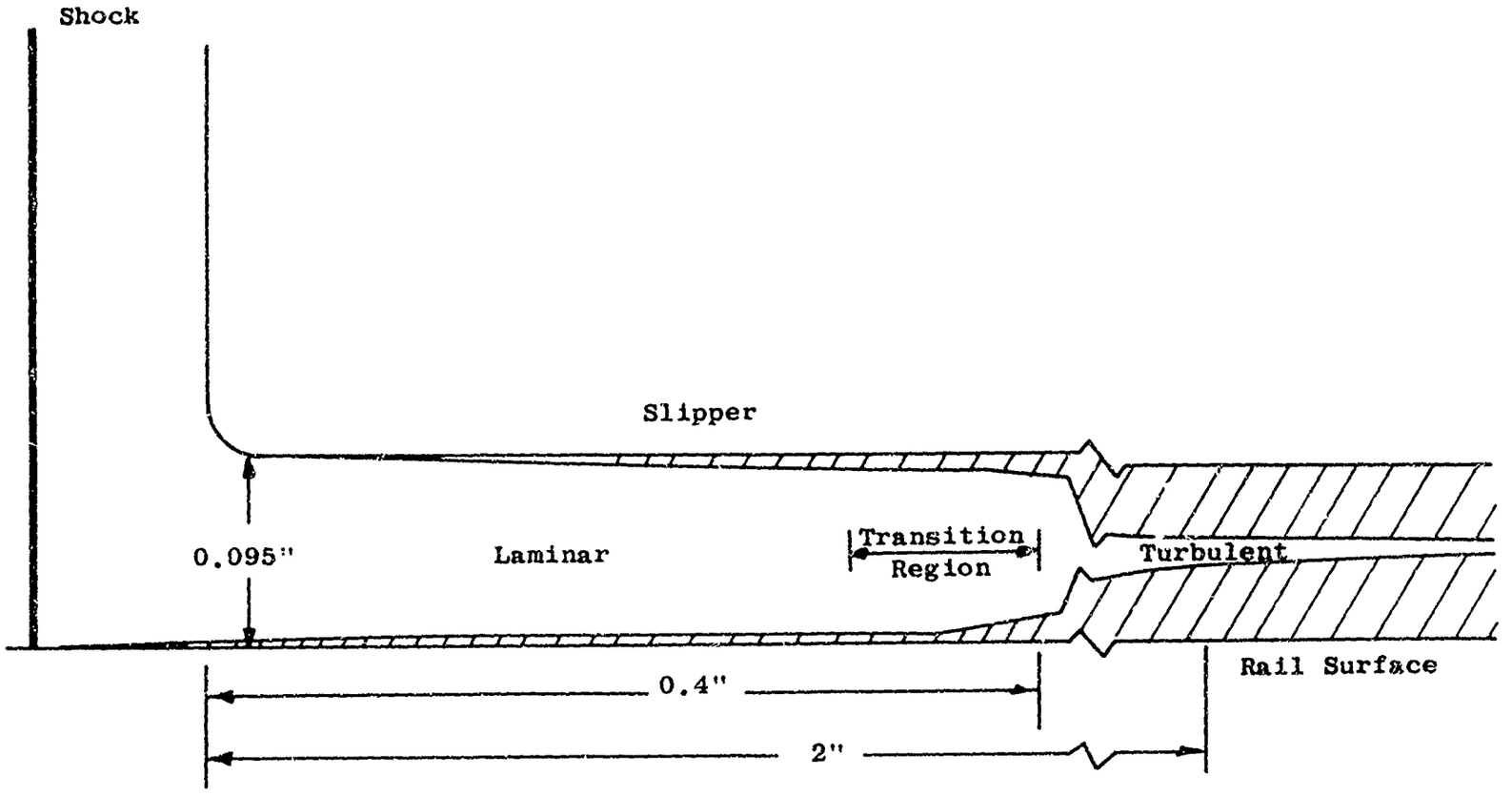

Figure 35. Typical Flow Pattern at the Slipper-Rail Gap Inlet

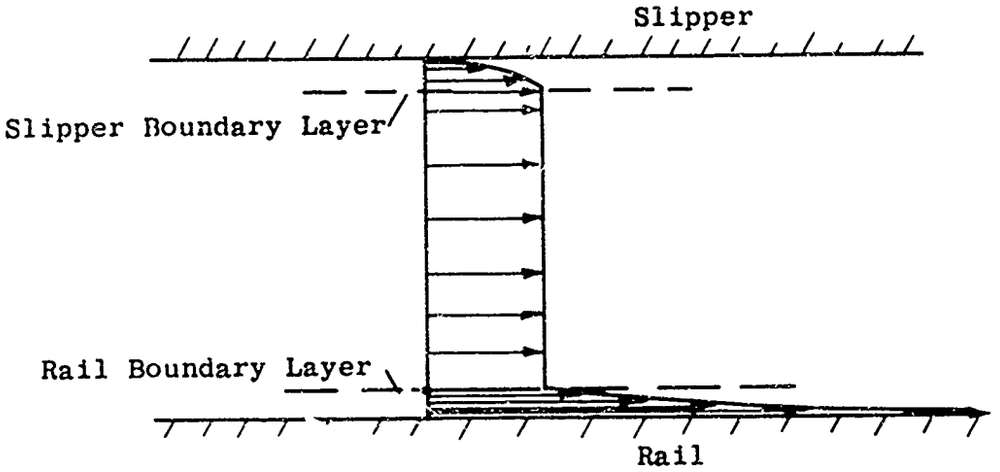

(a) Near Transition From Laminar to Turbulent Flow

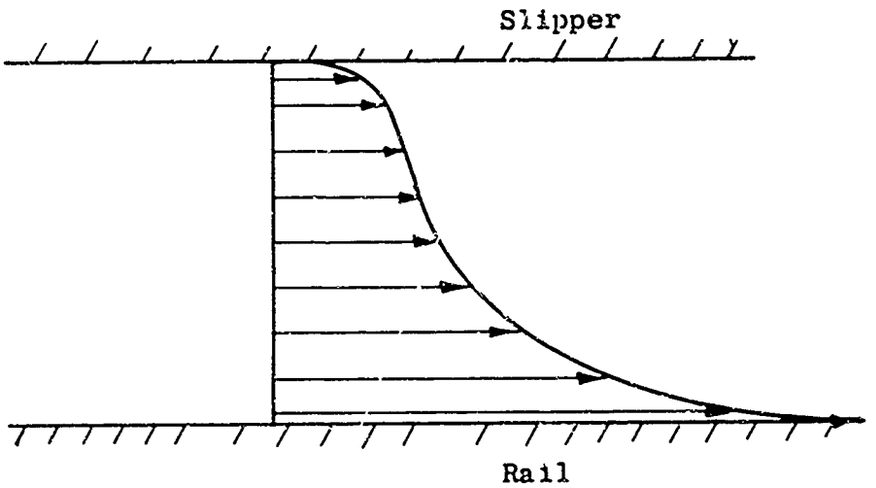

(b) Fully Developed Turbulent Film

Coordinate System Fixed in the Slipper

Figure 36. Typical Velocity Profiles in the Slipper-Rail Gap

small slippers (less than six inches), this effect is quite pronounced and a suitable correction factor must be included in the design.

Results

The computer program developed for this study was used to generate performance data for typical rocket sled self-acting slipper bearings. This performance data, in its most useful form, is presented in Figure 37 where the nondimensional load parameter and center of pressure are plotted as a function of minimum slipper-rail gap for various slipper lengths and gap slopes. In the load parameter (F/P_1L), F is the load per unit width of bearing surface, P_1 is the inlet pressure (the pressure behind a normal shock), and L is the slipper length. All units are consistent, and for this reason, the gap is given in feet rather than in inches (as in Figure 6).

It was found that no effect of Mach number for cases between Mach 1 and Mach 6 occurred if the performance was nondimensionalized with the pressure behind a normal shock at the desired Mach number. The slight differences that do occur are negligible and the curves may be used for any speed within this range. This result is due to the combination of pressure, velocity, and viscosity variations with the basic form of the equation.

The load per unit width of bearing surface is calculated assuming the pressure acting on the other side of the slipper is zero. Thus,

$$F = \int_0^L (P(x) - P_e)\, dx$$

where P_e is the exterior pressure, reduces to

$$F = \int_0^L P(x)\, dx$$

This form was chosen for convenience in calculating the actual bearing load, as explained in Appendix II.

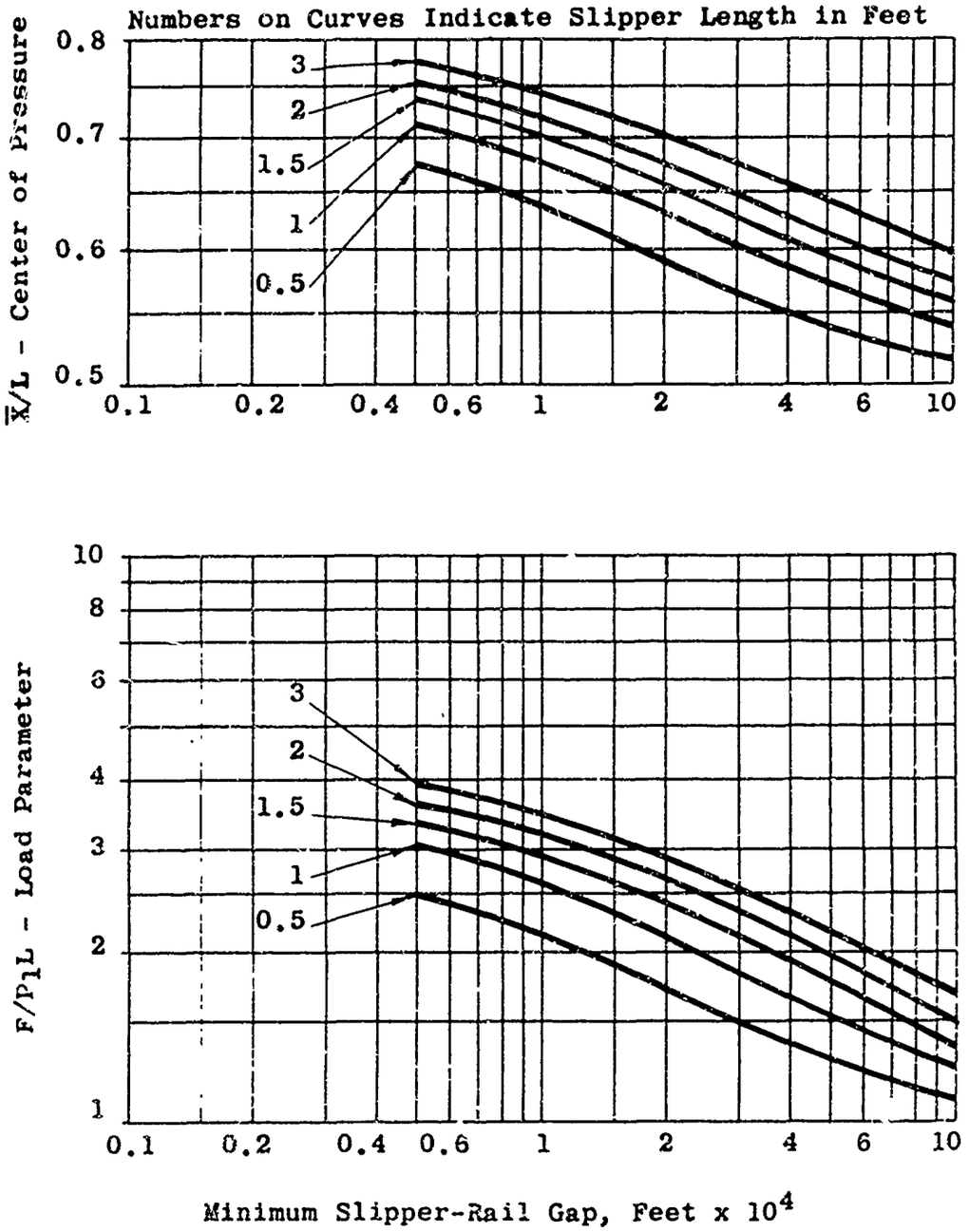

(a) Slipper Slope = 0.001

Figure 37. Self-Acting Slipper Bearing Performance

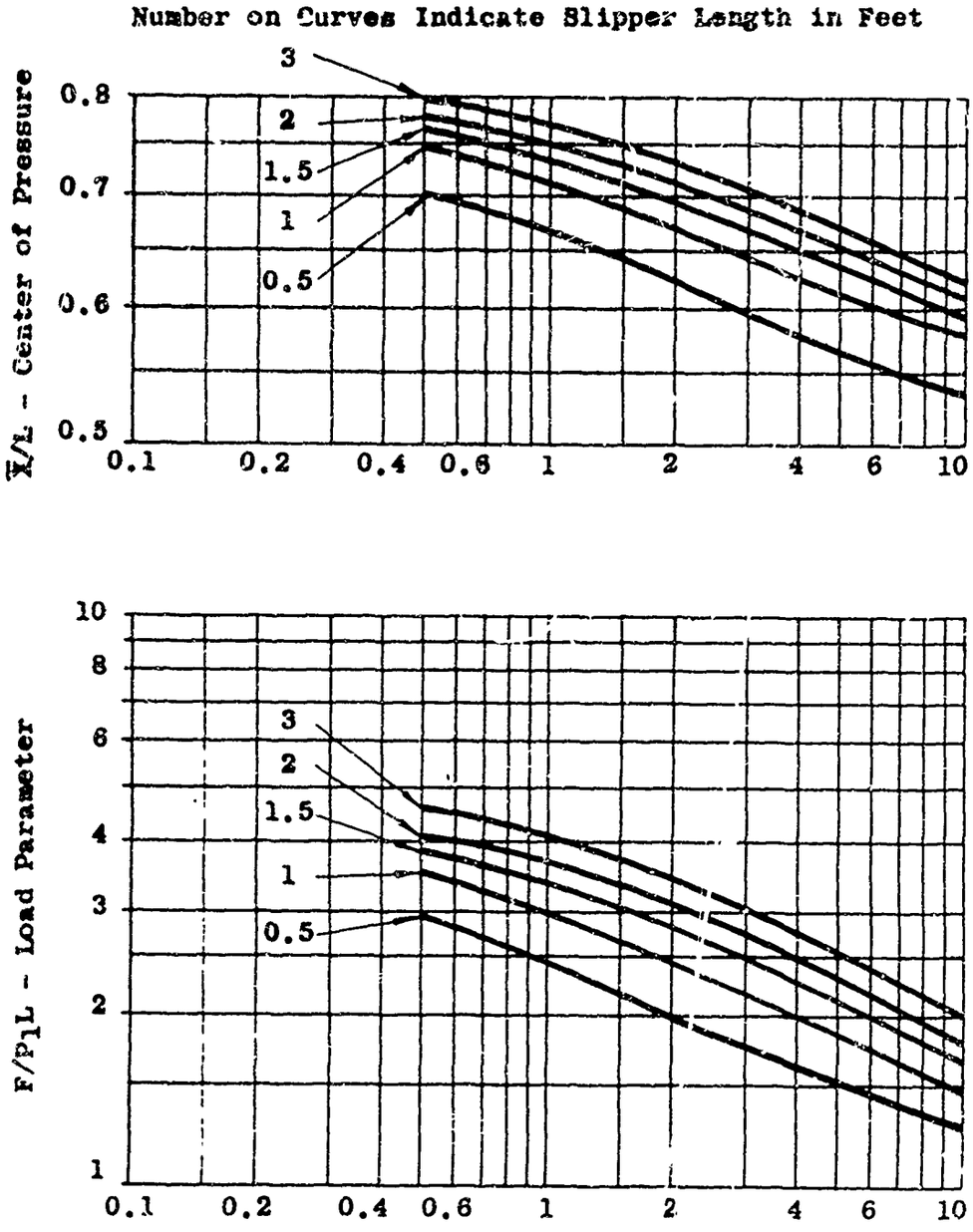

(b) Slipper Slope = 0.002

Figure 37. Continued

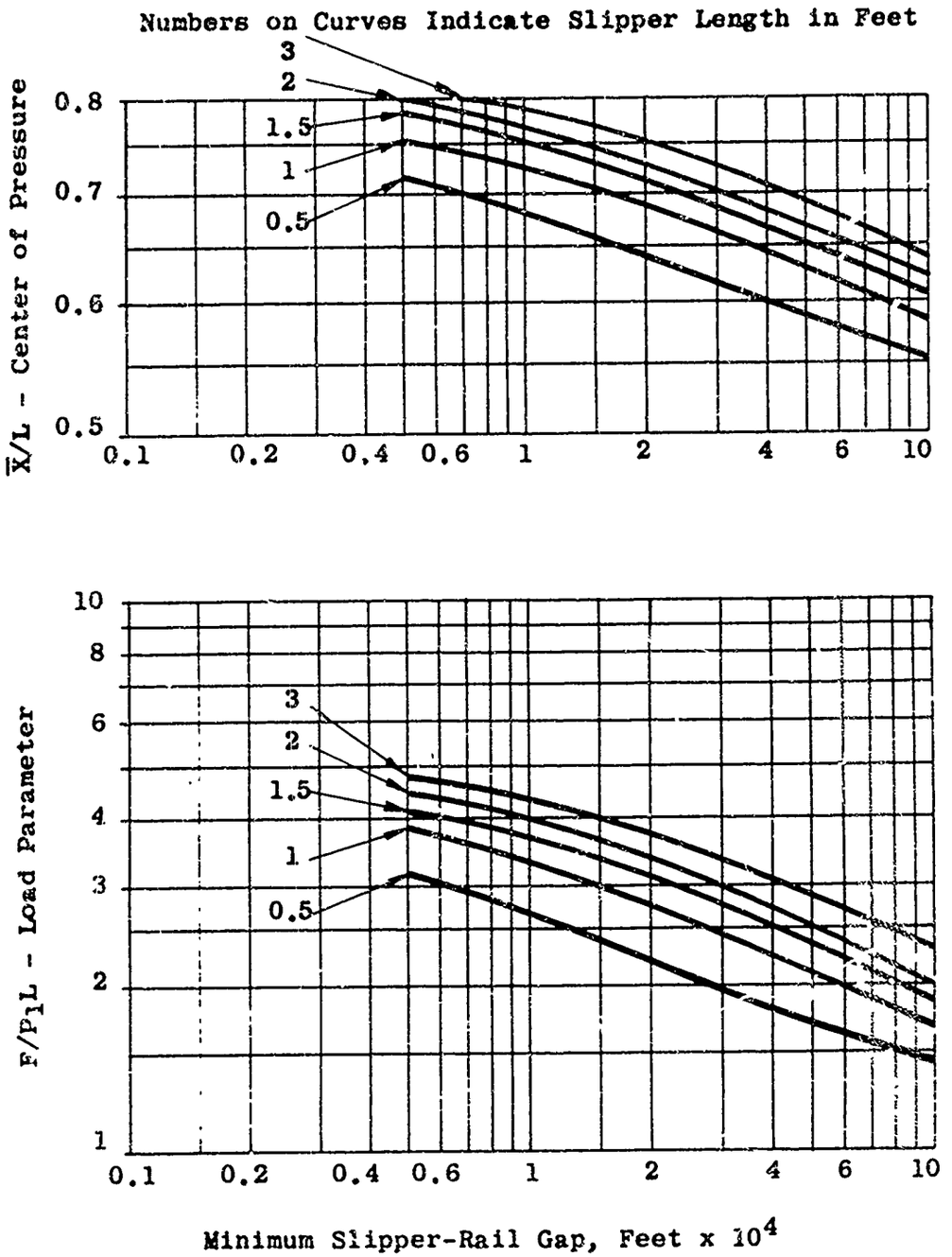

(c) Slipper Slope = 0.003

Figure 37. Continued

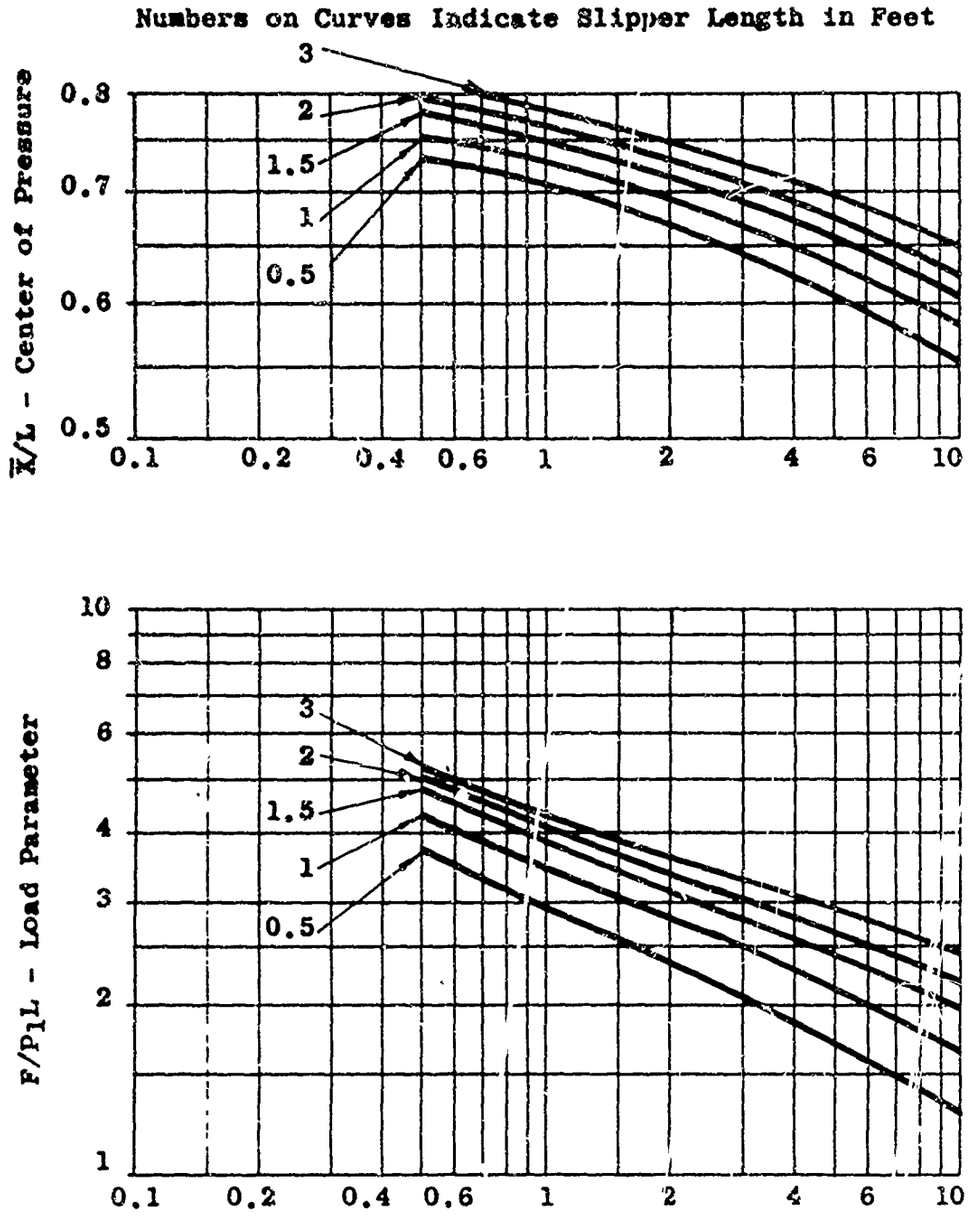

(d) Slipper Slope = 0.005

Figure 37. Concluded

APPENDIX II

USE OF THE SLIPPER PERFORMANCE CURVES

The application of the self-acting slipper bearing performance curves given in Figure 37 is presented below with a numerical example to clarify the procedure. The applicability of the curves to a typical sled run is also verified.

Determining the Slipper Bearing Requirements

To use the slipper performance curves it is first necessary to establish the actual load requirements. The actual load requirement is not only the applied load, but also includes (1) the opposing force developed by the opposite side of the slipper (discussed in Section 3.4.1) and (2) any net exterior force caused by the external flow field.

These forces are depicted in Figure 38. In Figure 38(a), the basic bearing force given in Figure 37 is based on assuming the exterior pressure is zero. The same system is used for calculating the opposing force as shown in Figure 38(b). Any net external aerodynamic force is calculated by assuming the pressure within the slipper gap is zero, as in Figure 38(c). When these forces are added, the reference pressure, (in this case zero), cancels out.

The opposing force may be calculated by assuming that the inlet pressure acts over the entire length of the slipper. Besides adding a slight safety factor, this assumption greatly simplifies the actual calculation. The external force may be obtained from Figure 42 in Appendix III or from other appropriate data.

Numerical Example

The case chosen for an example corresponds to the slipper shown in Figure 9. This slipper is 1.5 feet long and operates with a slope of 0.005 on the lower lip at Mach 6. The upper and lower bearing surfaces are both 0.1667 feet wide (2 inches) and the gap inlet pressure is 75,300 psf. A curve showing the gap inlet pressure as a function of Mach number is given in Figure 39.

The total bearing force required is:

$$Fb = Fa + Fp + Fe$$

where Fa is the applied slipper loading, Fp is the force developed by the opposite side of the slipper and Fe is the net external aerodynamic force. At the Mach 6 operating condition,

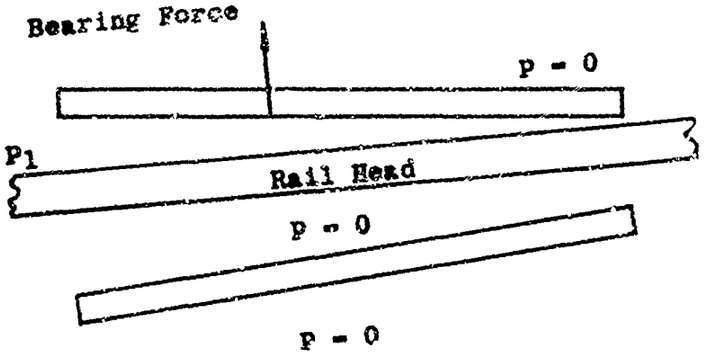

(a) Bearing Force

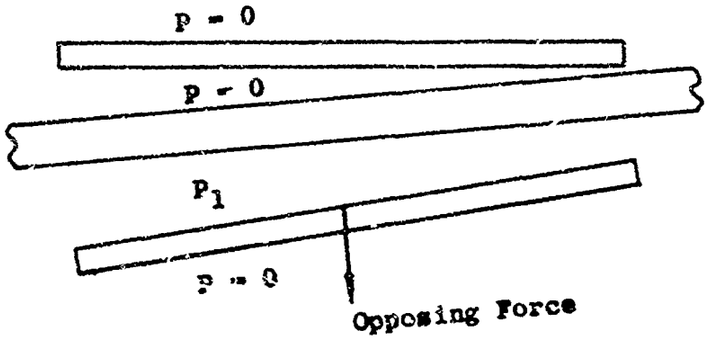

(b) Opposing Force

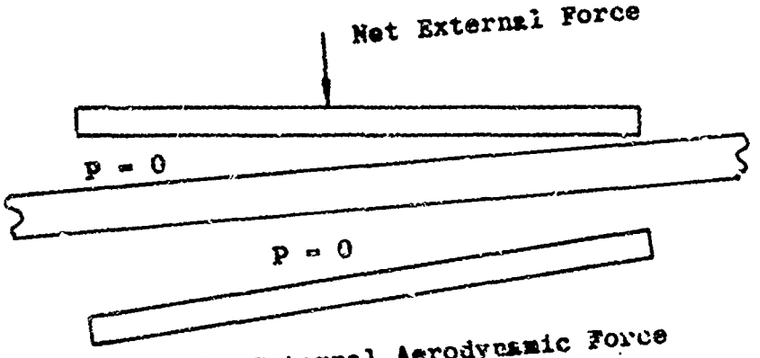

(c) External Aerodynamic Force

Figure 38. Forces on the Slipper Bearing

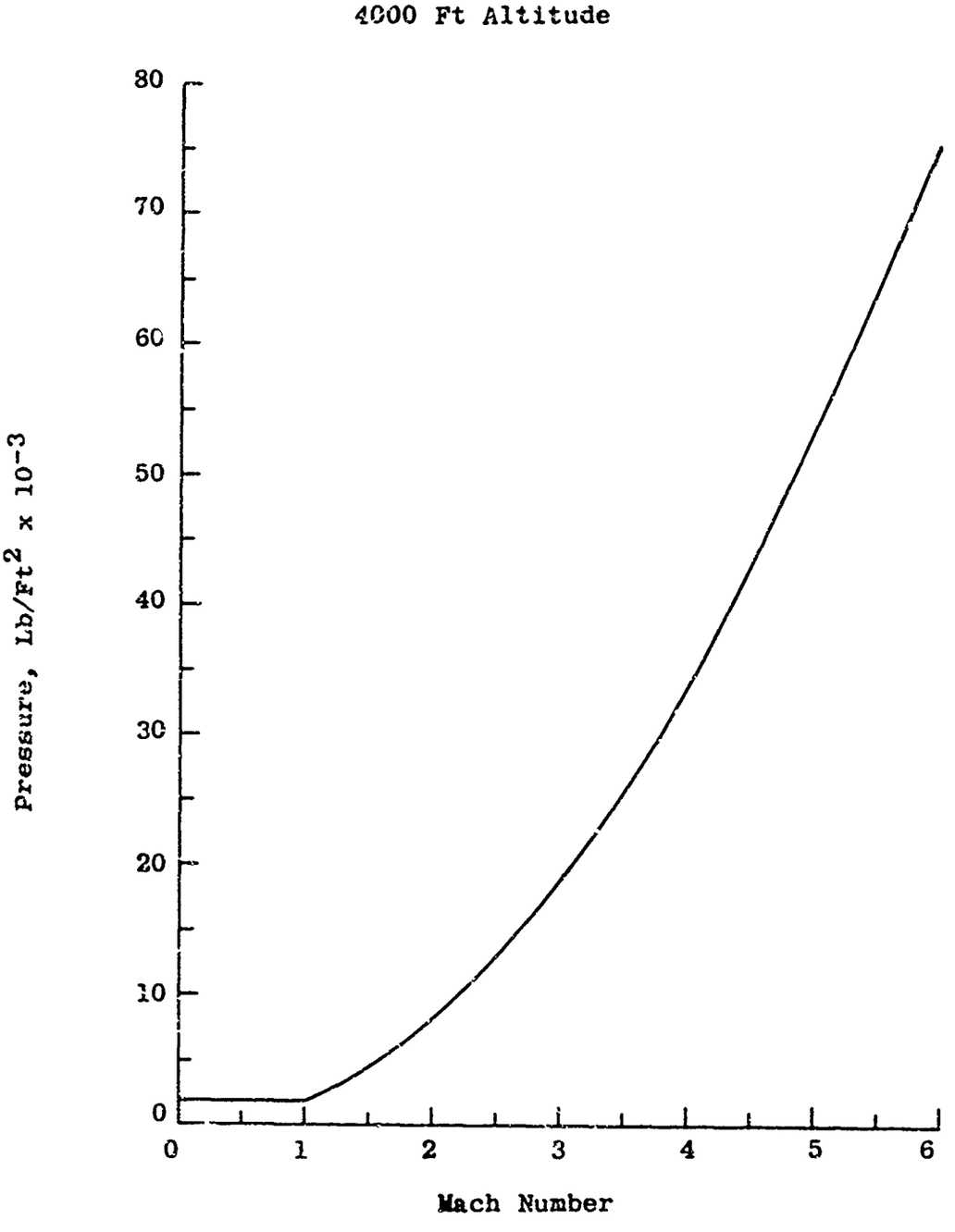

Figure 39. Gap Inlet Pressure Vs Mach Number

the applied force, Fa, is 37,000 pounds for the front monorail slipper. This force is an upload. The external force, Fe, is 6,750 pounds (Figure 42) and acts downward. The opposing force, Fp, is given by,

$$Fp = \text{inlet pressure} \times \text{slipper length} \times \text{bearing width}$$

$$= 75{,}300 \times 1.5 \times 0.1667 = 18{,}800 \text{ pounds.}$$

Therefore the total bearing force is;

$$Fb = 37{,}000 - 6{,}750 + 18{,}800 = 49{,}050 \text{ pounds}$$

To calculate the load parameter (F/P_1L) it must be remembered that F is the bearing force per unit width of surface. Therefore,

$$\frac{F}{P_1L} = \frac{Fb/\text{width of surface}}{P_1L}$$

$$= \frac{49{,}050/0.1667}{75{,}300 \times 1.5} = 2.61$$

From Figure 37(d), a load parameter of 2.61 and a slipper length of 1.5 feet corresponds to a minimum slipper-rail gap of 4.2×10^{-4} feet (0.005 inches). This is the value shown in Figure 10 at the Mach 6 operating condition.

In the preceding example a slipper slope of 0.005 was chosen. This slope is approximately optimum for all combinations of slipper length and minimum slipper-rail gap. A cross plot of data in Figure 37, illustrating this fact is presented in Figure 40. This figure shows the variation of the load parameter of a 1 foot slipper with slipper slope for various minimum slipper-rail gaps. As shown in the figure, all of the cases achieve a maximum load parameter (and therefore a maximum load capacity) at a slipper slope of 0.005.

The data shown in Figure 40 also illustrates that the variation of load parameter with slipper slope is small in the region of the optimum. This is a particularly desirable characteristic since it eliminates the need for precise alignment of the slipper on the sled. Slight misalignment of the slipper will not result in an appreciable change in load capacity.

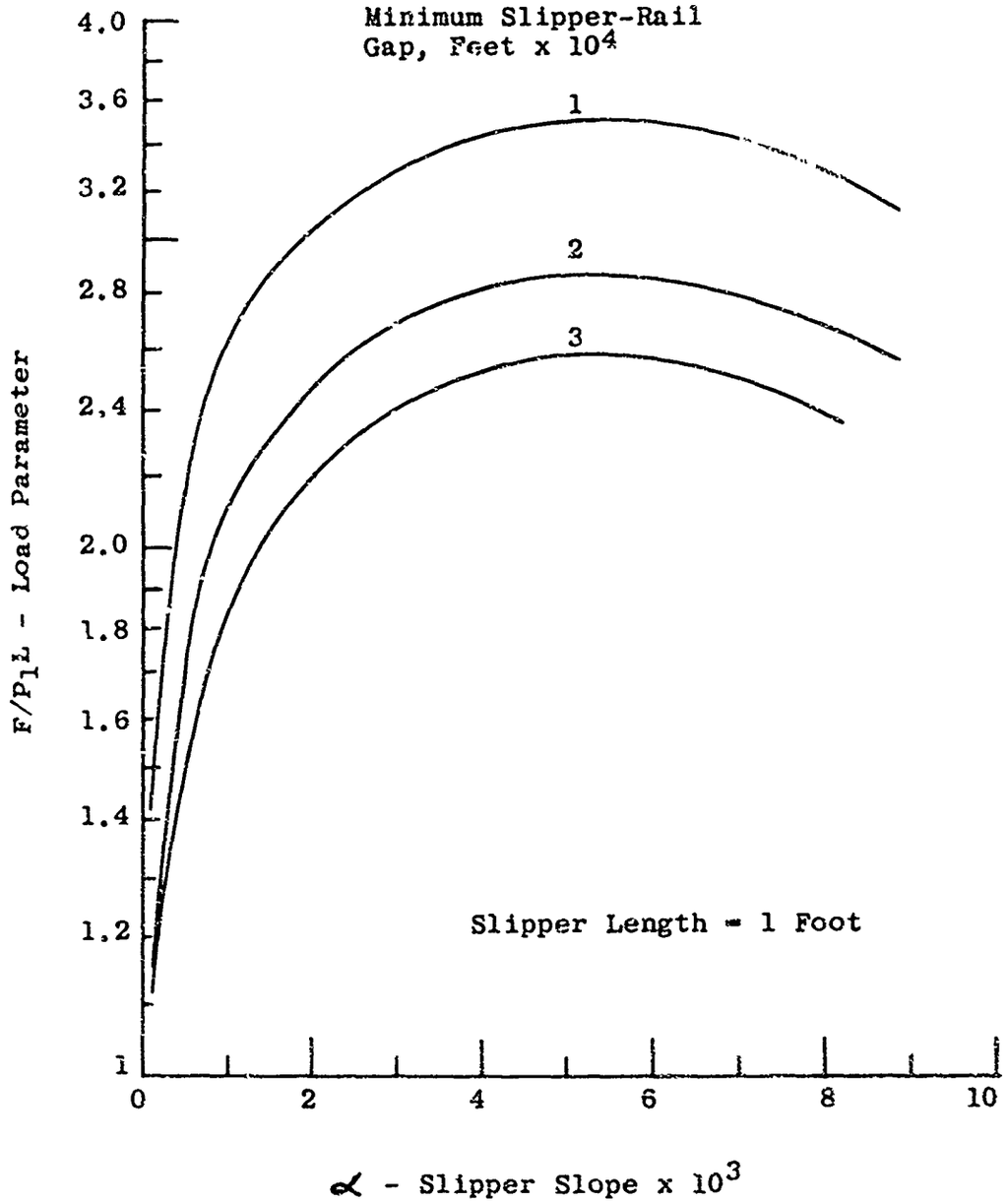

Figure 40. Effect of Slipper Slope on Performance

Application to a Typical Sled Run

The data shown in Figure 10 was obtained by applying the procedure outlined above to various speeds and the corresponding loads of the monorail sled front slipper. The validity of using the steady state performance of an air lubricated slipper for the highly transient loading conditions shown in Figure 2 can be verified by an order of magnitude calculation.

As an example, the highest rate of velocity and load changes occur near the maximum velocity of the monorail sled. These were estimated at 3500 ft/sec^2. and 150,000 lb/sec. from Figure 2. The characteristic time interval, during which variations in sled loading and velocity must be small for a quasi-steady analysis to be valid, is the time required for a mass of air to move from the inlet to the exit of the slipper. Since the air velocity within the gap varies from zero to the sled velocity, the average velocity may be approximated by a straight average. This time interval, for the maximum velocity point, is then

$$t \approx \frac{\text{Slipper Length}}{\frac{1}{2}\ \text{Sled Velocity}} = \frac{1.5}{\frac{1}{2}\ (6600)} = 4.55 \times 10^{-4}\ \text{sec.}$$

The corresponding load and velocity changes during this interval are 68 pounds and 1.6 ft/sec. These changes are very small compared to the absolute values of load and velocity. Therefore, the quasi-steady analysis of the slipper performance is valid. This conclusion also applies to the effect of unsteady heat input during a typical run, since the temperature of the air entering the slipper-rail gap is directly related to the sled velocity.

APPENDIX III

EXTERNAL AERODYNAMIC LOADS

To calculate the total slipper bearing load requirements, it is necessary to determine the net force on the slipper due to the external flow field. For this purpose, a slipper configuration which would have a maximum net external aerodynamic load was selected for analysis. This configuration, taken from Reference (7), is shown in Figure 41(a). A cross-section of this configuration, showing a strut inserted into the recess and approximate shock locations and shapes, is given in Figure 41(b).

In the arrangement shown in Figure 41, the shock generated by the lower lips of the slipper will curve backward from the lip, reflect off the lower flange of the rail, and then intersect the lower lip surface again. The shock eminating from the upper surface would be similar in shape but would merge with the shock sheet generated by the attachment structure. To determine the shock shapes and surface pressure distributions, the analysis presented in Reference (8) was used. It was found that the loads due to the lip generated shock were quite small. Also, the reflected shock (from the lower rail flange) did not intersect the lower lip of a 1.5 feet long slipper at speeds above Mach 2.5. Below this speed, the effect of the reflected shock on the surface pressure distribution is small, and no appreciable increase in external load occurs.

The main contribution to the external slipper bearing aerodynamic load is due to the flow around the slipper attachment structure. As shown in Figure 41(b), an irregularly-shaped shock sheet will stand off the front of this structure. A base flow region, where the pressure is very low, will exist directly behind this structure. If the strut is arranged as shown in the figure, air will flow through the internal recess of the slipper attachment mechanism from the area market "inlet" through the area marked "exit".

The pressure of the air entering the inlet area will be very high due to the shock sheet directly in front of the structure. The pressure directly outside the exit area would be quite low due to the base area effect. Since the "inlet" and "exit" areas would be approximately the same size, this passage acts like an unstarted supersonic wind tunnel and the pressure within the recess will be approximately the same as the inlet pressure. This pressure would be quite high (static pressure behind a normal shock) and the download caused by this

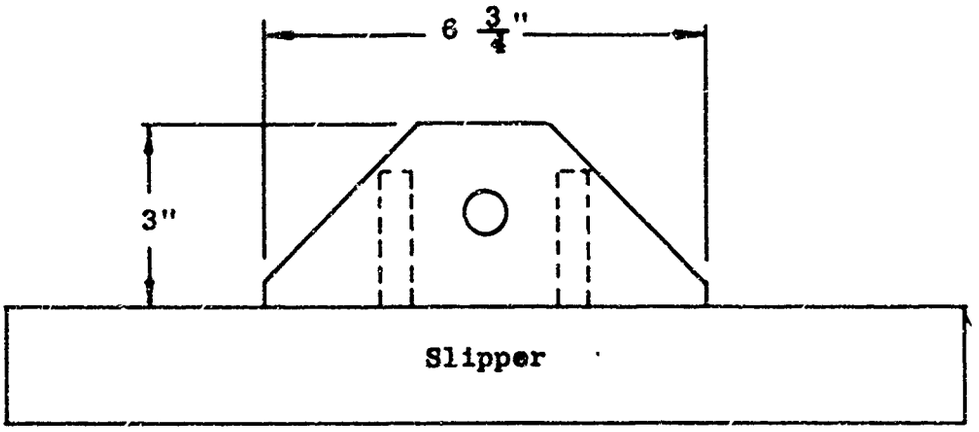

(a) Slipper Attachment Structure

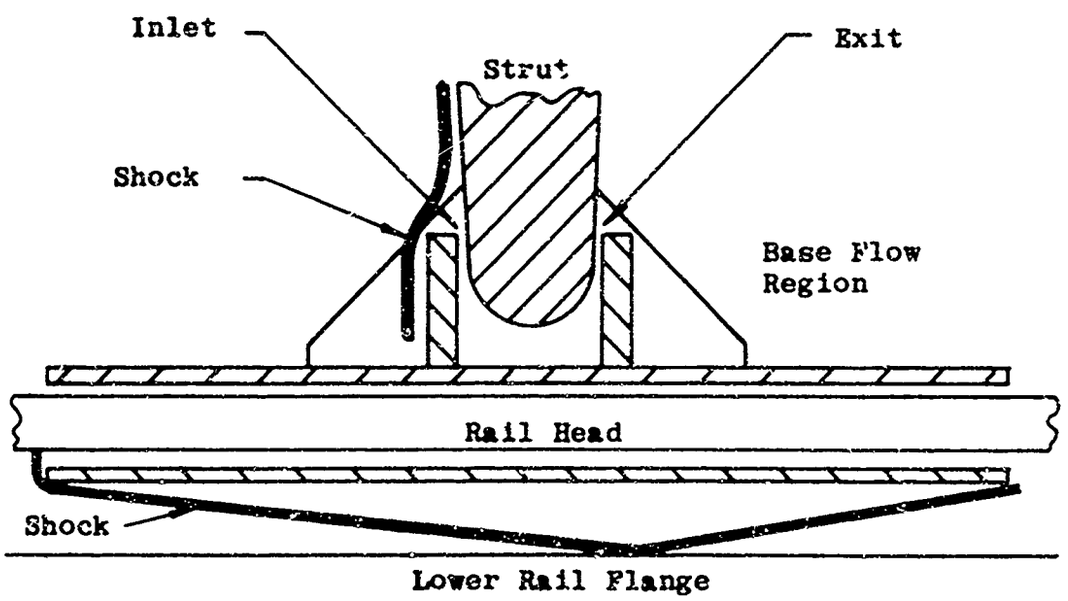

(b) Approximate Flow Field

Figure 41. Slipper Model for External Flow Analysis

effect would far outweigh any loads due to the surface pressure distribution.

The base pressure region behind the strut structure does result in a small upload which partially compensates for the download caused by the recess. The pressure within this region and the extent of the region were calculated using the data presented in Reference (9). (This data was also used to determine the exit pressure of the slipper gap).

The attachment structure for the sled strut was assumed to be the same size for any length slipper. Since the force due to the high pressure in the structure recess dominates the total external aerodynamic slipper force, this load may be used for any slipper length between 0.5 and 3 feet. This force, as a function of sled Mach number, is given in Figure 42.

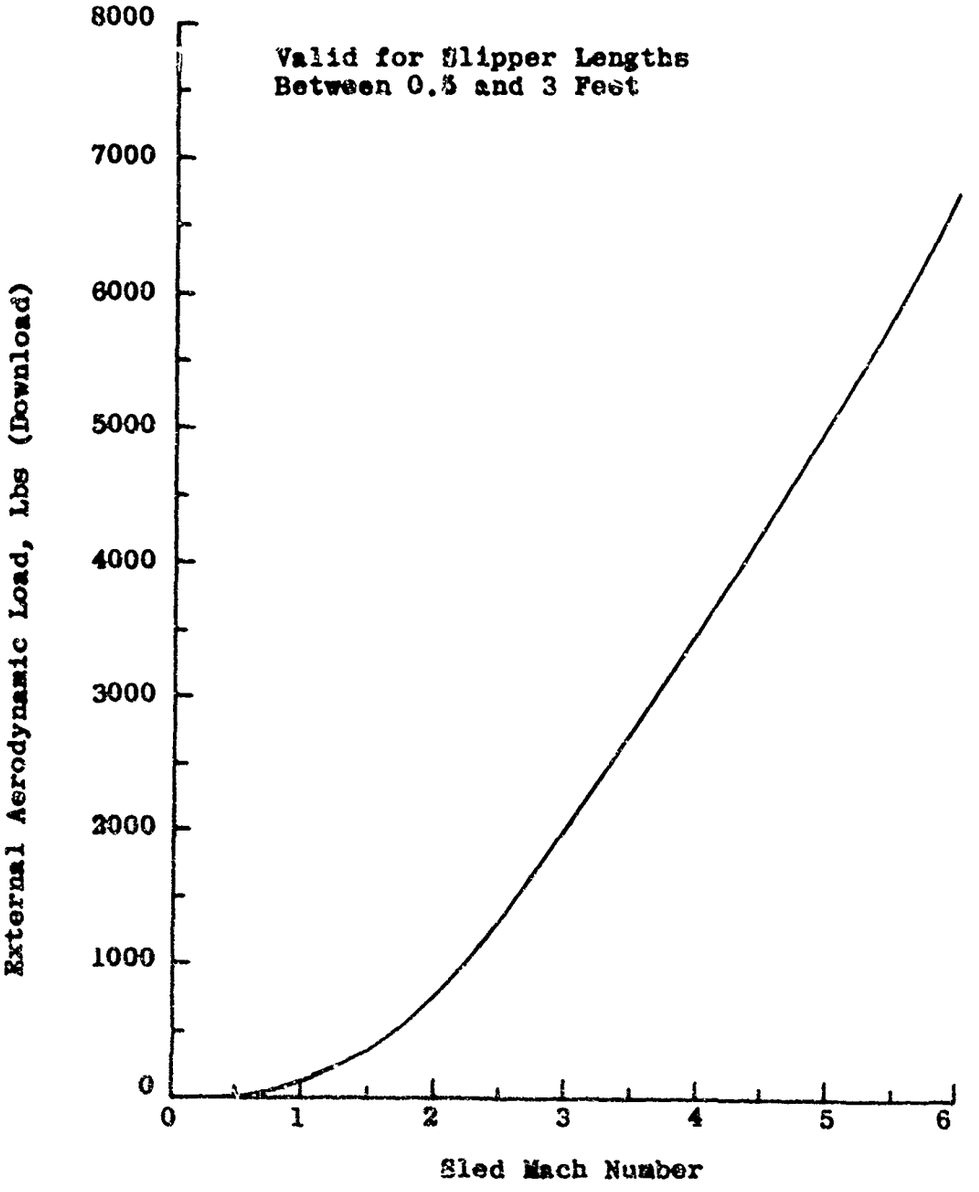

Figure 42. External Aerodynamic Slipper Loads

APPENDIX IV

TURBULENT BEARING ANALYSIS

The analysis used to derive the pressure gradient equation given in Appendix I is presented below with a brief description of the computer program used to numerically integrate the equation.

Approach

The approach used in the development of the basic pressure gradient equation presented in Appendix I follows the method given in References (3) and (10).

1. The components of the turbulent velocity vector and their properties are defined in the same manner as for the analysis of turbulent boundary layers.

2. These components are introduced into the Navier-Stokes equations and the time averaged values are used to reduce the equations. This procedure then limits the equations to the macroscopic flow properties.

3. Standard order of magnitude analyses for bearings are applied to the equations reducing them to the differential equations for turbulent bearings.

4. The Prandtl mixing length hypothesis is used to express the turbulent shear stresses in terms of the velocity gradients and the mixing length. This permits the integration of the differential equations.

5. An approximation on the "exact" solutions of the integration permits the pressure gradient within the bearing gap to be expressed in a simple form as a function of the bearing geometry, velocities of the boundaries, and the properties of the lubricant.

6. The overall bearing performance is then obtained by integrating the pressure gradient equation numerically.

Procedure

The analysis of the turbulent bearing begins with the Navier-Stokes equations, one of which is given in Equation (1)

$$\rho \frac{Du}{Dt} = -\frac{\partial p}{\partial x} + \frac{\partial}{\partial x}\left\{\mu\left[2\frac{\partial u}{\partial x} - \frac{2}{3}\left(\frac{\partial u}{\partial x} + \frac{\partial v}{\partial y} + \frac{\partial w}{\partial z}\right)\right]\right\}$$

$$+ \frac{\partial}{\partial y}\left[\mu\left(\frac{\partial v}{\partial x} + \frac{\partial u}{\partial y}\right)\right] + \frac{\partial}{\partial z}\left[\mu\left(\frac{\partial w}{\partial x} + \frac{\partial u}{\partial z}\right)\right] \qquad (1)$$

Similar equations are obtained for the Dv/Dt and Dw/Dt terms where

$$\frac{D}{Dt} = \frac{\partial}{\partial t} + u\frac{\partial}{\partial x} + v\frac{\partial}{\partial y} + w\frac{\partial}{\partial z}$$

The velocities of the turbulent flow are defined in the standard manner (See Reference (4), Chapter XVIII),

$$\begin{aligned} u &= \bar{u} + u' \\ v &= \bar{v} + v' \\ w &= \bar{w} + w' \end{aligned} \qquad (2)$$

where $\bar{u}$ is the mean velocity in the x direction, and u' is a pulsation or fluctuating velocity. In the same manner,

$$\begin{aligned} p &= \bar{p} + p' \\ \rho &= \bar{\rho} + \rho' \end{aligned} \qquad (3)$$

The mean values of these properties are defined as:

$$\bar{a} = \frac{1}{T}\int_{t-T/2}^{t+T/2} a\, dt \qquad (4)$$

where the time interval T is, by definition, long enough for the mean values to be independent of time. Thus:

$$\bar{u}' = \bar{v}' = \bar{w}' = \bar{p}' = \bar{\rho}' = 0 \qquad (5)$$

where the bar notation denotes the time averaged values of the pulsations.

The approach up to this point is identical with turbulent boundary layer analysis. Substituting expressions (2) and (3) into Equation (1), and taking the time averaged values, the right-hand side of Equation (1) remains the same with all of the quantities replaced by their mean values ($\bar{u}, \bar{v}, \bar{w}, \bar{p}$). However, the left-hand side of Equation (1) becomes

$$\bar{\rho}\frac{D\bar{u}}{Dt} + \frac{\partial}{\partial x}\left(\bar{\rho}\,\overline{u'^2}\right) + \frac{\partial}{\partial y}\left(\bar{\rho}\,\overline{u'v'}\right) + \frac{\partial}{\partial z}\left(\bar{\rho}\,\overline{u'w'}\right) \quad (6)$$

where continuity has been used to simplify the result.

$$\frac{\partial\bar{\rho}}{\partial t} + \frac{\partial}{\partial x}\left(\bar{\rho}\bar{u}\right) + \frac{\partial}{\partial y}\left(\bar{\rho}\bar{v}\right) + \frac{\partial}{\partial z}\left(\bar{\rho}\bar{w}\right) = 0 \quad (7)$$

Thus, the left-hand side of Equation (1) contains, in addition to the usual inertia terms, the so-called apparent or turbulent stresses. The complete set of stresses are given by:

$$\begin{pmatrix} \tau_{xx} & \tau_{xy} & \tau_{xz} \\ \tau_{yx} & \tau_{yy} & \tau_{yz} \\ \tau_{zx} & \tau_{zy} & \tau_{zz} \end{pmatrix} = -\bar{\rho}\begin{pmatrix} \overline{u'^2} & \overline{u'v'} & \overline{u'w'} \\ \overline{v'u'} & \overline{v'^2} & \overline{v'w'} \\ \overline{w'u'} & \overline{w'v'} & \overline{w'^2} \end{pmatrix} \quad (8)$$

To specialize the general expressions obtained above for a bearing problem, the standard order of magnitude analysis applied for bearing problems is used. Referring to Figure 43, which gives the coordinate system for the bearing, this procedure reduces the equations to

$$\frac{\partial\bar{p}}{\partial x} = \mu\frac{\partial}{\partial y}\left(\frac{\partial\bar{u}}{\partial y}\right) + \frac{\partial}{\partial y}\left(-\bar{\rho}\,\overline{u'v'}\right) \quad (9)$$

To obtain Equation (9), the following assumptions and procedures have been used.

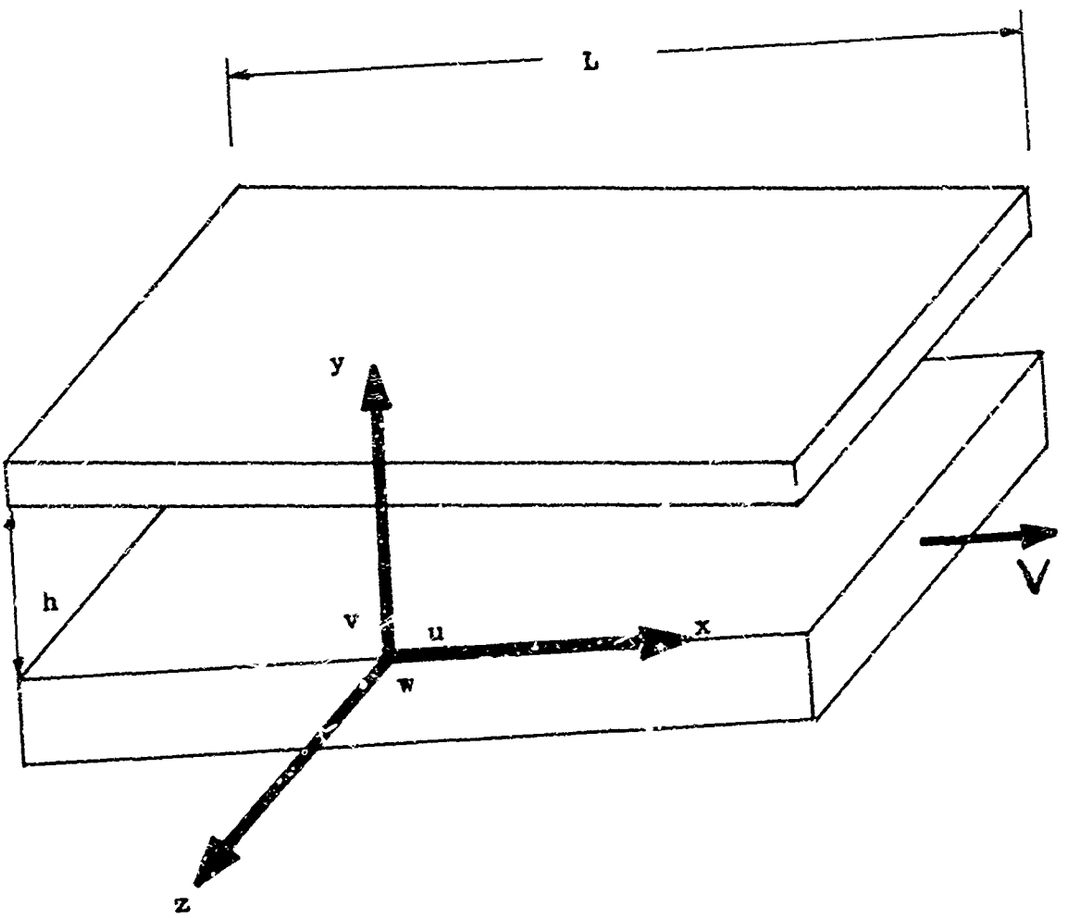

Figure 43. Bearing Coordinate System

1. The flow is considered two-dimensional. This eliminates one (z direction) of the Navier-Stokes equations.

2. The inertia terms, except for the turbulent stress terms, have been dropped. This is consistent with laminar bearing analysis, and in Reference (11), the author presents an estimate of the importance of the inertia terms which indicates these may be dropped for the slipper bearing problem.

3. An order of magnitude analysis, similar to that given in Chapter 8 of Reference (2), has eliminated many of the remaining terms. This analysis uses the fact that the characteristic dimension in the y direction, the bearing gap, is much smaller than the characteristic dimensions in the other directions. The net result is that variations of the fluid properties in the y direction (across the gap) are negligible, and the second Navier-Stokes equation may be eliminated as well as many of the terms in the first (x direction) equation.

At this point, the Prandtl mixing length hypothesis is introduced to handle the turbulent shear stress term,

$$-\bar{\rho}\,\overline{u'v'} = \bar{\rho}\,l^2 \frac{\partial \bar{u}}{\partial y}\left|\frac{\partial \bar{u}}{\partial y}\right| \tag{10}$$

In this expression, l is the mixing length, which must be determined experimentally. A complete discussion of the hypothesis and its physical significance may be found in Reference (4), Chapter XVIII. Substituting Equation (10) into Equation (9) yields:

$$\frac{\partial p}{\partial x} = \mu \frac{\partial}{\partial y}\left(\frac{\partial u}{\partial y}\right) + \rho \frac{\partial}{\partial y}\left(l^2 \frac{\partial u}{\partial y}\left|\frac{\partial u}{\partial y}\right|\right) \tag{11}$$

where the bar notation has been dropped. All terms are henceforth to be regarded as mean values.

Integrating Equation (11) and rearranging, the following expression is obtained

$$\rho l^2 \frac{\partial u}{\partial y}\left|\frac{\partial u}{\partial y}\right| + \mu \frac{\partial u}{\partial y} - \frac{\partial p}{\partial x} y + C_{x_1} = 0 \tag{12}$$

where

$$C_{x_1} = C_{x_1}(x)$$

The first term has the sign of $\partial u/\partial y$ and can be written as

$$\pm \rho l^2 (\partial u/\partial y)^2$$

Equation (12) then becomes

$$\frac{\partial u}{\partial y} = \frac{-\mu + \sqrt{\mu^2 \pm 4\rho l^2 [(\partial p/\partial x) y - C_{x_1}]}}{\pm 2\rho l^2} \qquad (13)$$

The solution of this equation will yield the velocity gradient across the bearing gap, and after integration, the velocity distribution. This process is described in Reference (3) and in more detail in Reference (10). The approach is to assume the form of the mixing length as

$$l = \sigma y \quad ; \quad 0 \le y \le h/2$$
$$l = \sigma (h - y) \quad ; \quad h/2 \le y \le h \qquad (14)$$

Thus, the mixing length varies linearly from the walls, where it is zero, out to the center of the gap where it is a maximum. The gradient, σ, is left as an open value to be determined experimentally. Next, the flow within the gap is broken up into laminar sublayers near the bearing walls and a fully turbulent flow in the remaining area. In the turbulent area, $\mu \partial u/\partial y$ may be neglected, and in the laminar areas, $\rho l^2 \partial u/\partial y |\partial u/\partial y|$ may be ignored (see Equation 12). There are various combinations of signs for $\partial p/\partial x$, C_x, and $\partial u/\partial y$ which yield different forms of the equations. For example, in the turbulent area, if $\partial p/\partial x$ is negative, $\partial u/\partial y$ is negative, and C_{x_1} is positive, then

$$\frac{\partial u}{\partial y} = -\sqrt{\frac{1}{\rho\sigma^2} \left(C_{x_1} - \partial p/\partial x \, y \right)} \Big/ y \qquad (15)$$

for $0 \le y \le h/2$. Consequently

$$u = C_{x_2} - \sqrt{\frac{C_{x_1}}{\sigma^2 \rho}} \left\{ 2M - \ln \frac{1+M}{1-M} \right\} \qquad (16)$$

where

$$M = \sqrt{1 - \frac{(\partial p/\partial x) y}{C_{x_1}}}$$

Equations similar to (16) for each combination of signs of $\partial p/\partial x$, $\partial u/\partial y$ and C_x, are obtained as shown in Reference (10). These are matched with the velocity profiles in laminar sublayers so that the velocity distribution and gradients agree when the sections are patched together. After determining the constants from the boundary conditions, complete velocity profiles are obtained.

It is then necessary to relate the pressure gradient to some easily determined property of the flow. For this purpose the mean velocity of the flow at any section is calculated.

$$u_m = \frac{1}{h}\int_0^h u \, dy \tag{17}$$

After this operation is performed, the results may be plotted as shown in Figure 44, which has been taken from Reference (3) and is also presented in Reference (10). As shown in the figure, the curves are very nearly straight lines and may be expressed as

$$\frac{\partial p}{\partial x} = -\left[12 + 0.14\left(\frac{\sigma^2}{0.16} R\right)^{0.725}\right]\frac{\mu}{h^2}\left(u_m - \frac{V}{2}\right) \tag{18}$$

where

$$R = \rho V h/\mu \quad .$$

The next step is to integrate the continuity equation (Equation 7) across the gap. If the quasi-steady, two-dimensional case with no surface velocities in the y direction is examined, the result is

$$\frac{d}{dx}\left(\frac{h^3 \rho}{\mu k_1}\frac{dp}{dx}\right) = \frac{1}{2}\frac{d}{dx}(\rho V h) \tag{19}$$

where $k_1 = 12 + 0.14\left(\sigma^2 R/0.16\right)^{0.725}$. This is the equation of turbulent flow comparable to the laminar Reynolds equation. Direct integration yields

$$\frac{h^3 \rho}{\mu k_1}\frac{dp}{dx} = \rho V h/2 + C$$

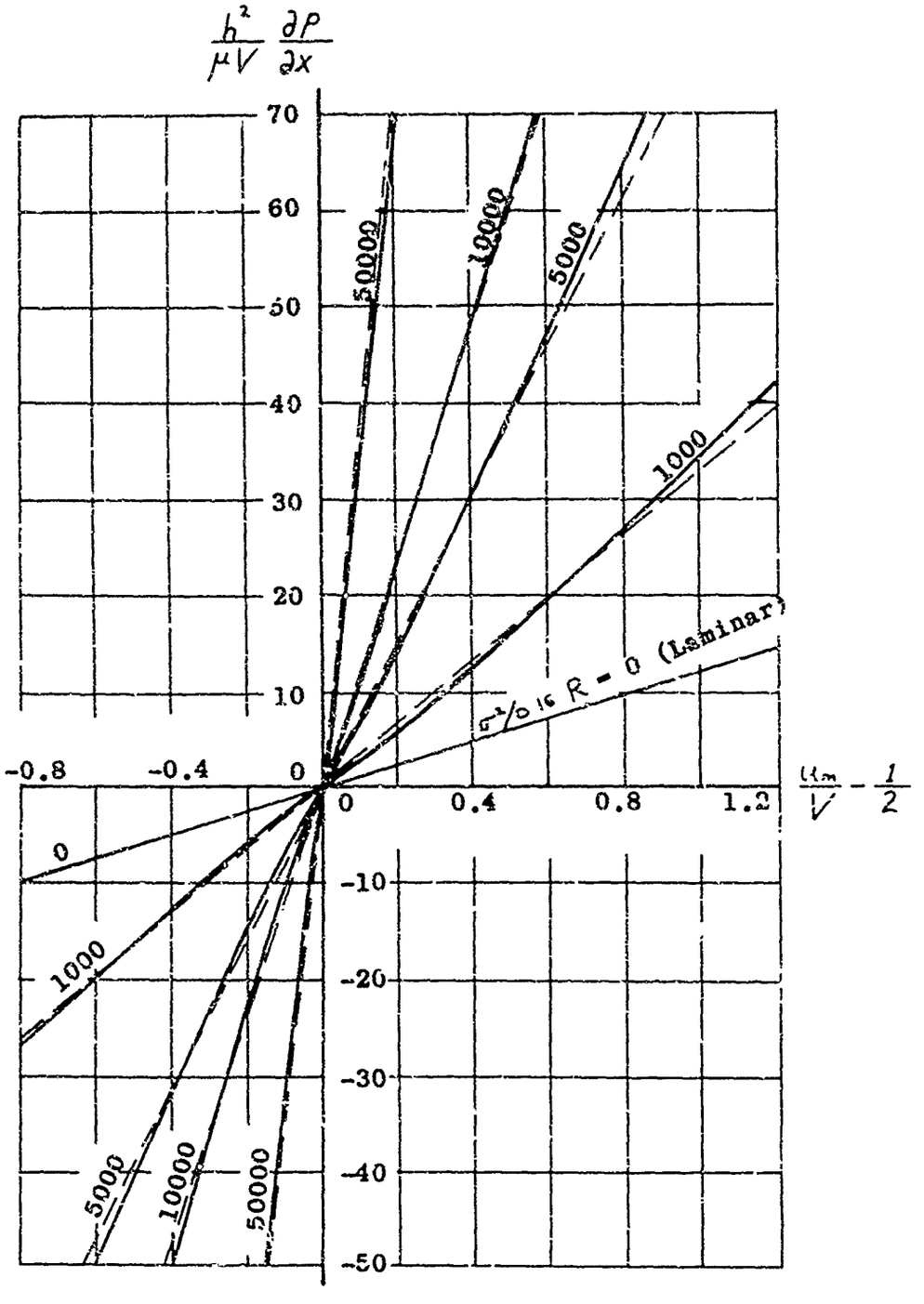

Figure 44. Turbulent Bearing Performance Parameters

As shown in Figure 5, the pressure in a bearing increases from the inlet value to a maximum value somewhere within the bearing, and then drops off to the exit value. At the maximum pressure point, $dp/dx = 0$ and

$$C = -\rho_M V h_M / 2 \tag{20}$$

where the M subscript denotes the conditions at the maximum pressure point. Combining Equation (20) with Equation (19), the result yields the basic differential equation for the pressure in the bearing gap.

$$\frac{dp}{dx} = \frac{\mu V k_1}{2h^2}\left[1 - \frac{\rho_M h_M}{\rho h}\right] \tag{21}$$

A relation between the density and pressure must be introduced at this point and for this purpose the polytropic equation is used.

$$P/\rho^n = \text{CONST} \qquad 1 \le n \le \gamma = c_p/c_v \tag{22}$$

Combining Equations (21) and (22) and substituting the expression for k_1, the result is:

$$\boxed{\frac{dp}{dx} = \frac{\mu V}{2h^2}\left[12 + 0.14\, R^{*0.725}\left(\frac{p^{1/n} h}{p_M^{1/n} h_M}\right)^{0.725}\right]\left(1 - \frac{p_M^{1/n} h_M}{p^{1/n} h}\right)} \tag{23}$$

where

$$R^* = \rho_M V h_M \sigma^2 / 0.16\,\mu$$

This is the basic equation for the pressure gradient within a quasi-steady, two-dimensional, turbulent gas bearing.

Computer Program

To calculate the bearing pressure profile, temperature profile, load, and center of pressure, Equation (23) must be integrated. As shown in Reference (3), Page 558, even for the isothermal case (n = 1), this requires linearizing a portion of the equation. To eliminate the required restrictions on the range of the final solution, and to permit future calculations employing a nonisothermal case, it was decided to integrate Equation (23) numerically.

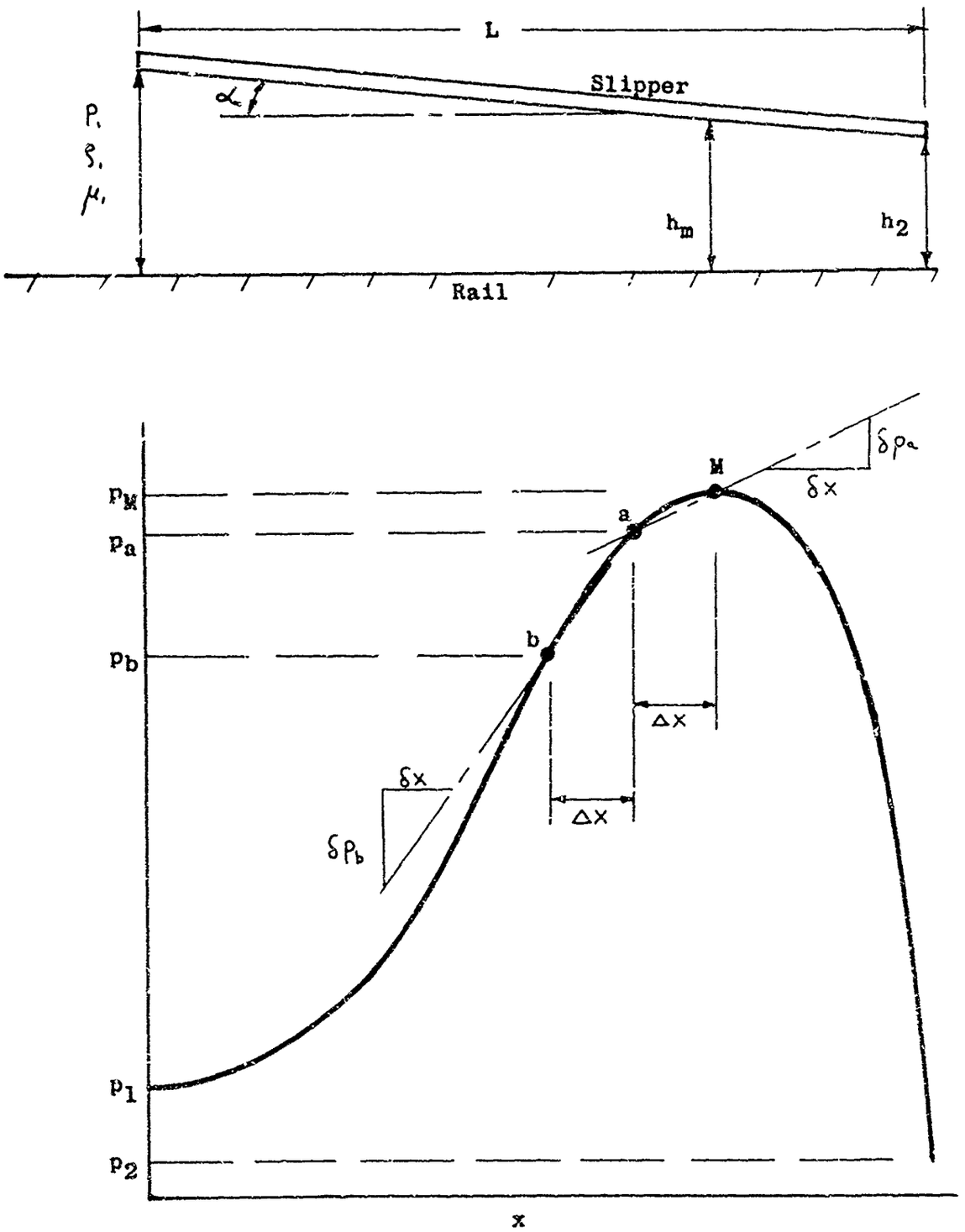

Figure 45. Numerical Integration Method

The essential steps are shown in Figure 45. Starting at the maximum pressure location, the value of the pressure and the bearing gap at this point are selected. The isothermal case was selected for the feasibility study since this case represents the lower performance range of an air bearing. Equation (23), with known values of P_M and h_M then becomes:

$$\frac{dp}{dx} \approx \frac{\delta p}{\delta x} = \frac{C_1}{h^2}\left[12 + C_2 (P h)^{0.725}\right]\left(1 - \frac{C_3}{P h}\right)$$

where C_1, C_2, and C_3 are constants.

Starting from the maximum pressure point

$$h_a = h_M \pm \Delta x(\alpha)$$

where Δx is a small increment. The pressure gradient is then

$$\left(\frac{\delta p}{\delta x}\right)_a = \frac{C_1}{h_a^2}\left[12 + C_2 (P_M h_a)^{0.725}\right]\left(1 - \frac{C_3}{P_M h_a}\right)$$

and the pressure at point a (Figure 45) is:

$$P_a = P_M + \Delta x \left(\delta p / \delta x\right)_a$$

This procedure is continued at the next section by replacing P_M and h_a by P_a and h_b. The process is continued until the inlet pressure (as specified by the sled velocity) and exit pressure are reached. Then

$$L = \bar{n}\,\Delta x$$

$$F = \Delta x \sum_{1}^{\bar{n}} P_i$$

$$\bar{x} = \sum_{1}^{\bar{n}} P_i x_i / F$$

where x_i is the distance from the front of the slipper to the location where the pressure is P_i.

With some additional complication, the process can be modified to calculate the nonisothermal cases.

UNCLASSIFIED

Security Classification

DOCUMENT CONTROL DATA - R&D

(Security classification of title, body of abstract and indexing annotation must be entered when the overall report is classified)

1. ORIGINATING ACTIVITY (Corporate author) Kaman Aircraft Corporation Bloomfield, Connecticut	2a. REPORT SECURITY CLASSIFICATION Unclassified 2b. GROUP N/A

3. REPORT TITLE

FEASIBILITY STUDY OF AIR BEARING ROCKET SLED SLIPPERS

4. DESCRIPTIVE NOTES (Type of report and inclusive dates)

Final Report

5. AUTHOR(S) (Last name, first name, initial)

Meier, R. C. and Smith, A. F.

6. REPORT DATE	7a. TOTAL NO. OF PAGES	7b. NO. OF REFS
July 1966	111	11

8a. CONTRACT OR GRANT NO. AF 29(600)-5516 b. PROJECT NO. 6876 c. Task No. 687629 d.	9a. ORIGINATOR'S REPORT NUMBER(S) R-638 9b. OTHER REPORT NO(S) (Any other numbers that may be assigned this report) MDC-TR-66-110

10. AVAILABILITY/LIMITATION NOTICES

Distribution of this document is unlimited.

11. SUPPLEMENTARY NOTES N/A	12. SPONSORING MILITARY ACTIVITY Air Force Missile Development Center Air Force Systems Command Holloman AFB, New Mexico

13. ABSTRACT

A study was conducted for the Air Force Missile Development Center to investigate the feasibility of applying the principle of air film lubrication to rocket sled slippers to (1) overcome erosive oxidation and severe melting effects experienced at hypersonic speeds and (2) alleviate rail-induced vibrations. Results of the study indicate that a simple self-acting type of bearing can support a typical monorail rocket sled, without contact between the slipper and the rail, at speeds between Mach 1.5 and Mach 6. With contact eliminated, the slipper can be coated with a refractory material to prevent erosive oxidation and melting of slipper structural material. This type of air bearing slipper appears to be the most suitable for AFMDC requirements. An externally pressurized type of slipper bearing is capable of preventing slipper-rail contact over the entire speed range of typical monorail and dual rail sleds. However, the weight and volume of the associated pressurization system are large, and are considered prohibitive for a practical design. The most critical track requirements for an application of air lubricated slippers are the vertical alignment and dimensional tolerances of the rail. It is recommended that AFMDC proceed with the development of a self-acting type of slipper bearing.

DD FORM 1 JAN 64 1473

UNCLASSIFIED

Security Classification

Security Classification

14. KEY WORDS	LINK A		LINK B		LINK C	
	ROLE	WT	ROLE	WT	ROLE	WT
AIR FILM LUBRICATION ROCKET SLED SLIPPERS AIR BEARINGS						

INSTRUCTIONS

1. ORIGINATING ACTIVITY: Enter the name and address of the contractor, subcontractor, grantee, Department of Defense activity or other organization (*corporate author*) issuing the report.

2a. REPORT SECURITY CLASSIFICATION: Enter the overall security classification of the report. Indicate whether "Restricted Data" is included. Marking is to be in accordance with appropriate security regulations.

2b. GROUP: Automatic downgrading is specified in DoD Directive 5200.10 and Armed Forces Industrial Manual. Enter the group number. Also, when applicable, show that optional markings have been used for Group 3 and Group 4 as authorized.

3. REPORT TITLE: Enter the complete report title in all capital letters. Titles in all cases should be unclassified. If a meaningful title cannot be selected without classification, show title classification in all capitals in parenthesis immediately following the title.

4. DESCRIPTIVE NOTES: If appropriate, enter the type of report, e.g., interim, progress, summary, annual, or final. Give the inclusive dates when a specific reporting period is covered.

5. AUTHOR(S): Enter the name(s) of author(s) as shown on or in the report. Enter last name, first name, middle initial. If military, show rank and branch of service. The name of the principal author is an absolute minimum requirement.

6. REPORT DATE: Enter the date of the report as day, month, year; or month, year. If more than one date appears on the report, use date of publication.

7a. TOTAL NUMBER OF PAGES: The total page count should follow normal pagination procedures, i.e., enter the number of pages containing information.

7b. NUMBER OF REFERENCES: Enter the total number of references cited in the report.

8a. CONTRACT OR GRANT NUMBER: If appropriate, enter the applicable number of the contract or grant under which the report was written.

8b, 8c, & 8d. PROJECT NUMBER: Enter the appropriate military department identification, such as project number, subproject number, system numbers, task number, etc.

9a. ORIGINATOR'S REPORT NUMBER(S): Enter the official report number by which the document will be identified and controlled by the originating activity. This number must be unique to this report.

9b. OTHER REPORT NUMBER(S): If the report has been assigned any other report numbers (*either by the originator or by the sponsor*), also enter this number(s).

10. AVAILABILITY/LIMITATION NOTICES: Enter any limitations on further dissemination of the report, other than those imposed by security classification, using standard statements such as:

(1) "Qualified requesters may obtain copies of this report from DDC."

(2) "Foreign announcement and dissemination of this report by DDC is not authorized."

(3) "U. S. Government agencies may obtain copies of this report directly from DDC. Other qualified DDC users shall request through _____."

(4) "U. S. military agencies may obtain copies of this report directly from DDC. Other qualified users shall request through _____."

(5) "All distribution of this report is controlled. Qualified DDC users shall request through _____."

If the report has been furnished to the Office of Technical Services, Department of Commerce, for sale to the public, indicate this fact and enter the price, if known.

11. SUPPLEMENTARY NOTES: Use for additional explanatory notes.

12. SPONSORING MILITARY ACTIVITY: Enter the name of the departmental project office or laboratory sponsoring (*paying for*) the research and development. Include address.

13. ABSTRACT: Enter an abstract giving a brief and factual summary of the document indicative of the report, even though it may also appear elsewhere in the body of the technical report. If additional space is required, a continuation sheet shall be attached.

It is highly desirable that the abstract of classified reports be unclassified. Each paragraph of the abstract shall end with an indication of the military security classification of the information in the paragraph, represented as (*TS*), (*S*), (*C*), or (*U*).

There is no limitation on the length of the abstract. However, the suggested length is from 150 to 225 words.

14. KEY WORDS: Key words are technically meaningful terms or short phrases that characterize a report and may be used as index entries for cataloging the report. Key words must be selected so that no security classification is required. Identifiers, such as equipment model designation, trade name, military project code name, geographic location, may be used as key words but will be followed by an indication of technical context. The assignment of links, rules, and weights is optional.

GPO 856-591

Security Classification